Synthesis of metal xanthates and their application as latent catalysts for curing of epoxy resin

GRADUATE SCHOOL OF LIFE SCIENCE AND SYSTEM ENGINEERING
KYUSHU INSTITUTE OF TECHNOLOGY

DISSERTATION

FOR THE DEGREE OF

DOCTOR OF PHILOSOPHY

Tarun Chand V

September - 2015

SUPERVISOR

Associate Professor. Shyam Sudhir Pandey

Abstract

Cured epoxy resins have emerged as one of the most demanding industrial materials due to their properties such as high stiffness, adhesive nature and environmental stability. Their versatile nature makes it valuable with tremendous application potential ranging from sports goods to aerospace industry.

Cured epoxy is a product of processed epoxy oligomer or polymer into a three dimension network generated by employing curing catalysts. The conventional curing catalysts however suffer from serious drawback of premature curing even undesired at ambient conditions limiting its pot-life. Therefore utilization of latent catalyst for thermoset applications is highly desired to extend the working life of a formulated mixture by passivating the activity of the catalyst until triggered by the external stimulus. The impetus for using latent catalysts is to impart the ability for developing the fully formulated resin systems with long storage life that can be applied directly by the end user. This, in turn, helps guaranteed consistency and improve process efficiency. To attain this, core shell encapsulation or matrix encapsulation are being currently used but they suffer from the problems like diffusion through the thermoset after release and sluggish release kinetics respectively.

We have found that metal sulfides exhibit the curing of epoxy resin composite like conventionally used acid and base catalysts. Normally such catalyst start reacting immediately having limitation on the pot-life. Since metal sulfides are generally insoluble in the solvent and by homogeneously mixing with the ingredients of the epoxy resin composite their latent catalytic property cannot be effectively utilized. Metal xanthates are well known soluble precursors for the metal sulfides whose solubility can be controlled by judicious modification of alkyl chain. Just upon heating to the threshold temperature, they generate the metal sulfide in the system releasing only the gaseous bi-products.

This dynamic latent capability of metal xanthates to form catalytically active metal sulfides was put to use in this current study. This thesis explores and demonstrates the investigation of metal xanthates as potential latent thermal catalysts for curing of epoxy resins.

Table of contents

Chapter 1. Introduction

1.1 Relevance of cured epoxy resin

Cured epoxy resins are potential industrial materials applied in endless variety of applications [1]. Cured epoxy resins industry market growth is increasingly being robust with global demand expected to increase at around 4% per year during 2013–2018 [2]. The worldwide epoxy resin market predicted at roughly US$18.6 billion in 2013. With development of new applications the demand for epoxy is increasing under demand [3]. Cured epoxy resins are employed in aerospace industry [4], packaging [5], electronics [6], construction [7] and several other industries [8]. The first commercial epoxy resin was synthesized by Dr. Pierre Castan in Switzerland during the development of material for dental restoration and in 1942, patent was assigned to Ciba-Geigy (Ciba AG of Basel) Switzerland. Bisphenol A diglycidyl ether (DGEBPA) is an important constituent of epoxy resin and is the basic building block for the volume of applications of epoxy resin which was invented and patented by Dr S. O. Greenlee, Devoe and Raynolds, in 1948 [9]. The simplest epoxy resin designed by Dr S. O. Greenlee involves reaction of Bisphenol-A (BPA) with epichlorohydrin (ECH) in presence of caustic soda producing DGEBPA (figure 1.1) [10]. Subsequently many polymers have been epoxidized and optimized for various desired applications. The tailoring of epoxy resins is achieved by several methods such as altering the functional groups, changing the processable conditions, modifying the structure and varying the curing agents catalyzing the formation of cured epoxy resin from monomers or polymers. Longer alkyl chain enhance the molecular weight of the epoxy monomer resulting in higher viscosity. Presence of reactive functional groups make the cured epoxy resin more intact and stable. The bond strength determines the modulus of the cured epoxy resin [11].

This flexibility and versatility allowed by cured epoxy resins formulations to be able to modify the material properties to meet the needs of the target application is the key for their wide spread demand in the industry. Cured epoxy resins can be processed to possess properties such as excellent thermal resistance [12], high tensile strength [13], low weight [14], high adhesiveness, flexibility [15], low shrinkage, electrical insulation [16], low cost, and environmental stability [17].

These properties make cured epoxy resins viable in several applications such as strong adhesives [18], semiconductor encapsulates [19], paints [20], coatings and adhesives [21]. Cured epoxy resins are even employed in several sports equipment such as cycling, golf and tennis [22]. Right from the beginning stages of commercial production of cured epoxy resins by Devoe-Reynolds Company the consumption level enhanced over the decades [23]. Commercial epoxy resins constitute varied types of backbones such as aromatic, aliphatic and cycloaliphatic chains. Apart from DGEBPA few other important well established epoxy resins include phenoxy epoxy resins, glycidyl ethers of novolac resins, epoxy cresol Novolac resins. Epoxidation of cycloaliphatic carboxylic acid and cycloaliphatic epoxy reisn leading to glycidyl esters are also commercially available. Novolac resins consists of several functional groups which enhances the cross linking density and therefore thermal stability. Multifunctional aromatic glycidyl amine resins for instance triglycidyl-p-aminophenol and tetraglycidyl- 4, 4'-diaminodiphenylmethane are reported to possess excellent thermal properties. On the other hand cycloaliphatic epoxy resins have properties of low viscosity and glass transition temperatures [24]. Cured epoxy resin are employed in several applications and few of them are listed in detail below

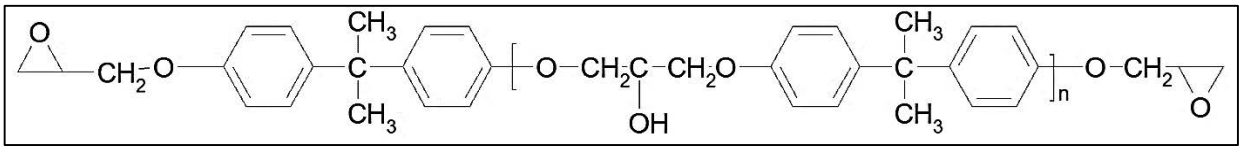

Figure 1.1: Bisphenol A diglycidyl ether (DGEBPA).

1.1.2 Fiber reinforced plastics

The liquid process ability and cured strength control of epoxy resin composites made these high performance materials as an obvious choice for matrices in fiber-reinforced composites and fiber reinforced plastics [25]. Fiber reinforced plastics are major components in medical prostheses, sports equipment and aircrafts [26].

1.1.3 Adhesives

The adhesive property is utilized in several military applications as well [27]. Almost all the substrates having a polar inclination form strong bonds with epoxy resin. The formulation of epoxy resin composite to form commercially viable adhesive system is indeed a specialized technology. The curing agent and the additives are chosen to meet the requirement of the target applications. For few adhesive systems the DGEBA is replaced with heterocyclic and alicyclic epoxides to meet the criteria of applications under consideration. The adhesive are available in different forms based on applications such a powders, films, tapes, two component liquids, heat melting adhesives and room temperature adhesives. High-strength structural adhesives are made from epoxy polyurethanes [28]. Adhesives that cure even under water were made utilizing rubber and elastomer [29].

1.1.4 Structural materials

Cured epoxies are used to bond concrete material [30] to other material such as stone or itself. They are also the primary raw materials in making boats. Cured epoxy resin employed in applying paints, to produce industrial floor covering, in pipelines as leak-proof sealants and in of construction of high-performance materials [31].

1.1.5 Coatings

Among all the applications coating industry is the highest market that is consuming the cured epoxies. The main reason for the use of cured epoxy resin for coatings [32] is its environmental stability, corrosion free surface [33]. This application is used in refrigerators, washing machines, ships, chemical plants and containers [34].

1.1.6 Laminates and composites

The employment of cured epoxy resins as laminated composites are gaining increased attention due to their low corrosion resistance, high strength to weight, low thermal expansion and stiffness to weight ratios [35]. Cured epoxy laminates are used as encapsulates in the semiconductor

industry for insulation. Glass fiber reinforced polymer (GFRP) [36] are materials in future fusion reactors as insulators for superconducting magnetic coils [37].

1.2 Curing process

Cured epoxy resin is the outcome of the processed parent epoxy compound. The uncured epoxy compound consists of one or more reactive epoxide functional groups in the monomer or polymer chains. The epoxy functional group is a three membered chain consisting of two carbon groups and one oxygen group. Due to its low membered cyclic structure a severe ring strain exists making the molecule highly reactive. Depending on the epoxy compound molecular weight and functional groups can either exist as liquid or solid [38].

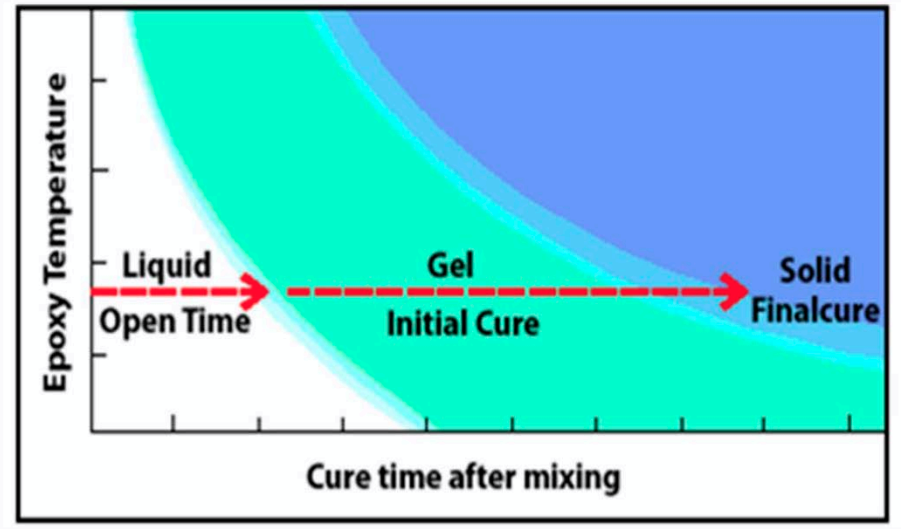

Figure 1.2: Schematic diagram of curing process.

Curing of epoxy resins is basically transformation of epoxy monomer or polymer chains of low molecular weight into a high molecular weight three dimensional network [39]. Ring strain and the polarity of the C-O bond due to the presence of electronegative oxygen atom of the epoxy group make it susceptible for the high reactivity. The addition of molecules to the main parent molecule by ring opening reaction of epoxy functional group leading to the formation of a three dimensional network system of high molecular weight is the curing reaction process. By the ring opening reaction, the active epoxide groups in the uncured epoxy can be made to react with many curing agents or hardeners that contain carboxyl, amine, phenols groups etc., depending on the

desired application. Curing reaction of the parent epoxy compound can be initiated with any other curing agents or epoxy compound in the presence or absence of a curing catalyst. Due to presence of a polar bond the epoxy group can react with both nucleophilic and electrophilic reaction centers and chemical structure of epoxides plays a crucial role in the curing reactions. The nature of the functional groups of the parent epoxy compound and the other substrates influence the rate of the reaction [40]. Physical changes of curing involve transformation of melted epoxy composite in liquid form to a highly viscous glassy state via highly viscous semi solid. This process is portrayed in figure 1.2. The time when the melted liquid epoxy composite fully forms the glassy state is recorded as the curing time.

The curing process consists of polymerization and crosslinking process. Polymerization process is an addition reaction whereas crosslinking process is interchain bonding of either intrachain reactive sites or secondary sites on co-reactive agents. In a simplified situation polymerization dominates crosslinking due to availability of free monomers leading to easy accomplishment of reaction of primary reactive sites resulting enhancement of molecular weight. Once all of the monomers possess one bond the polymer tends to become a high molecular weight thermoplastic and this is observed to be the gel point of the epoxy resin. This gel point is characteristic of the epoxy composite formulation. Upon reaching the gel point due to absence of free monomers crosslinking presides polymerization leading to formation of a three dimensional network. When the molecular weight exceeds than that of the energetically stable rubber state the polymer begins to transform into a glassy state. This process is referred to as vitrification process. At a stage where no more reactive sites are free to react a high modulus and insoluble network system results. This network system delivers the epoxy resin a high strength. Therefore the degree of network dictates the physical properties of the cured epoxy resin [41].

1.3 Curing catalysts

Curing catalysts are agents employed to catalyze the curing of the epoxy composite. The cure reactions can be accelerated by the use of curing catalysts [42]. There are several curing catalysts available and can be broadly classified as acids and bases. Several Lewis acids such as metal halide complexes are employed as acid catalysts [43]. Lewis bases act as nucleophilic catalytic curing agents due to presence of unshared pair of electrons attacking the electropositive reactive site of

the epoxy compound leading to propagation of ring opening reaction (figure 1.3) [44]. The base curing catalysts includes amines, amine adducts, ketimine and anhydrides [45]. On the other hand Lewis acids have an empty outer orbit so will tend to react with reaction centers with higher electron density [46]. BF_3, $FeCl_3$, $AlCl_3$, $SnCl_4$ and $ZnCl_2$ are the typical Lewis acid catalysts [47].

1.3.1 Amines

Amines such as aliphatic amines, primary amines, secondary amines, tertiary amines, aromatic amines, imidazole and alicyclic amines are utilized as curing agents [48]. The curing time of epoxy composite employing amines as curing agents depend on type of epoxy resin, type and loading of amine. The active hydrogen in the amine reacts with the epoxy group and forms a product containing a hydroxyl group. The primary amine upon reaction with epoxy compound becomes secondary amine and this further reacts with more reaction center further becoming a tertiary amine and again this further reacts thus leading to polymerization. The number of active hydrogens in the curing catalyst plays a very important role in deciding the stoichiometry of the curing agent to the epoxy compound. Compared to aliphatic amines aromatic amines have low basicity therefore curing occurs more gradually with the former than the later. In addition the steric hindrance of the aromatic ring further enhances the curing time. Few commonly used amine curing agents are Diethylenetriamine (DTA) [49], Triethylenetetramine (TTA) [50], N-aminoethylpiperazine (N-AEP), menthane diamine (MDA) [51], m-xylenediamine (m-XDA) [52], and Metaphenylene diamine (MPDA) [53].

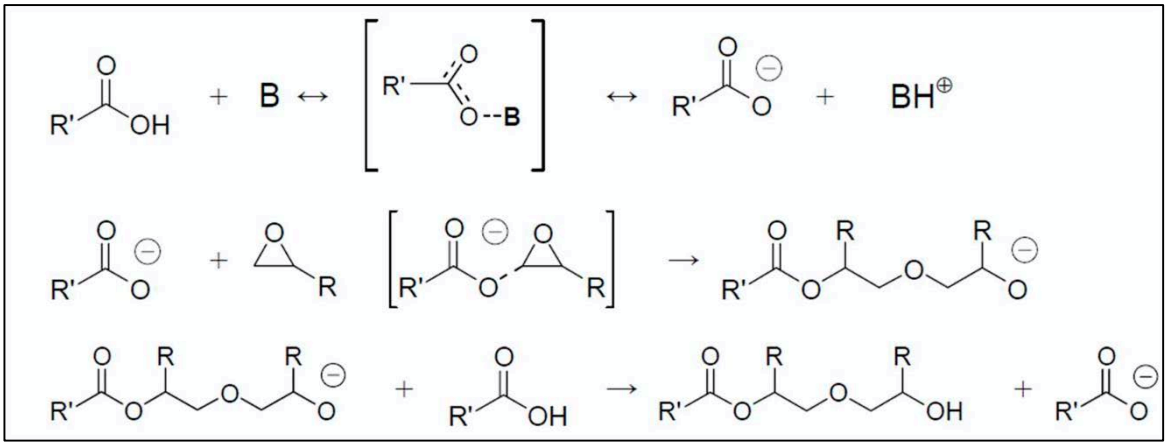

Figure 1.3: A typical base catalyzed curing reaction of epoxy resin.

1.3.2 Anhydrides

Even though compared to amine as curing agents, anhydrides require severe condition for curing to obtain large moldings. Their pot-life in general is much longer than amine curing agents and generate lower heat while curing. Alicyclic anhydrides are more common than aromatic anhydrides. Curing agents such as aromatic anhydrides curing agents are mostly solids. They are used in powder paints, insulating coating for casting and condensers [54]. Few anhydrides curing agents are tetrahydro phthalic anhydride [55], methylhexahydro phthalic anhydride and methyltetrahydro phthalic anhydride [56].

1.3.3 Boron trifluoride-amine complex .

Boron tri-fluoride is generally employed in combination with amine complexes as curing agents and fall under the category of cationic initiators [57]. The general scheme of curing of epoxy resin composite employing boron trihalide complex is presented in figure 1.4. The properties of the curing agent and the final cured epoxy resin such as melting point and reactivity depends on the type of the amine. Epoxy compound cured with these curing agents exhibited greater heat resistance and therefore employed in production of laminates for electrical insulation and reinforced plastics [58].

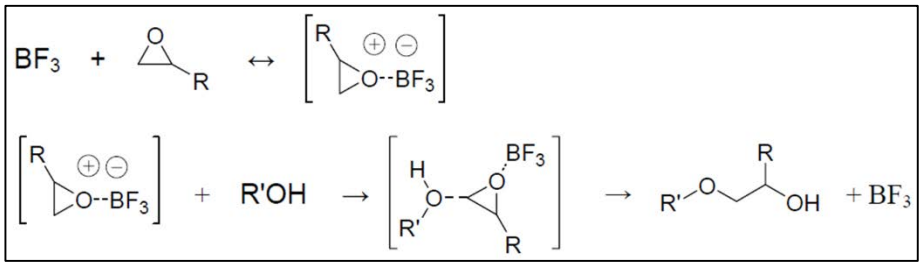

Figure 1.4: Acid catalyzed curing reaction of epoxy resin employing Boron trifluoride as complex.

1.4 Latent curing catalysts

The conventional curing agents although cure rapidly but suffers from many drawbacks. The traditional curing agents instigate curing even at ambient conditions making it infeasible to have easily storable mixtures which can be put to use only when desired [59]. The premature curing is

a major setback for the standard curing agents. Due to instigation of curing even at ambient conditions the shelf-life of the formulated composite mixtures is greatly reduced. In addition the uncertainty of the optimum conditions necessary for curing by employing these catalysts makes it very difficult to have precise control over cure processing [60].

To eliminate these limitations latent curing agents were explored as an alternative. The latent catalyst enable curing of the formulated mixture only when desired upon trigger by external stimuli [61]. The use of latent catalyst preserves the formulated mixture as there is no premature curing due to passivation of curing catalytic activity until the threshold external stimuli when required is provided thus enhancing the shelf-life of the composite [62]. In the case earlier catalytic systems to eliminate premature curing a two stable component mixture is required. Wherein at the desired time the two components consisting of epoxy compound and the curing agent are homogenously mixed and processed for the further use. This process is a highly tedious step and causes delay in the production line consuming both time and labor. The storing and transportation of two pot mixture is disadvantageous on a large scale. An extra burden of additional handling of the homogeneity and regulation of stoichiometry of multiple components is demanded during the mixing step. However with the utilization of latent catalysts endeavoring advantages such as easing of production line by elimination of several stages of processing such as requirement of control over mixing, homogenization of multiple components the cure processing is highly simplified [63]. As with formulated mixtures consisting of latent catalysts its feasible to have a storable and stable one pot mixture making processing more economical. Since the curing condition such as threshold stimuli required for initiation of curing by latent catalysts is precisely known the knowledge about the optimum conditions required for curing is made very emphatic [64]. These advantages are the driving force for the scientific pursuit of investigation of new latent catalysts. Thus the challenge for latent catalysts possessing ability to catalyze the curing process only upon instigation by threshold external stimuli is of huge demand.

1.5 Metal sulphides

Metal sulfides are well known for their wide range of applications such as catalysis, fuel cell technology, semiconductor industry and petroleum industry and photovoltaics. Predominantly metal sulfides are utilized as catalysts for several processes. Due to their significance they are

extensively pursued both academically as well as industrially. They are employed as catalysts in several reactions such as hydrodesulphurization, photo catalytic water splitting, electro catalytic hydrogenation of ketones, hydrogenation, hydrodenitrogenation and Hydrogen production reactions [65]. For instance, rhenium sulfide catalyst is used in hydrodesulphurization of thiophene [66], dehydrogenation of tetrahydroindole to indole with a nickel sulfide catalyst [67] and molybdenum sulfide catalyst for hydrogen production [68]. Even in several industrially important reactions on a large scale metal sulfides were employed as catalysts for processes such as hydrodesulphurization of the petroleum feedstock supported by MoS_2 nanocrystallites dispersed on alumina [69], hydrocracking of heavy oils, ruthenium sulfide as hydrotreating catalyst supported by alumina [70], NiMo/Al2O3 sulfide catalyst for hydrodenitrogenation of fast pyrolysis bio-oil obtained from sewage sludge [71]. Metal sulfide as nanoparticles are of high interest and is drawing tremendous scientific pursuit especially due to application as semiconductors. The copper zinc tin sulfide (Cu_2ZnSnS_4, CZTS) is one of the promising semiconductors for non-toxic and environment friendly thin-film solar cells [72]. Polymer nanocomposites comprising of conjugated polymers such as polythiophenes, poly-para-phenylenevinylenes, or various low bandgap polymers with metal sulfide nanoparticles are explored for fabrication hybrid solar cells. Fluorescing chalcogenide particles are put to use as biological labels. Antimony sulfide has been utilized in thermoelectric cooling technologies, SnS due to low-toxicity is investigated as a photoconductor for the preparation of photoelectric energy conversion and near-infrared (NIR) detector materials. Cadmium sulfide is one of the most important chalcogenide systems playing a pertinent role in semiconductor systems [73]. Thus the application potential and the invention of novel technology utilizing metal chalcogenides is ever increasing.

1.6 Metal xanthates

Xanthates are basically organic compounds bearing $–OCS_2-$ functional group and the name is derived from xanthic acid. They are derivatives of xanthic acid obtained by replacing the active thiol proton of xanthic acid either with alkyl group or metals. When the active proton is replaced with metals these compounds are referred to as metal xanthates or metal dithiocarbonates. The first of xanthates compounds were reported in 1822 [74]. Xanthates are found to be useful in several industrial processes such as flotation and collection in mineral and mining industries. Cellulose

xanthates are worth mentioning compounds due to their application for separation by column chromatographic method [75].

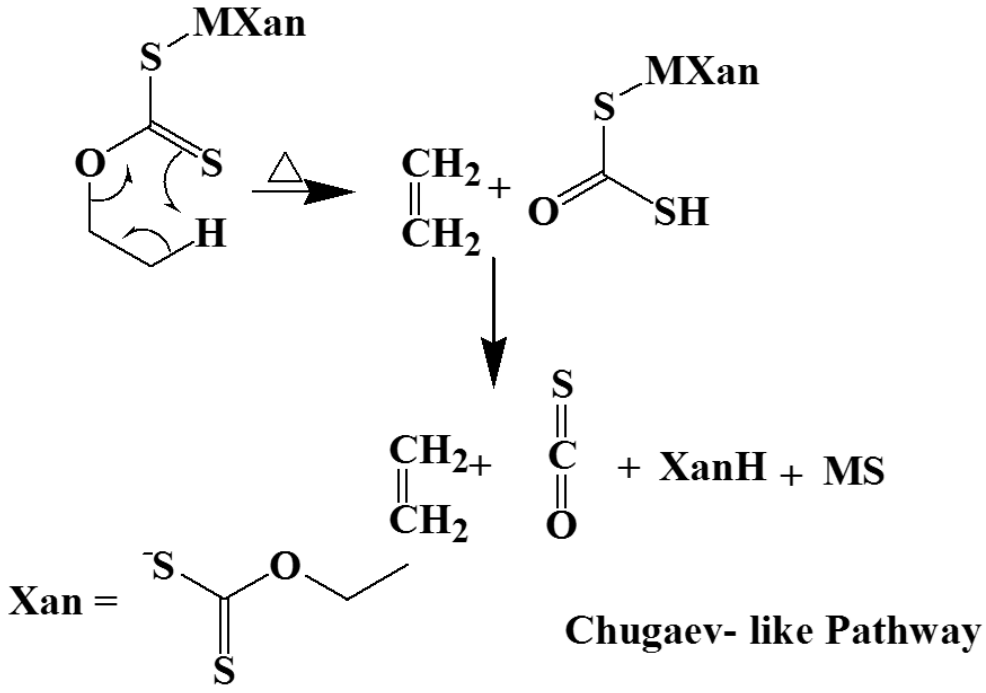

Figure 1.5: The Chugaev-like thermal decomposition pathway of metal xanthate.

method [75]. Xanthates are also well known for their anti-fungal activity therefore known for their use as fungicides and pesticides [76]. They are employed as catalysts in polymerization reaction such as RAFT polymerization [77]. Xanthates are also employed as capping agent for controlling the particle size of nanoparticles.

One of the most significant applications of metal xanthates is as precursors to metal sulfides for metal- organic chemical vapor deposition (MOCVD) and synthesis of semiconductor nanoparticles. Metal xanthates are the sources of metal sulfides. By thermal annealing at their threshold temperature metal xanthates decompose to yield metal sulfides [78]. It is suggested that metal xanthates decompose via chugaev elimination mechanism wherein by a concerted syn-elimination from a six-membered cyclic transition state leads to formation of an alkene followed by elimination of carbon disulfide and hydrogen sulfide gases. Thus the gases and the alkene are eliminated from the system with the residual metal sulfide (figure 1.5) [79]. In some situations the ligand gets departed from the metal xanthate complex and acts like a capping agent thus controlling

the size of the nanoparticles [80]. Literature reports on the preparation of CdS, Sb_2S_3, ZnS, Bi_2S_3 and other metal sulfide nanoparticles from their respective metal xanthate salts by thermal annealing for various applications is abundant [81]. Several advantages of metal xanthates over direct use of metal sulfides include formation of thin films, homogeneity of nanoparticles, tailoring of size of the nanoparticles and solubility.

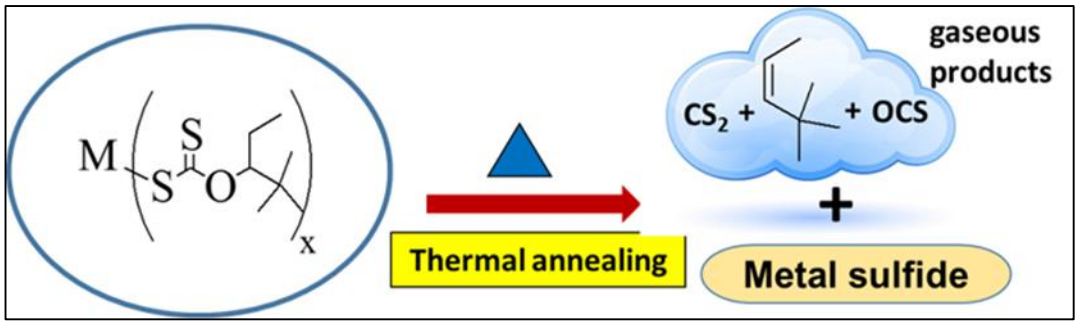

Figure 1.6: Metal xanthate decomposition upon thermal annealing at the threshold temperature.

1.7 Scope of study

As metal xanthates decompose to yield metal sulfides upon heating at threshold temperature as external thermal stimuli. This latent capability of metal xanthates yielding catalytically active metal sulfides upon thermal annealing is taken as an advantage and utilization of this principle for the curing of epoxy resin composite was investigated. The epoxy resin composite consisting of metal xanthates was subjected to thermal annealing. The in-situ formed metal sulfides formed by latent thermal decomposition of metal xanthates due to high catalytically surface area was expected to trigger curing of epoxy resin composite.

1.8 Organization of the present thesis

This thesis explores and demonstrates the utilization of metal xanthates as latent catalysts for curing of epoxy resin. First chapter describes the relevance of cured epoxy resins, curing process, curing catalysts, need for latent catalysts. Followed by the potential application of metal sulfides,

the use of metal xanthates as precursors to metal sulfides and finally the aim of the current study that is the use of metal xanthates as latent in-situ catalysts for curing of epoxy resin composite.

Second chapter deals with the details of instruments, techniques and characterization methods used for the confirming of material synthesized, cure time study and cure kinetics.

Third chapter describes the influence of alkyl ligand on zinc xanthates thermal decomposition temperature and in curing of epoxy resin composite utilizing zinc xanthate as catalyst. .

Fourth chapter gives the study of influence of metal by varying the metals on the xanthate species. The trend in thermal decomposition temperature and catalytic activity in curing of epoxy resin was investigated by various metal xanthates consisting of similar alkyl ligand is reported.

Fifth chapter deals with comparison of study of curing time versus temperature study, cure kinetics and mechanism of curing of epoxy resin with gallium (III) xanthate and standard catalyst.

Finally the sixth chapter work will summarize the main results and provide this works role in future investigation.

1.9 References

[1] M. Aldridge, W. Alan, W. Anthony, K. John, Macromolecules, 2014, 47, 8368.

[2] Epoxy Resins Chemical Economics Handbook (CEH), HIS, 2014, 2.

[3] Market Report, Global Epoxy Resin Market, Acmite Market Intelligence, 2014, 1.

[4] R. Senthil, S. W. Vedakumari, T. Hemalatha, B. N. Das, T. P. Sastry, *Fibers and Polymers* 16 2015, 1, 181.

[5] H. Luo, D. Zhang, C. Jiang, X. Yuan, C. Chen, K. Zhou, *ACS Applied Materials & Interfaces,* 2015, *7* (15), 8061.

[6] D. Xin, Q. Han, *Electronic Materials Letters*, 2014, 3, 535.

[7] P. N. Kumar, A. Rajadurai, Applied Mechanics and Materials, 2014, 592, 186.

[8] S. Sprengera, M. H. Kothmannb, V. Altstaedtb, *Composites Science and Technology,* 2014, 105, 86.

[9] B. Ellis, *Chemistry and Technology of Epoxy Resins*, 1993, 1.

[10] J. O. Simpson, S. A. Bidstrup, Journal of Polymer Science, Part B: Polymer Physics, 1995, 33, 55.

[11] B. Bilyeu, W. Brostow, K. P. Menard, Journal of Materials Education, 2000, 22 (4-6), 107.

[12] F. Hu, J. J. L. Scala, J. M. Sadler, G. R. Palmese, Macromolecules, 2014, 47 (14), 4548.

[13] H. Gu, S. Tadakamalla, X. Zhang, Y. Huang, Y. Jiang, H. A. Colorado, Z. Luo, S. Wei, Z. Guo, Journal of Materials Chemistry C, 2015, **3**, 162.

[14] H. Jin, C. L. Mangun, A. S. Griffin, J. S. Moore, N. R. Sottos, S. R. White, Advanced Materials 2014, 2, 282.

[15] R. Verker, A. Rivkin, G. Zilberman, O. Shoseyov, Cellulose, 2014, 21 (6), 4369.

[16] M. Hsiao, C. M. Ma, J. Chiang, K. Ho, T. Chou, X. Xie, C. Tsai, L. Changa, C. Hsieh, *Nanoscale, 2013,* 5(13), 5863.

[17] C. Aoufa, H. Nouailhas, M. Fache, S. Caillol, B. Boutevin, H. Fulcrand, European Polymer Journal, 2013, 49 (6), 1185.

[18] G. Zhanga, J. Chenga, L. Shia, X. Linb, J. Zhanga, Thermochimica Acta, 2012, 538, 36–42.

[19] J. Hou, G. Li, N. Yang, L. Qin, M. E. Grami, Q. Zhang, N. Wanga, X. Qu, RSC Advances, 2014, 4, 44282.

[20] Y. Edaoa, Y. Kawamuraa, T. Yamanishia, S. Fukadab, Fusion Engineering and Design, 2014, 89 (9–10), 2062.

[21] P. Kuo, M. Saina, N. Yan, Green Chem., 2014, 16, 3483.

[22] T. Deng, Y. Liu, X. Cui, Y. Yang, S. Jia, Y. Wang, C. Lu, D. Li, R. Caia, X. Hou, Green Chemistry, 2015, 17, 2141.

[23] C. A. May, Introduction to Epoxy Resins, Marcel Dekker, Inclusive, 1988, New York, 1, 1988.

[24] Cheremisinoff, Handbook of Ceramics and Composites: Mechanical Properties and Specialty Applications, 1991, 107.

[25] J. Bai, Advanced Fiber-Reinforced Polymer (FRP) Composites for Structural Applications, Elsevier, 201, chapter 5, 88.

[26] H. T. Corten, Composite Materials: Testing and Design, 1972, 170.

[27] J. Keller, Literature Review: An Overview of Epoxy Resin Syntactic Foams with Glass Microballoons, Los Alamos National Laboratory, 2012, 2.

[28] J. Jiaa, Y. Qina, Q. Meia, Z. Huanga, Journal of Macromolecular Science, Part B: Physics, 2014, 53 (10), 1621.

[29] Y. Ahn, Y. Jang, N. Selvapalam, G. Yun, K. Kim, Angewandte Chemie, 2013,125 (11), 3222.

[30] L. Tu, D. Kruger, Materials Journal, 1996, 93 (1), 26.

[31] W.K. Goertzen, M.R. Kessler, Composites Part B: Engineering, 2007, 38 (1), 1.

[32] L. Nie, A. Burgess, A. Ryan, Macromol. Chem.Phys., 2013, 214, 225.

[33] S. S. Qureshi, Z. Zheng, M. I. Sarwar, O. Félix, G. Decher, ACS nano, 2013, 7(10), 9336.

[34] C. H. Zhang, S. L. Luan, X. S. Qian, B. H. Sun, W. S. Zhang, Advanced Materials Research, 2011, 391, 1445.

[35] R. Murugana, R. Ramesh, K. Padmanabhan, Procedia Engineering, 2014, 97, 459.

[36] R. M. Boumbimbaa, C. Froustey, P. Viota, J.M. Olivec, F. Léonardid, P. Gerarde, R. Inoublie, Composite Structures, 2014, 116, 414.

[37] T. Tanabea, K. Nodab, T. Yosiyukic, M. Hosinoc, I. Watanabec, K. Chidaa, T. Watanabea, T. Honmab, I. Katayamad, Y. Arakakia, Y. Haruyamae, M. Saitoe, I. Nomuraf, K. Hosonog, Nuclear Instruments and Methods in Physics Research Section A: Accelerators, Spectrometers, Detectors and Associated Equipment, 2000, 441 (3), 326.

[38] C. May, Epoxy Resins: Chemistry and Technology, CRC Press, Technology & Engineering, 1987, 2, 285.

[39] A. Dimopoulos, A. A. Skordos, I. K. Partridge, Journal of Applied Polymer Science, 2012, 124, 1899.

[40] Y. Tanaka, R. S. Bauer, Curing Reactions, Epoxy Resins Chemistry and Technology, Marcel Dekker, Inclusive, 1988, 2, 285.

[41] B. Bilyeu, W. Brostow, K. P. Menard, Journal of Materials Education, 2000, 22 (4-6), 107.

[42] J. Wan, Z. Bu, C. Xu, H. Fan, B. Li, Thermochimica Acta, 2011, 525, 31.

[43] M. Flores, X. Fernández-Francos , J. M. Morancho, À. Serra, X. Ramis, Thermochimica Acta, 2012, 543, 188.

[44] C. Wang, Z. Liao, Polymer Bulletin, 1991, 25(5), 559.

[45] A. A. Azeez, K. Y. Rhee, S. J. Park, D. Hui, Composites: Part B, 2013, 45, 308.

[46] C. Su, C. Wei,B. Li, Advances in Materials Science and Engineering, 2013, 1.

[47] W. J. Blank, Z. A. He, M. Picci, International Waterborne, High-Solids and Powder Coatings Symposium, New Orleans, 2001.

[48] V. J. Eddy, J. E. Hallgren, R. E. Colborn, Journal of Polymer Science: Part A Polymer Chemistry, 1990, 28, 2417.

[49] W. Xu, S. Bao, P. He1, Journal of Applied Polymer Science, 2002, 84(4), 842.

[50] H. B. Fan, M. M.F. Yuen, Polymer, 2007, 48 (7), 2007, 2174.

[51] R. Nixon, J. Cahill, R. Jolanki, Kanerva's Occupational Dermatology, 2012, 559.

[52] M. Lettieria, M. Frigione, Construction and Building Materials, 2012, 30, 753.

[53] Y. Chenga, L. Chaob, Y. Wangc, K. Hoa, S. Shena, T. Hsieha, Y. Wang, Synthetic Metals, 2013, 168, 48.

[54] J.H. Luft, Journal of Cell Biology, 1961, 9 (2), 409.

[55] S. Huo, G. Wua, J. Chena, G. Liua, Z. Konga, Thermochimica Acta, 2014, 587, 18.

[56] V. Kumar, Dielectrics and Electrical Insulation, IEEE Transactions on, 2012, 19 (3), 968.

[57] C. O. Bounds, R. Goetter, J. A. Pojman1, M. Vandersall, Journal of Polymer Science Part A: Polymer Chemistry, 2012, 50 (3), 409.

[58] P. Ramesha, L. Ravikumar, A. R. Burkanudeenc, Polymer-Plastics Technology and Engineering, 2012, 51 (2), 140.

[59] M. J. Shin, Y. J. Shin, S. W. Hwang and J. S. Shin, Journal of applied polymer science, 2013, 129, 1036.

[60] K. Huang, Y. Zhang, M. Li, J. Lian, X. Yang, J. Xia. Progress in Organic Coatings, 2012, 74, 240.

[61] W. G. Kim, H. G. Yoon, J. Y. Lee, Journal of applied polymer science, 2001, 81, 2711.

[62] M. Kirino, I. Tomita, Macromolecules, 2010, 43, 8821.

[63] S. Naumann, M. R. Buchmeiser, Macromolecular rapid communications, 2014, 35, 682.

[64] A. M. Tomuta, X. Ramis, F. Ferrando, A. Serra, Progress in Organic Coatings, 2012, 74, 59.

[65] S. Wang, C. An, J. Yuan, Materials 2010, 3, 401.

[66] P. T. Vasudevana, J. L. G. Fierro, Catalysis Reviews: Science and Engineering, 1996, 38 (2), 161.

[67] O. Y. Gutiérrez, S. Singh , E. Schachtl, J. Kim, E. Kondratieva, J. Hein, J. A. Lercher, ACS Catal., 2014, 4 (5), 1487.

[68] X. Zong, Z. Xing, H. Yu, Y. Bai, G. Q. Lu, L. Wang, Journal of Catalysis, 2014, 310, 51–56.

[69] S. Garg, K. Soni, V. V. D. N. Prasad, M. Kumar, T. Bhaskar, J. K. Gupta, G. M. Dhar, C S Gopinath, Journal of Chemical Sciences, 2014, 126 (2), 437.

[70] M. Fang, R. A. S. Delgado, Journal of Catalysis, 2014, 311, 357.

[71] S. G. A. Ferraz, B. M. Santos, F. M. Z. Zotin, L. R. R. Araujo, J. L. Zotin, Industrial & Engineering Chemistry Research, 2015, 54 (10), 2646.

[72] J. Embden, A. S. R. Chesman , E. D. Gaspera , N. W. Duffy , S. E. Watkins, J. J. Jasieniak, Journal of the American Chemical Society, 2014, 136 (14), 5237.

[73] W. Boncher, H. Dalafu, N. Rosa, S. Stoll, Coordination Chemistry Reviews, 2015, 289–290, 279.

[74] W. H. Dennis, Metallurgy, 35.

[75] C. Denga, J. Liub, W. Zhoua, Y. Zhanga, K. Dua, Z. Zhaoa, Chemical Engineering Journal, 2012, 200–202, 452.

[76] K. Singh, G. Kour, R. Sharma, R. Sachar, V. K. Gupta, R. Kant, European chemical bulletin, 2014, 3 (5), 463.

[77] Y. Lei, T. Wang, J. W Mitchell, L. C Chow, Journal of Basic & Clinical Medicine, 2014, 3(1), 1.

[78] F. T. F. O'Mahony, U. B. Cappel1, N. Tokmoldin, T. Lutz1, R. Lindblad, H. Rensmo, S. A. Haque, Angewandte Chemie International Edition, 201, 52 (46), 12047.

[79] N. Alam, M. S. Hill, G. Kociok-Ko¨hn, M. Zeller, M. Mazhar, K. C. Molloy, Chemistry Materials, 2008, 20, 6157.

[80] C. Zhang, S. Zhang, L. Yu, Z. Zhang, P. Zhang, Z. Wu, Materials Letters, 2012, 85, 77.

[81] A. S. R. Chesman, J. Embden, N. W. Duffy, N. A. S. Webster, J. J. Jasieniak, Crystal Growth & Design, 2013, 13 (4), pp 1712.

Chapter 2. Experimental methods

2.1 Instrumentation for study of curing time

Cure time is defined as the time required for a material to reach maximum viscosity or modulus at a given temperature [1]. Lower the cure time at a given temperature means faster curing process indicating the higher efficiency of the catalyst under consideration. The cure time versus temperature study was utilized to analyse and compare the curing catalytic property of the metal xanthates. Wherein, the epoxy resin composite including metal xanthate was placed on a hot plate maintained at a specific temperature and the time to form complete solid (maximum viscosity) was recorded. The cure time at different temperatures was studied using Panasonic (KT4) hot plate (figure 2.1). The hot plate consists of an in-built function to monitor temperature and can be maintained at a constant temperature. The reaction mixture can be placed on the hot plate platform directly which is maintained at a desired temperature. The composite is constantly mixed until the mixture which initially becomes liquid due to melting later on becomes solid once the curing is finished. This entire time until the reaction mixture turns highly viscous is recorded and considered to be the curing time [2].

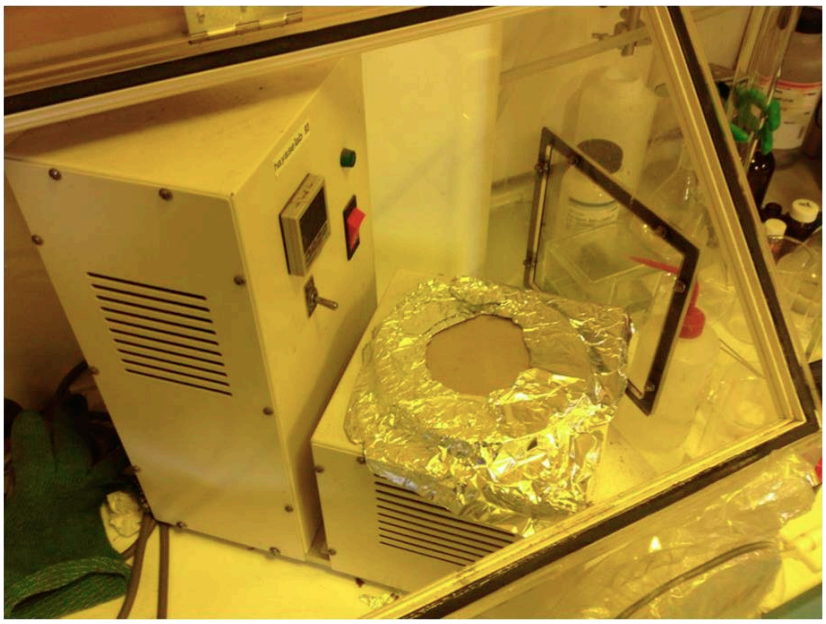

Figure 2.1: Panasonic (KT4) hot plate used for studying cure time at different temperatures.

2.2 Instrumentation for characterization of material

This section describes the various techniques utilized to characterize and confirm metal xanthates synthesized, metal sulfides obtained by thermal annealing of metal xanthates and epoxy composite cured by employing metal xanthates as catalysts.

2.2.1 Thermogravimetric analysis

The Thermogravimetric analyzer (TGA) was utilized to determine the thermal behaviour of metal xanthates under investigation.The Thermogravimetric analyzer (TGA) is an essential laboratory tool used for material characterization. This technique is utilized to characterize materials used in various environmental, petrochemical, food, and pharmaceutical applications. This technique requires monitoring the mass of a substance as a function of temperature or time [3].

Figure 2.2: Thermogravimetric analysis apparatus used in this present thesis.

A TGA instrument includes a sample pan placed on mass balance. Both of the reference empty and sample pans are placed inside furnace during the experiment. The sample mass is monitored during the analysis relative to the reference empty pan. A sample gas purged controls the sample

environment. The thermogravimetric analysis was performed using DTG-60 simultaneous DTA-TG apparatus, Shimadzu (figure 2.2). The TGA curve indicates percentage weight loss with respect to temperature. The final weight loss percentage is used to determine the final product of decomposition. The temperature at which decline in percentage mass curve is observed is determined as the decomposition temperature. The decomposition temperature was determined and compared among the metal xanthates using this technique. Also with conjunction to other techniques is utilized to characterise the final product of decomposition of metal xanthates [4].

2.2.2 Differential scanning calorimetry

The differential scanning calorimeter (DSC) is a fundamental tool in thermal analysis of materials. It was employed in studying and characterizing the cure reaction of epoxy resin composite. Differential thermal analysis was studied using DSC-60 Differential scanning calorimeter, Shimadzu (figure 2.3). DSC is employed in many industries – from pharmaceuticals and polymers, to food products and nanomaterials. The information provided by DSC is used to understand polymorph and eutectic transitions, amorphous and crystalline behavior, curing and degree of cure, and many other material properties used to manufacture, design and test products. In DSC the reference cell and the sample cell are heated in a single furnace in an inert atmosphere maintained by continuous flow of nitrogen gas. An aluminum pan was used in our case for the DSC study. The difference in heat flow between them is recorded as function of temperature and time. As the pressure of the system is constant heat flow measured gives the enthalpy changes in the system. In case of exothermic process heat is released and therefore heat flow to the reference is higher than that to the sample pan. In DSC-60 Differential scanning calorimeter, Shimadzu this is recorded as a positive exotherm.

Traditionally DSC is being used for the study of cure kinetics as cure reaction is an exothermic process [4] [5] [6]. Therefore DSC was utilized to the study the cure reaction of epoxy composite including curing catalysts. DSC is employed to determine the cure onset and peak temperatures for various heating rates [7]. This data was used to determine the activation energy by utilizing Flynn-Wall-Ozawa method 8 and Kissinger's method 9. The activation energy values and the heat

flow data as a function of temperature was further used to obtain various key kinetic parameters and enabled to determine the kinetic model for the mechanism of curing.

Figure 2.3: Differential scanning calorimetry apparatus used in this present thesis.

2.2.3 X – ray diffraction (XRD)

X-ray diffraction (XRD) analysis is based on constructive interference of monochromatic X-rays and a crystalline sample. This technique applied to crystalline materials for determining crystal structures, measure stress, identify phase composition, crystallinity and preferred orientation. XRD is primarily used to ID crystalline material. The interaction of the sample with incident X-rays produces constructive interference when Bragg's Law ($n\lambda=2d \sin \theta$) is satisfied. The characteristic x-ray diffraction pattern generated in XRD analysis gives the unique "fingerprint" of the crystals present in the sample. The analysis obtained can be interpreted, by comparison with standard reference measurements and patterns, allowing the identification of the crystalline form. Since metal xanthates are well known to form metal sulfides upon thermal annealing. Rigaku RINT-2000/PC X-ray diffraction apparatus was utilized to characterize these metal sulfides exhibiting crystalline behavior [10].

2.2.4 Scanning Electron Microscopy with X-ray microanalysis (SEM-EDS)

Electron dispersive spectroscopic (EDS) analysis involves generation of an X-ray spectrum from the scan area of the SEM. The EDS analysis plots Y-axis shows the counts (number of X-rays received and processed by the detector) and the energy level of those counts is shown by the X-axis. The EDS software recognizes the associated energy level of the X-rays with the elements and the shell levels responsible for the generation the X-rays. Hitachi S-5200 Scanning Electron Microscope (SEM) - Energy-dispersive X-ray spectroscopy (EDS) was utilized for elemental analysis and mapping of the material. EDS measurement using the above model required attachment filled with liquid nitrogen to maintain the temperature required by the instrument. Metal sulphides obtained by thermal annealing and not exhibiting crystalline behaviour were characterised using this technique [11].

2.2.5 Nuclear Magnetic Resonance Spectroscopy

The nuclear magnetic resonance (NMR) spectrum is utilized in structure elucidation because the properties given by it can be related to the molecular structure of the sample compound. The scalar coupling (or J-coupling) indicates an indirect interaction between individual nuclei in a chemical bond, mediated by electrons, and under suitable conditions. Metal xanthates synthesised were characterised by both proton ^{1}H NMR and carbon ^{13}C NMR spectroscopy [12]. ^{1}H NMR spectrum was recorded at 26 ^{0}C on JEOL JNM-A500 Nuclear Magnetic Resonance Spectrometer operated at 500 MHz. ^{13}C NMR spectrum was recorded at 24 ^{0}C on JEOL Nuclear Magnetic Resonance Spectrometer at 125 MHz. NMR spectra were measured in solution with TMS as an internal reference. All ^{1}H shift values are given in parts per million (s = singlet; d = doublet; t = triplet; m = multiplet).

2.2.6 Infrared (IR) spectroscopy

IR study involves triggering molecular vibrations through irradiation with infrared light. IR spectroscopy aides in providing the information about the presence of certain functional groups.

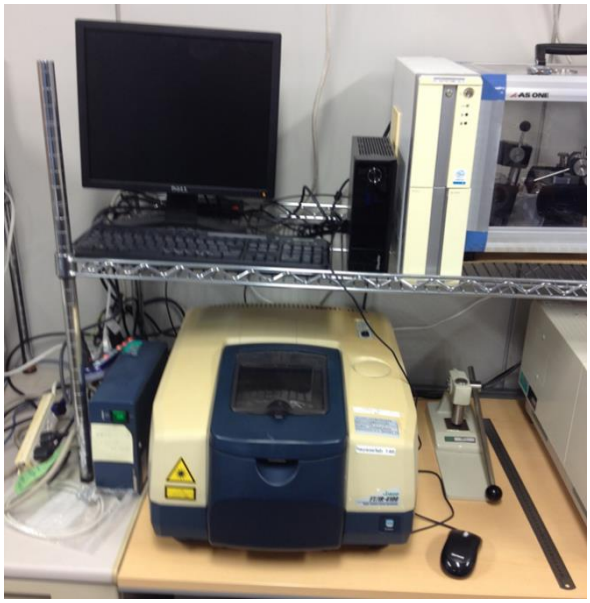

Figure 2.4: Fourier transform Infrared spectrometer used in this present work.

Infrared spectroscopy is based on the fact that when an infrared light is incident on the sample. The material absorbs specific frequencies characteristic of the bonds present. Upon incidence of infrared light the bonds or the functional groups present in the molecule vibrate and resonance occurs when the vibration frequency of incident light matches leading to absorption. These vibration frequencies are characteristic to a particular function group or bond. Thus based on the absorbed vibration frequency the nature of the bond or functional group can be identified.

In Fourier transform infrared (FTIR) spectroscopy infrared light is incident on the sample. The output light signal is detected and the instrument gives absorbance as a function of infrared wavelength (or equivalently, wavenumber). IR is used to identify the functional groups or bonds in a molecule [13] [14] [15]. The IR spectrum was recorded on a JASCO FT/IR 4100 (figure 2.4). Potassium bromide pellet sample form was used for the compounds to measure IR.

2.2.7 Elemental analysis

Elemental analysis in conjunction with other techniques provides a quick and inexpensive method to find sample purity, and can be used to characterize a compound. Elemental analysis was performed using Yanaco MT-5 CHN analyzer. The analytical method is based on instantaneous oxidation of the sample by "flash combustion" converting all organic and inorganic substances into combustion products. Elemental analysis gives the percentage composition of the various elements present in a material [16]. Elemental analysis of the metal xanthates was performed using Yanaco MT-5 CHN (carbon, hydrogen, nitrogen) analyzer.

2.2.8 Electronic absorption spectra

In case of electronic absorption spectroscopy, the electron is made to excite from an initial low energy state to a higher state by the photon energy provided by the spectrophotometer and is detected in the absorbance spectrum. Upon incidence of light on the material either gets reflected back or pass through or get absorbed. Absorbance is the difference the incident light (I_0) and transmitted light intensity (I). The absorbed light is either defined in terms of transmittance or absorbance.

Transmittance is defined as ratio of transmitted light and incident light intensity. When expressed in percentage is defined as percentage transmission.

Transmittance (T):

$$T = I / I_0$$

Percentage transmission (%T):

$$\% T = (I/I_0) \times 100$$

Absorbance is defined as negative log of Transmittance

Absorbance (A)

$$A = - \log T$$

Electronic absorption spectroscopy is a measurement technique that allows to measure the transmittance. Light is guided through the sample and by detecting output light intensity absorbance is plotted as a function of wavelength (or equivalently, wavenumber) is measured. The presence of an absorbance band at a particular wavelength is used for identifying the material as the absorption peak is characteristic to a particular compound and therefore utilized to identify the material composition. The utilization of absorbance studies for characterization of material is very well reported [17] [18]. Gallium sulfide obtained by thermal annealing of gallium (III) xanthate was confirmed by electronic absorption spectroscopy [19]. JASCO V-670 spectrophotometer was used to study the Electronic absorption spectra.

2.2.9 Electron probe microanalyser for electron probe microanalysis (EPMA)

EPMA involves bombardment by an accelerated and focused electron beam onto a sample. This leads to evolution of back-scattered electrons and x-rays due to electron-sample interactions. These signals are detected generating a surface image and allows to obtain an average composition of the material. Thus elemental composition and mapping can be achieved by EPMA. JEOL JXA-8530F Field Emission Electron Probe Microanalyser was used for electron probe microanalysis. The cured epoxy composite utilizing gallium (III) xanthate as catalyst was characterised by this technique [20].

2.3 References

[1] “Cure time" McGraw-Hill Dictionary of Scientific & Technical Terms, The McGraw-Hill Companies, Inc. 24, 2003, 6.

[2] Tarun Chand Vagvala, Shyam Sudhir Pandey, Yuhei Ogomi, Shuzi Hayase, RSC Advances, 2014, 4, 24658.

[3] C. D. Doyle, Analytical Chemistry 1961, 33 (1), 77.

[4] D.P. Dutta, G. Sharma, A.K. Tyagi, S.K. Kulshreshtha, Materials Science and Engineering B, 2007, 138, 60.

[5] M. J. Yoo, S.H. Kim, S.D. Park, W.S. Lee, J. Sun, J. Choi and S. Nahm., Eur. Polym. J., 2010, 46, 1158.

[6] W. M. McDanel, M. G. Cowan, J. A. Barton, D. L. Gin, R. D. Noble, Industrial & Engineering Chemistry Research, 2015, 54 (16), 4396.

[7] K Pielichowski, P Czub, J Pielichowski, Polymer, 2000, 41 (12), 2000, 4381.

[8] G. M. Roudsari, A. K. Mohanty, M. Misra, ACS Sustainable Chemistry & Engineering 2014 2 (9), 2111-2116.

[9] Y. S. Ye, Y. J. Huang, F. C. Chang, Z. G. Xuea, X. L. Xie, Polymer Chemistry, 2014, 5, 2863.

[10] L. K. Macreadie, H. E. Maynard-Casely, S. R. Batten, D. R. Turner, A. S. R. Chesman, ChemPlusChem, 2015, 80(1), 107.

[11] K. H. Park, J. Choi, H. J. Kim, J. B. Lee, S. U. Son, Chemistry of materials, 2007, 19, 3861.

[12] T. Rath, M. Edler, W. Haas, A. Fischereder, S. Moscher, A. Schenk, R. Trattnig, M. Sezen,

G. Mauthner, A. Pein, D. Meischler, K. Bartl, R. Saf, N. Bansal, S. A. Haque, F. Hofer, E. J.W.

List, G. Trimmel, Advanced Energy Materials, 2011, 1, 1046.

[13] G. Rajput, V. Singh, S. K. Singh, L. B. Prasad, M. G. B. Drew, N. Singh, European Journal of Inorganic Chemistry, 2012, 24, 3885.

[14] T. Khoo, M. Break, K.A. Crouse, M. Ibrahim, M. Tahir, A.M. Ali, A.R. Cowley, D.J. Watkin, M.T.H. Tarafder, Inorganica Chimica Acta, 2014, 413, 68.

[15] M. Tariq, S. Ali, N. Muhammad, N. A. Shah, M. Sirajuddin, M. N. Tahir, N. Khalid, M. R. Khan, Journal of Coordination Chemistry, 2014, 67 (2), 323.

[16] S. Kapoor, R. Sachar, K. Singh, V. K. Gupta, V. Rajnikant, Journal of Chemical Crystallography, 2012, 42(3), 222.

[17] N. Soltania, E. Saiona, W. M. M. Yunusa, M. Erfania, M. Navaserya, G. Bahmanrokha, K. Rezaeeb, Applied Surface Science, 2014, 290, 440.

[18] M. Buscema, D. J. Groenendijk, S. I. Blanter, G. A. Steele, H. S. J. Zant, A. Castellanos-Gomez, Nano Letters, 2014, 14 (6), 3347.

[19] M.A. Malik, M. Afzaal and P. O'Brien, Chem. Rev., 2010, 110, 4417; M. Lazell, P. O'Brien, D. J. Otway and J. Park, J. Chem. Soc., Dalton Trans., 2000, 4479.

[20] N.O. Lottera, J.F. Oliveiraa, A.L. Hannafordb, 1, S.R. Amosb, Minerals Engineering, 2013, 52, 8.

Chapter 3. Zinc xanthates with varying alkyl chains on curing

3.1 Introduction

Properties of metal xanthates are very much influenced by the alkyl chains as ligand of the xanthate [1]. Properties such as solubility, stability of the xanthate complexes [2], decomposition temperature, and crystal structure of the metal sulfide formed are dependent on the alkyl chain of the xanthate [3]. Branched alkyl metal xanthates tend to be more soluble non polar organic solvents than the linear alkyl metal xanthates counterparts. For instance zinc n-pentyl xanthate is insoluble while the 2,2- dimethyl-3-pentyl zinc xanthate is soluble in dichlorobenzene. Metal xanthates having methyl [4], isopropyl [5] [6], and ethyl [7] as alkyl chain substituent are reported to show very low solubility in non-polar organic solvents. This solubility difference should be taken into account especially for the preparation of thin films of metal sulfides [8, 9]. The stability of metal xanthates is also dependent on the alkyl chain ligand of the xanthates [10] e.g. n-hexyl potassium xanthate was found to be more stable than cyclohexyl potassium xanthate. It is reported that tertiary alkoxy metal xanthates are relatively unstable than secondary alkoxy metal xanthates [11]. Therefore, choice of the ligand of the metal xanthate determines stability in turn influences its decomposition temperature. As the metal sulfide crystal dimensions and configuration are dependent on the alkyl chains of the metal xanthates formed upon decomposition, size of the nanoparticle formed upon thermal annealing of metal xanthates can be controlled by the alkyl chain ligand of the metal xanthates.

For instance, when silver sulfide nanoparticles were prepared from silver carnaubyl, hexadecyl and octyl-xanthates. Ag_2S nanoparticles formed upon thermal annealing of silver carnaubyl xanthate showed the smallest mean diameter compared to silver hexadecyl xanthate and silver octyl xanthates [12]. The thermal decomposition process resulted in simultaneous formation of both Ag_2S nanoparticles and xanthate ligands. Xanthate ligands thus formed act as a capping agent hindering the enlargement of nuclei limiting the size of the silver sulfide nanoparticle. Thus greater the size of the alkyl ligand of the metal xanthate better the limitation on the nanoparticles nuclei growth, therefore, smaller the size of the nanoparticles. This clearly indicates that the crystallinity

and the size of the metal sulfide formed are strongly influenced by the alkyl ligand of the metal xanthate. Since the alkyl ligand of the metal xanthates has tremendous influence on the properties of the metal xanthates [13]. The effect of changing alkyl chain of metal xanthates on curing of epoxy composite was thought to be very essential.

To achieve this purpose, series of zinc xanthates consisting of varied linear and branched alkyl chain ligands were synthesized (figure 3.1) and characterized by ^{1}H NMR, ^{13}C NMR, IR and elemental analysis. In the linear chain series, n-butyl, n-amyl, n-hexyl zinc xanthates were synthesized. While the branched alkyl ligand zinc xanthates series consisted of 2,2-dimethyl butyl, pentyl and hexyl zinc xanthates. All zinc xanthates under investigation were derived from their respective potassium xanthate precursors. Influence of alkyl ligand on the thermal behavior and decomposition temperature was studied by performing TGA analysis under nitrogen atmosphere for zinc xanthates with varying alkyl ligands. The final decomposition product upon thermal annealing of all the zinc xanthates was characterized by employing XRD. Apart from this, investigation and comparison of curing time of epoxy composite at various temperatures employing 5% zinc xanthates with varied alkyl ligands as catalysts was also conducted. The final post thermally annealed product of cured epoxy resin utilizing zinc xanthates as catalysts was also characterized by XRD..

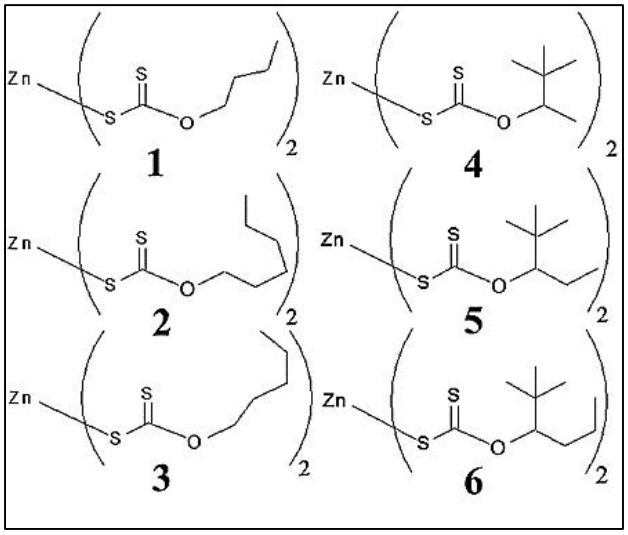

Figure 3.1: Zinc xanthates with linear and branched alkyl chains.

3.2 Materials

Potassium tert-butoxide, carbon disulphide, 1-hexanol and zinc (II) chloride were purchased from Wako Japan. 2, 2 - dimethyl-3-pentanol was purchased from Sigma Aldrich, Japan. 3,3-dimethyl-2-butanol, 2,2-diemthyl-3-hexanol, Potassium butyl xanthate and potassium amyl xanthate were purchased from Tokyo Chemical Corporation, Japan. Epoxy resin (CNE200ELB65) and phenolic resin (BRG556) used in this work were supplied by Kyocera Company, Japan.

3.3 Synthesis and Characterization

Potassium -O-2,2- dimethylbutan-3-yl dithiocarbonate [14], Potassium -O-2,2- dimethylpentan-3-yl dithiocarbonate [15] , were synthesized following literature reports.

Potassium O-hexan-1-yl dithiocarbonate

Potassium *tert*-butoxide (10.5 g, 93 mmol, 1.0 equiv.) was dissolved in Tetrahydrofuran (THF) in an inert atmosphere (nitrogen). The solution was cooled down to 0 °C, then 1-hexanol (8.8 g, 86 mmol, 1.1 equiv.) was slowly added. After stirring for fifteen minutes, carbon disulphide (6.5 g, 86 mmol, 1.1 equiv.) was added dropwise and the solution was stirred for about 5 hours. The reaction mixture was evaporated completely and then extracted into acetone followed by filtration to remove insoluble impurities. The solution was again rotaevaporated, dried and washed with ample diethyl ether to obtain yellow residue. (Yield: 14 g, 72%).

^{1}H NMR (500 MHz, 26 ^{0}C, acetone-d_6) δ = 4.34-4.32 (t, 2H), 1.69-1.38 (m, 2H), 1.34-1.30 (m, 6H) ppm, 0.91-0.88 (t, 3H) ppm.

^{13}C NMR (125 MHz, 24 °C, $CDCl_3$) δ = 233.37, 71.94, 32.35, 29.66, 26.57, 23.19, 14.22 ppm.

IR (KBr pellet, cm^{-1}): 2953, 2870, 1458, 1380, 1194, 1131, 1040, 919.

Elemental analysis: $KC_7H_{13}OS_2$ calculated: C 39.1%, H 6.1%, found: C 40.18%, H 6.6%.

Potassium -O-2,2- dimethylhexan-3-yl- dithiocarbonate

Potassium tert-butoxide (8 g, 71.3 mmol) was dissolved in THF under nitrogen atmosphere. The solution was cooled to 0 ^{0}C and 15 g of 3, 3-dimethyl-2-hexanol (10.15 g, 78.2 mmol)

was added slowly. After stirring for fifteen minutes, carbon disulfide (6 g, 78.2 mmol) was added drop wise, and the solution was stirred for 5 h. The reaction mixture was rotaevaporated completely. The yellow solid obtained was dissolved in acetone and the solution was subsequently filtered to eliminate insoluble impurities. The solution was rotaevaporated again and washed with diethyl ether to obtain a yellow powder. (Yield: 7 g, 73 %).

^{1}H NMR (500 MHz, 26 ^{0}C, acetone-d_6) δ = 2.48-2.47 (t, 1H), 1.95-1.90 (m, 4H), 1.34-1.32 (d, 9H) ppm, 1.31-1.29 (t, 3H) ppm.

^{13}C NMR (125 MHz, 24 °C, $CDCl_3$) δ = 235.30, 87.40, 36.28, 33, 20.35, 15.05 ppm.

IR (KBr pellet, cm^{-1}): 2953, 2870, 1458, 1380, 1194, 1131, 1040, 919.

Elemental analysis: $KC_9H_{17}OS_2$ calculated: C 44.2%, H 7%, found: C 43.4%, H 5.9%.

Zinc (II) -O-butan-1-yl dithiocarbonate (1)

An aqueous solution of potassium-O-butan-1-yl dithiocarbonate 1 (3 g, 16.3 mmol) was added drop wise to a solution of Zinc (II) chloride (1 g, 7.4 mmol), while stirring at room temperature. A white precipitate resulted was collected by suction filtration and washed with methanol. (Yield: 4.9 g, 82.6%).

^{1}H NMR (500 MHz, 26 ^{0}C, $CDCl_3$) δ = 4.51-4.49 (t, 2H), 1.84-1.79(m, 2H), 1.50-1.44 (m, 2H) ppm, 0.97-0.95 (t, 3H) ppm.

^{13}C NMR (125 MHz, 24 °C, $CDCl_3$) δ = 229.73, 77.88, 30.34, 19.08, 13.86 ppm.

IR (KBr pellet, cm^{-1}): 2953, 2870, 1458, 1380, 1194, 1131, 1040, 919.

Elemental analysis: Zn (II) $C_{10}H_{18}O_2S_4$ calculated: C 33.6%, H 4.9%, found: C 34.48%, H 5.2%.

Zinc (II) -O-pentan-1-yl dithiocarbonate (2)

An aqueous solution of Zinc (II) chloride (1 g, 7.4 mmol) was added to an aqueous solution of potassium-O-pentan-1-yl dithiocarbonate (3.3 g, 16.3 mmol) drop wise and the solution was stirred for 2 h. The precipitate obtained was filtered and washed with methanol to obtain the desired product as white solid (yield: 5.3 g, 86.1%).

^{1}H NMR (500 MHz, 26 ^{0}C, $CDCl_3$) δ = 4.50-4.47 (t, 2H), 1.85-1.81 (m, 2H), 1.43-1.33 (m, 4H) ppm, 0.94-0.90 (t, 3H) ppm.

^{13}C NMR (125 MHz, 24 ^{0}C, $CDCl_3$) δ = 229.82, 78.04, 28.06, 27.92, 22.29, 13.93 ppm.

IR (KBr pellet, cm^{-1}): 2950, 2855, 1461, 1220, 1129, 1075, 1028, 946.

Elemental analysis: Zn (II) $C_{12}H_{22}O_2S_4$ calculated: C 36.8%, H 5.6%, found: C 37.6%, H 5.6%.

Zinc (II) -O-hexan-1-yl dithiocarbonate (3)

To an aqueous solution of Zinc (II) chloride (1 g, 7.3 mmol), potassium-O-hexan-1-yl dithiocarbonate (3.8 g, 15.4 mmol) dissolved in water was added drop wise while stirring at room temperature. The solid obtained was filtered and washed with methanol to give white solid (yield: 2.7 g, 76.5 %).

^{1}H NMR (500 MHz, 26 ^{0}C, $CDCl_3$) δ = 4.49-4.47 (t, 2H), 1.85-1.78 (m, 2H), 1.43-1.29 (m, 6H) ppm, 0.91-0.88 (t, 3H) ppm.

^{13}C NMR (125 MHz, 24 ^{0}C, $CDCl_3$) δ = 229.80, 78.04, 31.38, 28.34, 25.52, 22.53, 14.02 ppm).

IR (KBr pellet, cm^{-1}): 2952, 2850, 1459, 1207, 1132, 1064, 1032, 936.

Elemental analysis: Zn (II) $C_{14}H_{26}O_2S_4$ calculated: C 40.1%, H 6.2%, found: C 39.7%, H 6.05%.

Zinc (II) -O-2,2- dimethylbutan-3-yl dithiocarbonate (4)

Zinc (II) -O-2,2- dimethylbutan-3-yl xanthate in the yield of 5.7 g, 83.2 % was synthesized according to the literature report [14].

^{1}H NMR (500 MHz, 26 ^{0}C, $CDCl_3$) δ = 4.88-4.92 (m, 1H), 1.34-1.32 (d, 3H), 1-0.99 (d, 9H) ppm.

^{13}C NMR (125 MHz, 24 ^{0}C, $CDCl_3$) δ = 228.93, 94.29, 35.06, 25.68, 14.34 ppm.

IR (KBr pellet, cm-1): 2965, 2873, 1462, 1364, 1252, 1129, 1058, 907.

Elemental analysis: Zn (II) $C_{14}H_{26}O_2S_4$ calculated: C 40%, H 6.2%, found: C 45.7%, H 6.9%.

Zinc (II)-O-2,2- dimethylpentan-3-yl dithiocarbonate (5)

To an aqueous solution of zinc (II) chloride (1 g, 7 mmol), potassium-O-2,2-dimethyl pentan-3-yl dithiocarbonate (3.71 g, 16 mmol) dissolved in water was added drop wise while stirring at room

temperature. A white precipitate formed was collected by suction filtration and washed with methanol. The solid obtained was extracted into chloroform and recrystallized from methanol to obtain white powder (yield: 6.4 g, 89%).

^{1}H NMR (500 MHz, 26 ^{0}C, $CDCl_3$, δ): 4.92-4.98 (m, 1H), 1.79-1.72 (m, 2H), 0.96-0.98 (m, 12H) ppm.

^{13}C NMR (125 MHz, 24 ^{0}C, $CDCl_3$, δ): 230.79 (CS_2O), 100.56 (CH), 35.88 (C (CH_3)), 25.95 (C (CH3), 23.20 (CH2), 10.96 (CH2-CH3) ppm).

IR (KBr pellet, cm-1): 2965, 2875, 1468, 1367, 1236, 1129, 1056, 902.

Elemental analysis: Zn (II) $C_{16}H_{30}O_2S_4$ calculated: C 42.9%, H 6.7%, found: C 42.0%, H 6.5%.

Zinc (II) -O-2,2- dimethylhexan-3-yl- dithiocarbonate (6)

To an aqueous solution of zinc (II) chloride (1 g, 7.4 mmol), potassium-O-2,2-dimethylhexan-3-yl dithiocarbonate (3.9 g, 16 mmol) dissolved in water was added drop wise while stirring at room temperature. A white precipitate formed was collected by suction filtration and washed with methanol. The solid obtained was extracted into chloroform and recrystallized from methanol to obtain slightly yellow powder as titled compound (yield: 5.6 g, 72.1%).

^{1}H NMR (500 MHz, 26 ^{0}C, $CDCl_3$) δ = 4.99-4.97 (m, 1H) 1.76-1.74 (m, 2H), 1.52-1.47 (2H), 1.01-1.0(d,9H), 0.96-0.89 (m, 3H) ppm.

^{13}C NMR (125 MHz, 24 ^{0}C, $CDCl_3$) δ = 230.72, 99.44, 35.85, 32.22, 25.89, 19.51, 14.15 ppm.

IR (KBr pellet, cm-1): 2954, 2870, 1461, 1369, 1222, 1130, 1038, 901.

Elemental analysis: Zn (II) $C_{18}H_{34}O_2S_4$ calculated: C 45.4%, H 7.2%, found: C 44.2%, H 6.9%.

3.4 Thermogravimetric analysis

The comparison of thermal behavior and decomposition temperature of zinc xanthates by varying alkyl chain was investigated utilizing thermogravimetric (TGA) analysis under nitrogen atmosphere. Several reports on utilization of TGA for the study of thermal decomposition behavior and determining the final product of decomposition of zinc xanthates are available [16] [17] [18]. The TGA plots of linear and branched alkyl chain zinc xanthates were presented in figure 3.2. The TGA plot indicates that the metal xanthates are quite stable at room temperature conditions but upon further the increasing temperature they decompose. This tendency to decompose only by providing threshold external thermal stimuli to yield metal sulfide can be attributed to the latent capability of zinc xanthates to yield metal sulfides.

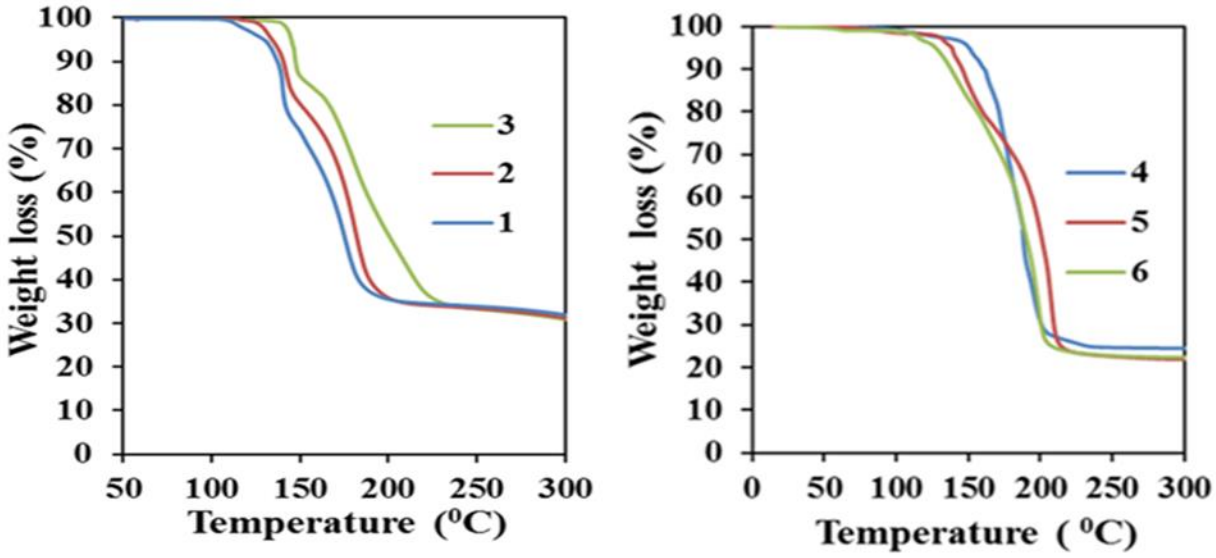

Figure 3.2: Thermogravimetric analysis of Zinc xanthates with linear chains 1, 2, 3 (left) and branched chains 4, 5, 6 (right).

All the zinc xanthates show expected weight loss percentage corresponding to the formation of zinc sulfide. The decomposition temperature of zinc xanthates with change in alkyl chain showed interesting results. The thermal decomposition temperature in case of linear alkyl zinc (II) xanthates varied in the order **1** < **2** < **3.** This indicates that with increase in alkyl chain length the decomposition temperature is enhanced in case of linear alkyl chain zinc xanthates. On the other hand in the case of branched alkyl chain zinc xanthates the trend observed is opposite where in with increase in alkyl chain length the thermal decomposition temperature decreases as the TGA

analysis potrays the thermal decomposition temperature in the order **4** > **5** > **6**. This leads to conclusion that the decomposition temperature trend in case of linear chain zinc xanthates gets enhanced with increase in chain length and in contrary in case of branched alkyl zinc xanthates increase in alkyl chain length causes decrease decomposition temperature.

3.5 XRD analysis of thermally annealed zinc xanthates

In the previous section about TGA investigation, it was found that beyond about 200^{o}C temperature, there was no further weight loss as function of increasing temperature was explained to be zinc sulfide (ZnS) based on stoichiometry calculations.

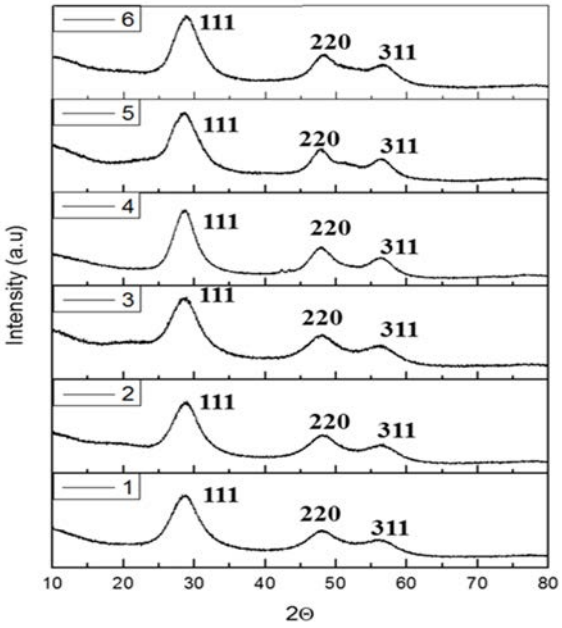

Figure 3.3: XRD analysis of Zinc xanthates with linear chains 1, 2, 3 and branched chains 4, 5, 6 under investigation after thermal annealing at 200 ^{0}C.

To verify this explanation by another independent technique, X-ray diffraction (XRD) was employed to characterize the final product of decomposition upon thermal annealing. Since in the TGA curve for both the branched and linear alkyl chain zinc (II) xanthates a stabilized flat curve around 250 ^{0}C can be observed. All of the zinc (II) xanthates were thermally annealed for about 15 min at 250 ^{0}C. The sample powders obtained were grinded thoroughly and subjected to powder XRD investigations. The XRD spectra of zinc xanthates presented in figure 3.3.spectra

show various diffraction peaks at 2θ values of 28.6°, 47.6° and 56.4° corresponding to the diffraction planes (111), (220) and (311) respectively. This peak pattern perfectly describe a zinc blend structure (JCPDS No. 80-0020) [19] [20]. The XRD analysis confirm the formation of ZnS upon thermal annealing by **1, 2, 3, 4, 5, 6** zinc xanthates.

3.6 Cure time versus temperature studies

To study the latent catalytic activity of metal xanthates to cure the epoxy resin composite, cure time study was conducted at different temperatures to observe implication of molecular structure on the curing time of the epoxy resin. A 1:1 mixture of epoxy resin and phenol was homogenously grinded including 5 % of the respective Zinc (II) xanthates for performing cure time study at various temperatures. The formulated composite was placed on the hot plate maintained at definite temperature. The composite begins to melt followed by formation of semi solid and then leading to final formation of highly viscous glassy state. This entire time until the formation of highly viscous glassy state was recorded as cure time at a given temperature. There was no significant curing observed below 180^0C. Therefore, the cure time was recorded at different temperatures ranging from 180 to 200^0C utilizing 5 % zinc xanthates and presented in figure 3.4. The cure time study at different temperatures with varying alkyl chains of zinc xanthate in figure 3.4 gives comparison of the cure trend of zinc xanthates under investigation.

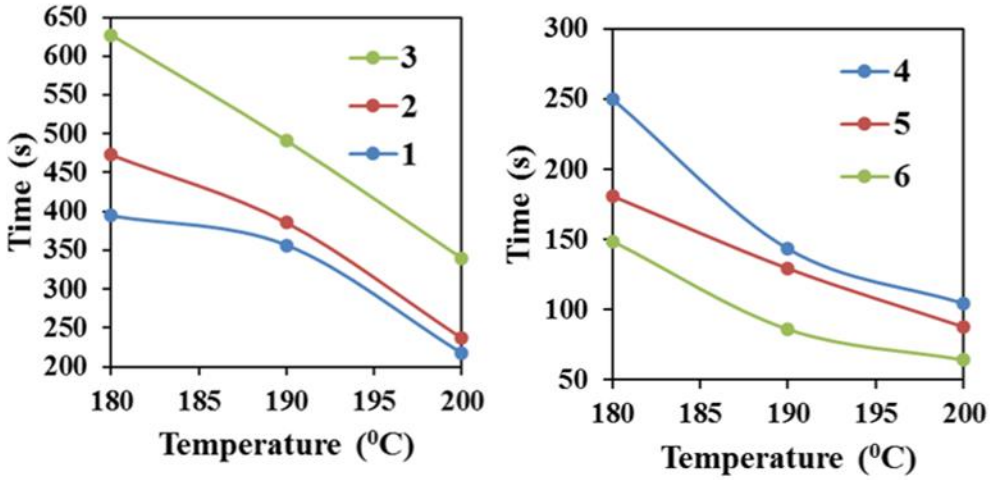

Figure 3.4: Cure time versus temperature with 5% zinc xanthates with linear alkyl chains (left) and branched alkyl chains (right) under investigation as catalysts.

This behavior of curing only after a particular temperature indicates the latent capability of zinc xanthates. As curing is observed only above 180 ^{0}C and no significant curing below 180 ^{0}C indicates that curing can be achieved only upon reaching threshold temperature. This Catalytic activity behavior wherein significant curing is initiated by the catalyst only upon providing optimum external stimuli can be attributed to the latent curing activity of zinc xanthates. The cure time trend by zinc xanthates with varying alkyl ligands at a particular temperature showed results in parallel to the order of thermal decomposition temperature as revealed by TGA of zinc xanthates. In case of linear alkyl zinc xanthates the cure time increased with increment in alky chain length following the order **1** < **2** < **3**. In contrast the cure time decreased with increase in alkyl chain length in the case of branched alkyl zinc xanthates following the order **4** > **5** > **6**. This situation is similar to the trend observed in the case of TGA. This trend can be explained based on our communication [21] where the mechanism of curing was reported to occur via the formation of metal sulfide. The epoxy resin composite including zinc xanthate upon thermal annealing yields in-situ catalytically active zinc sulfide which is responsible for cure initiation. Since in the case of the linear alkyl chain zinc xanthates by increase in alkyl chain length the thermal decomposition temperature enhanced. Therefore the increase in cure time at a particular temperature with increase in alkyl chain length can be observed as the time to decompose to form zinc xanthates gets enhanced with increase in alkyl chain length of zinc xanthates owing to higher decomposition temperature. On the other hand in case of branched alkyl chain zinc (II) xanthates the thermal decomposition temperature decreased with increment in alkyl chain length. This results in decrease in time to form zinc sulfide from zinc xanthate with increase in alkyl chain length therefore the decrease in cure time of epoxy composite at a particular temperature. This trend also explains the possible mechanism of curing of epoxy resin composite including metal xanthates via formation of in-situ formation of metal sulfides in the epoxy resin matrix.

3.7 XRD analysis of cured epoxy resin consisting of zinc xanthates

To further validate our results that the in-situ formed metal sulfide is responsible for curing of epoxy resin upon thermal annealing epoxy resin composite including zinc (II) xanthates, XRD analysis was also performed for the cured epoxy resin samples obtained by thermally annealing at 250 ^{0}C consisting of zinc (II) xanthates.

Figure 3.5 represents the XRD spectra of thermally annealed zinc (II) xanthates (20 % by mass) including epoxy resin composite. The XRD spectra of all the cured epoxy samples consisting of various zinc (II) xanthates under investigation confirm the presence zinc sulfide in the matrix. As the XRD analysis pattern of the cured epoxy resin including zinc xanthates consisted of similar peaks as presented in figure 3.3. In addition to the peaks similar to figure 3.3 an extra broad amorphous peak can be observed in the figure 3.5. This broad peak is due to the presence of amorphous cured epoxy resin. Thus the presence of zinc sulfide peaks in the cured epoxy composite matrix clearly indicates that the metal xanthate decomposition reaction to form metal sulfide in-situ in the polymer matrix leads to curing of epoxy resin.

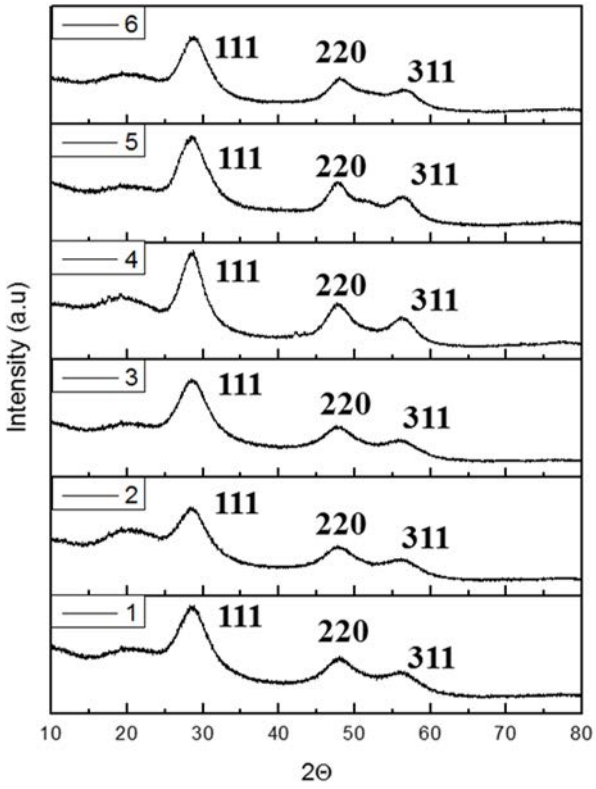

Figure 3.5: XRD analysis of cured epoxy resin consisting of Zinc xanthates with linear chains 1, 2, 3 and branched chains 4, 5, 6 after thermal annealing at 200 ^{0}C.

3.8 Conclusion

Linear and branched zinc (II) xanthates with varying chain length were synthesized and characterized by ^{1}H NMR, ^{13}C NMR, IR and elemental analysis. The thermal decomposition behavior was analyzed employing TGA under nitrogen atmosphere. In case of linear alkyl zinc xanthates with increase in alkyl chain length increase in thermal decomposition temperature was observed. In contrary with increase in chain length in case of branched alkyl zinc xanthates decrease in thermal decomposition temperature resulted. The formation of zinc sulfide as final product of thermal decomposition was confirmed by XRD analysis of thermally annealed zinc xanthates. Cure time at various temperatures was conducted and the results for curing of epoxy resin with various zinc xanthates followed the same trend as shown by the TGA of zinc xanthates. The cure time increased with increase in alkyl chain length in case of linear alkyl chain zinc xanthates while in the case of branched zinc (II) xanthates with increase in alkyl chain length decrease in cure time was observed. The formation of zinc sulfide in-situ in the epoxy resin matrix was confirmed by XRD analysis of the thermally annealed cured epoxy resin composite consisting of zinc xanthates indicating that the decomposition of zinc xanthate to zinc sulfide is probably responsible for curing of epoxy resin.

3.9 References

[1] G.A. Hope, K. Watling, R. Woods, Colloids and Surfaces A: Physicochemical and Engineering Aspects, 2001, 178, 157.

[2] J. He, K. Yee, Z. Xu, M. Zeller, A. D. Hunter, S. S. Chui, C. Che, Chemistry of materials, 2011, 23, 2940.

[3] Y. Li, X. Li, C. Yang, Y. Li, Journal of physics and chemistry B, 2004, 108, 16002.

[4] Pradhan N, Katz B, Efrima S, Journal of physical chemistry, 2003, 107, 13843.

[5] Xu K, Ding W, Material Letters, 2008, 62, 4437.

[6] Barreca D, Gasparotto A, Maragno C, Seraglia R, Tondello E, Venzo A, Krishnan V, Bertagnolli H, Applied Organometallic chemistry, 2005, 19, 59.

[7] Barreca D, Tondello E, Lydon D, Spalding TR, Fabrizio M, Chemical vapor deposition, 2003, 9, 93.

[8] J. R. Castro, K. C. Molloy, Y. Liu, C. S. Lai, Z. Dong, T. J. White, E. R. T. Tiekink, Journal of material Chemistry, 2008,18, 5399.

[9] D. Barreca, A. Gasparotto, C. Maragno, R. Seraglia1, E. Tondello, A. Venzo1, V. Krishnan, H. Bertagnolli, Applied Organometallic Chemistry, 2005, 19 (1), 59.

[10] N. Alam, M. S. Hill, G. Kociok-Köhn, M. Zeller, M. Mazhar, K. C. Molloy, Chemistry of materials, 2008, 20 (19), 6157.

[11] Whitmore WF, Lieber E, Industrail Engineering Chemistry, 1935,127.

[12] C. Zhang, S. Zhang, L. Yu, Z. Zhang, P. Zhang, Z. Wu, Materials Letters, 2012, 85, 77.

[13] A. A. Saboury, M. Alijnianzadeh, H. Mansoori-Torshizi, Acta biochimica polonica, 2007, 54 (1), 183.

[14] A. Fischereder, A. Schenk, T. Rath, W. Haas, S. Delbos, C. Gougaud, N. Naghavi, A. Pateter, R. Saf, D. Schenk, M. Edler, K. Bohnemann, A. Reichmann, B. Chernev, F. Hofer, G. Trimmel, Monatshefte für Chemie, 2013, 144 (3), 273.

[15] T. Rath, M. Edler, W. Haas, A. Fischereder, S. Moscher, A. Schenk, R. Trattnig, M. Sezen, G. Mauthner, A. Pein, Advanced Energy Materials, 2011, 1, 1046.

[16] D. Barreca, E. Tondello, D. Lydon, T. R. Spalding, M. Fabrizio, Chemical vapor deposition, 2003, 9(2), 93.

[17] Shiny Palaty, Rani Joseph, Journal of Applied Polymer Science, 2000, 78, 1769-1775.

[18] D. C. Onwudiwe, P. A. Ajibade, International Journal of Molecular Sciences, 2012, 13, 9502.

[19] S. H. Choi, K. An, E. G. Kim, J. H. Yu, J. H. Kim, T. Hyeon, Advanced Functional Materials, 2009, 19, 1645.

[20] P. An, Z. Liang, X. Xu, X. Wang, H. Jin, N. Wang, J. Wanga, F. Zhuc, RSC Advances, 2015, 5, 6879.

[21] Tarun Chand Vagvala, Shyam Sudhir Pandey, Yuhei Ogomi, Shuzi Hayase, RSC Advances, 2014, 4, 24658.

4. Effect of alkyl-metal xanthates with varying metals on the curing of epoxy resin

4.1 Introduction

From the parent potassium xanthate precursor by treating with soluble salts of metals, respective metal xanthates can be synthesized in aqueous solution [1, 2]. Properties of the metal xanthates are controlled by the alkyl ligand of metal-xanthates with same metal by varying alkyl ligands as discussed in the previous chapter. In this case, generated metal sulfide is always the same but physical properties like solubility, decomposition temperature etc. only can be fine-tuned. On the other hand, metal xanthates can also be prepared keeping the same alkyl chain as ligand and varying the metals under consideration. Properties of metal xanthates such as thermal decomposition temperature [3, 4], nature of metal sulfide formed upon thermal annealing and their properties [5, 6], stability and many other factors are determined by the metal ion of the xanthates [7]. The thermal decomposition temperature of gallium xanthate was observed to lower than decomposition temperature of copper (I) xanthate. 2, 2 - dimethyl-3-hexane zinc xanthate is stable while 2,2-diemthyl-3-hexyl gallium, indium and cadmium xanthates were found to be highly unstable. Several reports can be found in literature on the application of metal xanthates as precursors of metal sulfide. For instance metal xanthates were employed for the generation of metal sulfides layers used for fabrication of nanostructured hybrid polymer-inorganic solar cells [8]. Synthesis of metal sulfide nanoparticles $CuInS_2$ from a mixed complex of copper and indium metal xanthates by solvent thermolysis method [9]. Size controlled synthesis of CdS nanorods using cadmium xanthates by altering the reaction conditions such as reaction temperature, single-source precursor concentration and reaction time [10].

Since the properties are determined by the metal ion for the xanthate species with same alkyl ligand, influence of cure time at a given temperature utilizing various metal xanthates consisting of same alkyl ligand was investigated and compared. Even though from the previous study described in chapter 3 indicated that 2, 2-diemthyl-3-hexane zinc (II) xanthate as the most effective catalyst in curing of epoxy resin. As described earlier 2, 2-dimethyl-3-hexyl gallium, indium and cadmium xanthates were observed to be highly unstable and hence not suitable for the

study. Therefore, 2, 2 - dimethyl – 3-pentanyloxy ligand was chosen for the study as this species was able to form highly stable complexes with all the metals under investigation.

2,2 – dimethyl – 3-pentane copper (I), lead (II), antimony (III), zinc (II), cadmium (II), indium (III), gallium (III) xanthates were synthesized from 2,2-dimethyl-3-pentane potassium xanthate precursor as shown in the figure 4.1 and confirmed by ^{1}H NMR, ^{13}C NMR, IR and elemental analysis. The influence of metal ion on xanthates thermal behavior and decomposition temperature was studied by performing TGA analysis under nitrogen atmosphere for 2, 2-diemthyl-3-pentyl ligand based metal xanthates with varying metal ions. The final decomposition product upon thermal annealing of the metal xanthates under examination was characterized by employing XRD and SEM/EDS techniques. Investigation and comparison of curing time of epoxy composite at various temperatures employing 5% xanthate with varied metal ions as catalysts was also performed. The final post thermal annealed product of cured epoxy resin utilizing metal xanthates as catalysts was also characterized by XRD and SEM/EDS techniques.

4.2 Materials

Potassium tert-butoxide, carbon disulphide, zinc (II) chloride, cadmium (II) chloride, lead (II) nitrate, copper (II) chloride anhydrous were purchased from Wako Japan. Antimony potassium tartrate hydrate was purchased from Alfa Aesar. 2, 2 - dimethyl-3-pentanol and indium (III) chloride tetrahydrate were purchased from Sigma Aldrich, Japan. Anhydrous gallium (III) chloride was purchased from Tokyo Chemical Corporation, Japan. Epoxy resin (CNE200ELB65) and phenolic resin (BRG556) used in this work were supplied by Kyocera Company, Japan.

4.3 Synthesis and Characterization

Potassium xanthate (K-O-2,2-dimethyl pentan-3-yl-dithiocarbonate) was synthesized following the literature report [11].

Zinc (II) -O-2,2- dimethylpentan-3-yl- dithiocarbonate [4]

To an aqueous solution of zinc (II) chloride (1 g, 7 mmol) of potassium-O-2,2-dimethyl pentan-3-yl dithiocarbonate (3.71 g, 16 mmol) dissolved in water was added drop-wise while stirring at room temperature. A white precipitate formed was collected by suction filtration and washed with

methanol. The solid obtained was extracted into chloroform and recrystallized from methanol to obtain white powder (yield: 2.9 g, 89%).

^{1}H NMR (500 MHz, 26 ^{0}C, $CDCl_3$, δ): 4.92-4.98 (dd, 1H, CH), 1.79-1.72 (m, 2H, CH_2), 0.96-0.98 (m, 12H, 4 x CH3) ppm.

^{13}C NMR (125 MHz, 24 ^{0}C, $CDCl_3$, δ): 230.79 (CS_2O), 100.56 (CH), 35.88 (C (CH_3)), 25.95 (C (CH_3), 23.20 (CH_2), 10.96 (CH_2-CH_3) ppm).

IR (KBr pellet, cm^{-1}): 2965, 2875, 1468, 1367, 1236, 1129, 1056, 1033, 902.

Elemental analysis: Zn (II) $C_{16}H_{30}O_2S_4$ calculated: C 42.9%, H 6.76%, found: C 42.02%, H 6.55%.

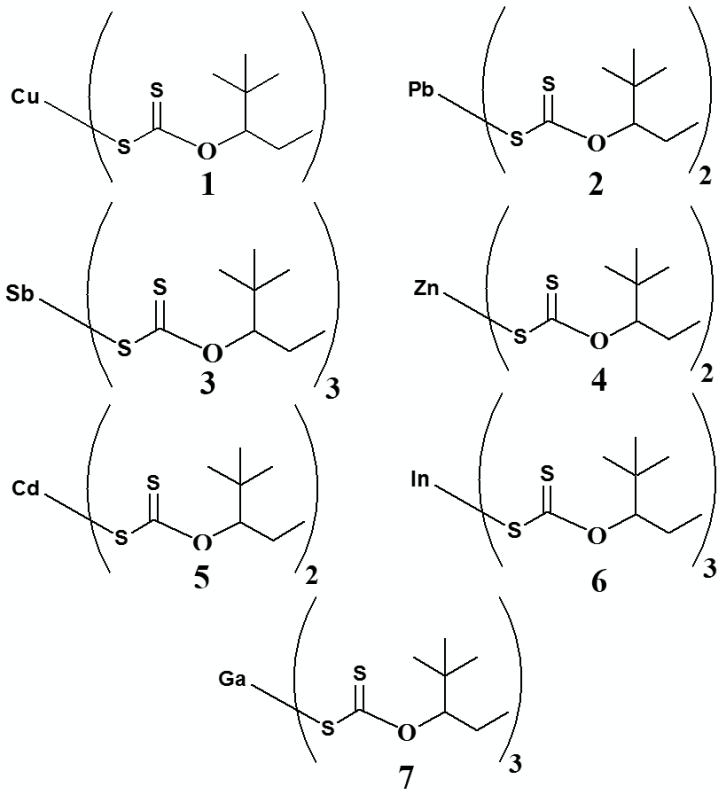

Figure: 4.1 Structure of metal xanthates under investigation.

Cadmium (II) -O-2, 2- dimethylpentan-3-yl dithiocarbonate [5]

An aqueous solution of potassium-O-2, 2-dimethylpentan-3-yl dithiocarbonate **1** (2.8 g, 15 mmol) was added drop wise to a solution of cadmium (II) chloride anhydrous (1 g, 6 mmol), while stirring at room temperature. A white precipitate resulted was collected by suction filtration and washed with methanol. The solid was recrystallized from methanol after extracting into chloroform (Yield: 2.4 g, 5 mmol, 87%).

^{1}H NMR (500 MHz, 26 ^{0}C, $CDCl_3$, δ): 4.98-5 (dd, 1H, CH), 1.70-1.79 (m, 2H, CH_2), 1-1.02 (m, 12H, 4 x CH3) ppm.

^{13}C NMR (125 MHz, 24 ^{0}C, $CDCl_3$, δ): 230.71 (CS_2O), 101.03 (CH), 35.90 (C (CH_3)), 25.12 (C (CH_3), 23.37 (CH_2), 11.14 (CH_2-CH_3) ppm).

IR (KBr pellet, cm^{-1}): 2965, 2874, 1468, 1365, 1230, 1130, 1029, 947, 902.

Elemental analysis: Cd (III) $C_{16}H_{30}O_2S_4$ calculated: C 38.81%, H 6.11%, found: C 38.48%, H 5.93%.

Lead (II) -O-2, 2- dimethylpentan-3-yl dithiocarbonate [2]

An aqueous solution of Lead (II) nitrate (1 g, 3.02 mmol) was added to an aqueous solution of Potassium-diemthylpentan-3-yl dithiocarbonate (1.53 g, 6.64 mmol) drop-wise and the solution was stirred for 2 h. The precipitate obtained was filtered and washed with methanol, dissolved in $CHCl_3$ and recrystallized in methanol to obtain the desired product as grey solid (yield: 1.3 g, 71%).

^{1}H NMR (500 MHz, 26 ^{0}C, $CDCl_3$, δ): 5.45-5.47 (dd, 1H, CH), 1.78-1.87 (m, 2H, CH_2), 1.04-1.01 (m, 12H, 4 x CH3) ppm.

^{13}C NMR (125 MHz, 24 ^{0}C, $CDCl_3$, δ): 229.51 (CS_2O), 94.11 (CH), 35.76 (C (CH_3)), 26.19 (C (CH_3), 23.08 (CH_2), 11.13 (CH_2-CH_3) ppm).

IR (KBr pellet, cm^{-1}): 2965, 2874, 1464, 1370, 1212, 1125, 1056, 1017, 904.

Elemental analysis: Pb (II) $C_{16}H_{30}O_2S_4$ calculated: C 32.58%, H 5.13%, found: C 32.47%, H 5.05%.

Antimony (IV) -O-2,2- dimethylpentan-3-yl dithiocarbonate [3]

Antimony chloride is insoluble in water, therefore, antimony potassium tartrate hydrate which is clearly soluble in water was employed [12]. To an aqueous solution of antimony potassium tartrate hydrate (1 g, 1.63 mmol), potassium-O-2,2-dimethylpentan-3-yl dithiocarbonate (1.20 g, 5.216 mmol) dissolved in water was added drop wise while stirring at room temperature. The mixture was centrifuged and washed with methanol. The solid obtained was extracted into chloroform and recrystallized from methanol to give yellow solid (yield: 0.78 g, 69 %).

^{1}H NMR (500 MHz, 26 ^{0}C, $CDCl_3$, δ): 5.37-5.35 (dd, 1H, CH), 1.78-1.71 (m, 2H, CH_2), 0.95-0.96 (m, 12H, 4 x CH3) ppm.

^{13}C NMR (125 MHz, 24 ^{0}C, $CDCl_3$, δ): 223.99 (CS_2O), 96.57 (CH), 35.93 (C (CH_3)), 26.05 (C (CH_3), 23.26 (CH_2), 11.04 (CH_2-CH_3) ppm).

IR (KBr pellet, cm^{-1}): 2965, 2872, 1462, 1369, 1212, 1131, 1053, 1043, 910.

Elemental analysis: Sb (III) $C_{24}H_{45}O_3S_6$ calculated: C 41.43%, H 6.51%, found: C 41.17%, H 6.28%.

Gallium (III) -O-2, 2- dimethylpentan-3-yl dithiocarbonate [7]

Gallium (III) -O-2, 2- dimethylpentan-3-yl dithiocarbonate was synthesized following our previously published work [13].

^{1}H NMR (500 MHz, 26 ^{0}C, $CDCl_3$, δ): 4.78-4.74 (dd, 1H, CH), 1.78-1.71 (m, 2H, CH_2), 1.02-0.89 (m, 12H, 4 x CH_3) ppm.

^{13}C NMR (125 MHz, 24 ^{0}C, $CDCl_3$, δ): 228.42 (CS_2O), 101.17 (CH), 35.94 (C (CH_3)), 25.94 (C (CH_3), 23.28 (CH_2), 10.97 (CH_2-CH_3) ppm).

IR (KBr pellet, cm^{-1}): 2965, 2873, 1462, 1364, 1252, 1129, 1058, 1027, 907.

Elemental analysis: Ga (III) $C_{24}H_{45}O_3S_6$ calculated: C 44.77%, H 7.0%, found: C 44.75%, H 6.9%.

Indium (III) -O-2,2- dimethylpentan-3-yl dithiocarbonate [6]

Indium (III) -O-2,2- dimethylpentan-3-yl dithiocarbonate with yield 6.18 g, 88 % was synthesized according to the literature report [14].

^{1}H NMR (500 MHz, 26 ^{0}C, $CDCl_3$, δ): 4.77-4.71 (dd, 1H, CH), 1.78-1.72 (m, 2H, CH_2), 1-0.99 (m, 12H, 4 x CH3) ppm.

^{13}C NMR (125 MHz, 24 ^{0}C, $CDCl_3$, δ): 228.79 (CS_2O), 104.47 (CH), 35.95 (C (CH_3)), 25.99 (C (CH_3), 23.33 (CH_2), 11.18 (CH_2-CH_3) ppm).

IR (KBr pellet, cm^{-1}): 2965, 2874, 1466, 1365, 1240, 1130, 1052, 948, 905.

Elemental analysis: In (III) $C_{24}H_{45}O_3S_6$ calculated: C 41.85%, H 6.59%, found: C 41.77%, H 6.38%.

Copper (I) -O-2,2- dimethylpentan-3-yl dithiocarbonate [1]

Copper (I) -O-2,2- dimethylpentan-3-yl dithiocarbonate with yield 2.84 g, 86 % was synthesized following the literature report [14]. Even though Copper (II) xanthate is theoretically expected to form due to unstable nature of copper (II) xanthate further undergoes reaction to form stable copper (II) xanthate as reported in the literature [15].

^{1}H NMR (500 MHz, 26 ^{0}C, $CDCl_3$, δ): 5.23-5.25 (dd, 1H, CH), 1.69-1.77 (m, 2H, CH_2), 0.94-0.91 (m, 12H, 4 x CH3) ppm.

^{13}C NMR (125 MHz, 24 ^{0}C, $CDCl_3$, δ): 230.18 (CS_2O), 98.72 (CH), 36.02 (C (CH_3)), 26.08 (C (CH_3), 23.20 (CH_2), 11.22 (CH_2-CH_3) ppm).

IR (KBr pellet, cm^{-1}): 2965, 2873, 1464, 1368, 1235, 1125, 1078, 1014, 898.

Elemental analysis: Cu (I) $C_8H_{15}OS_2$ calculated: C 37.71%, H 5.94%, found: C 37.92%, H 6.01%.

4.4 Thermogravimetric analysis

Thermogravimetric analysis under nitrogen atmosphere was used to investigate the thermal decomposition behavior of the different metal xanthates under investigation. The TGA plot shown in figure 4.2 portrays the thermal decomposition of metal xanthates in order **7** < **8** < **9** < **10** <**11** < **12** < **13**. The difference in decomposition can be attributed due to difference of bond strength among the metal xanthates under investigation determined by the nature of metal ion of the xanthate species. The TGA analysis confirms the thermal decomposition of metal xanthates starts at their threshold temperature but all of xanthates studied are stable from room temperature. This

indicates the latent capability of the metal xanthate under investigation to yield metal sulfides as they decompose only upon providing optimum external thermal stimuli.

A perusal of the Fig. 4.2 clearly indicates that after onset of the weight loss owing to the decomposition of corresponding metal xanthates, there is no further weight loss beyond about 200^{o}C. This could be attributed to the formation of corresponding metal sulfides after the thermal decomposition. A good agreement between the expected and observed residual weights after thermal annealing of metal xanthates confirms the formation of metal sulfides after thermal decomposition as shown in table 4.1.

Table 4.1 Thermogravimetric analysis of metal xanthates.

Metal xanthate	Expected residual weight (%)	Observed residual weight (%)	Product of decomposition
Cu (I) xanthate	37.4	36.2	CuS
Pb (II) xanthate	40.6	39.4	PbS
Sb (III) xanthate	48.8	47.3	Sb_2S_3
Zn (II) xanthate	21.7	22.5	ZnS
Cd (II) xanthate	29.1	30.1	CdS
In (III) xanthate	21.2	22.4	InS
Ga (III) xanthate	36.5, 15.7	97.1, 18	Ga_2S_3, GaS

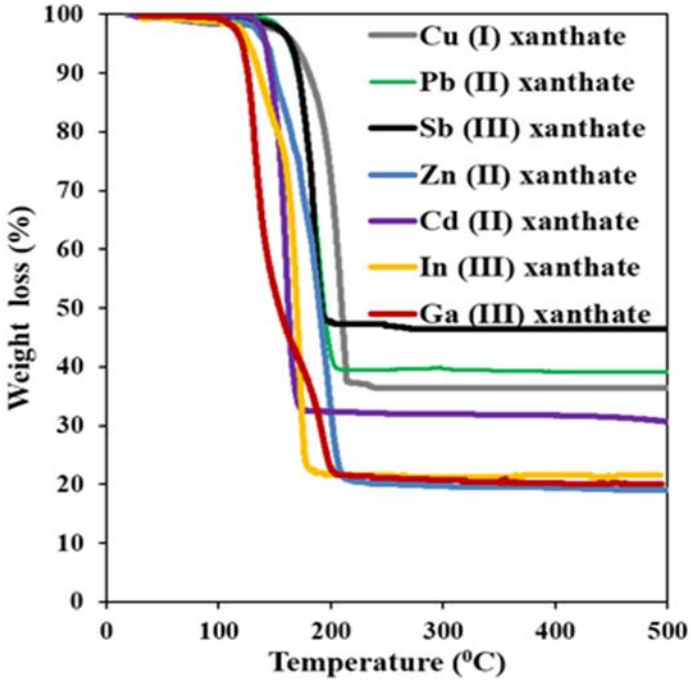

Figure 4.2 Thermogravimetric analysis curve of metal xanthates under investigation.

This reveals the latent property of metal xanthates to yield metal sulfides (figure 4.3) [16, 17] triggered by thermal heating after the threshold temperature. Amongst metal xanthates under investigation Ga (III) xanthate showed lowest decomposition temperature. Its TGA curve was found to be distinct from other metal xanthates indicates a two-step decomposition yielding GaS via formation of a metal stable Ga_2S_3 [18].

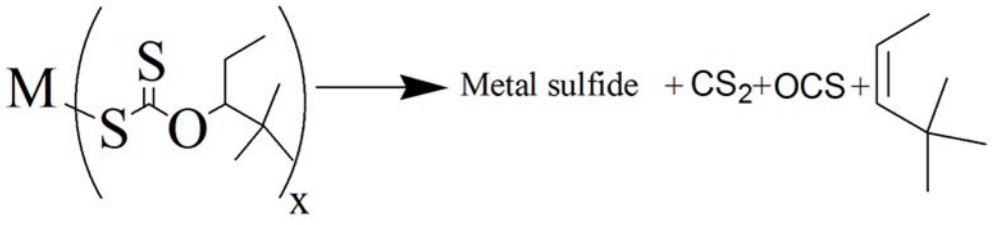

Figure 4.3 Thermal decomposition of metal xanthates under decomposition.

4.5 XRD analysis of thermally annealed metal xanthates

To confirm and characterize the metal sulfides obtained by thermal decomposition of metal xanthates, powder X-ray diffraction (XRD) was utilized.

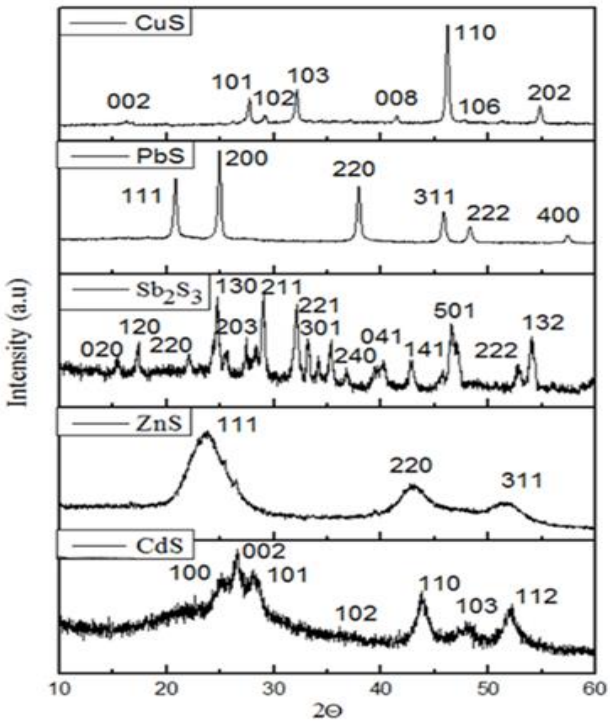

Figure 4.4: The XRD pattern of metal xanthates under investigation after thermal annealing at 200 ^{0}C.

All of the metal sulfides are obtained by thermal annealing of the corresponding metal xanthates at 200^{0}C for 15 min. Figure 4.4 shows the XRD patterns of CuS with hexagonal covellite structure (JCPDS No. 6-464) [19], PbS with cubic structure (JCPDS No. 78-1901), ZnS with zinc blende structure (JCPDS No. 80-0020) and CdS with wurtzite structure (JCPDS No. 80-0006) [20] and Sb_2S_3 with stibnite structure (JCPDS No. 06-0474) [21]. In (III) and Ga (III) xanthates resulted in an amorphous metals sulfides, therefore, energy dispersive X-ray spectroscopy (EDS) was employed to characterize the product of decomposition.

4.6 EDS analysis of thermally annealed Indium (III) and Gallium (III) xanthates

In (III) and Ga (III) xanthates resulted in an amorphous metals sulfides, therefore, energy dispersive X-ray spectroscopy (EDS) was employed to characterize the product of decomposition [22].

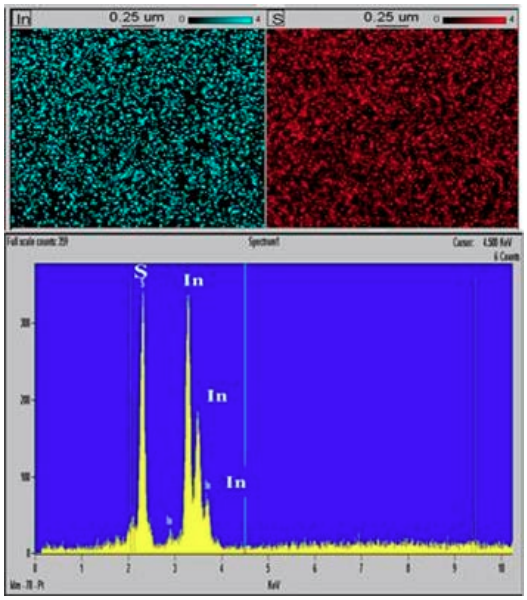

Figure 4.5: EDS spectra of In (III) xanthate after thermal annealing at 200 ^{0}C.

Figure 4.5 and 4.6 represents the EDS elemental mapping and spectra of the InS and GaS resulted from In (III) and Ga (III) xanthates, respectively upon thermal decomposition. The EDS spectra in figure 4.5 and 4.6 shows that the atomic ratio of In to S is 1:1.1 and Ga to S is 1:1.2 respectively. This confirms the final species formed by thermal decomposition of In (III) and Ga (III) xanthates as InS and GaS, respectively.

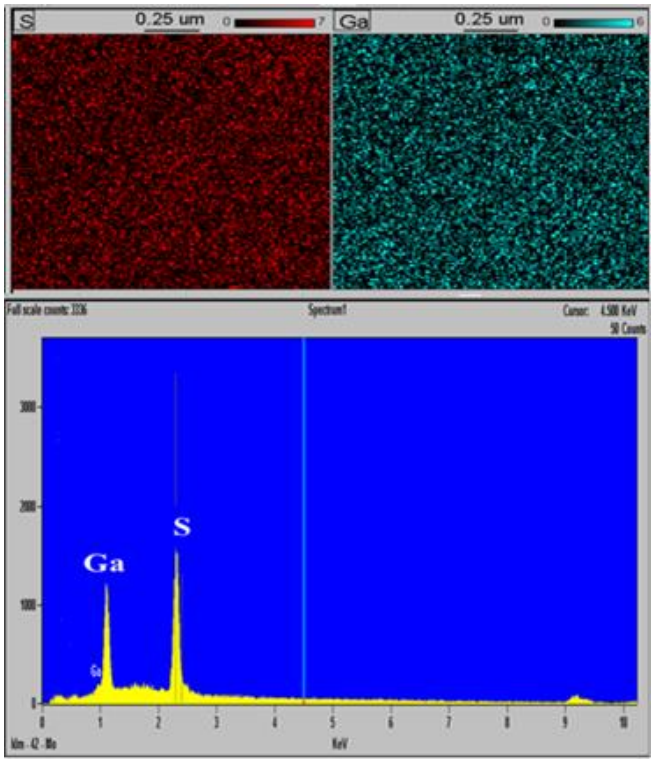

Figure 4.6: EDS spectra of Ga (III) xanthate after thermal annealing at 200 ^{0}C.

4.7 Curing of epoxy resin by metal xanthates

In order to investigate the use of different metal-xanthates as latent curing catalyst for the curing of the epoxy-resin, they were subjected for the gelation. Curing time at various temperatures was recorded for a mixture of 1:1 molar ratio of epoxy resin and phenolic resin after grinding homogenously and employing 5 % metal xanthates as catalyst. The temperature range used for curing studies was between 150 – 200 ^{0}C. It was observed that none of the metal xanthates showed significant curing below the temperature of 170^{0}C. This clearly reveals the latent capability of metal xanthates in the curing of epoxy resins. The curing time as a function temperature as shown in the Figure 4.7 indicate the curing ability of metal xanthates varies in the order **7** < **8** < **9** < **10** < **11** < **12** < **13**. Interestingly, the order of ability to cure the epoxy resin composite by metal xanthates is same as the order of decomposition temperature as revealed by TGA curve of metal xanthates to form metal sulfides supporting that the thermal decomposition

reaction of metal xanthates forming metal sulfide to be the probable mechanism for curing of epoxy resin composite.

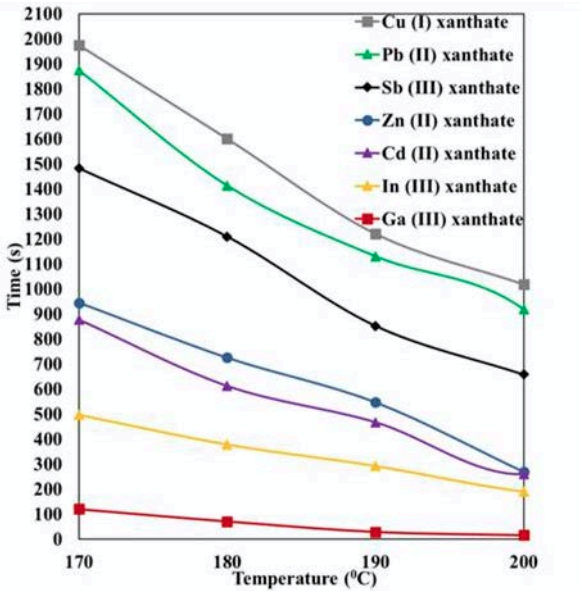

Figure 4.7: Cure time versus temperature study of 1:1 epoxy/phenolic resin with 5% metal xanthates under investigation as catalysts.

In addition, all of the metal xanthates used in this work exhibit thermal decomposition temperature beyond 170^0C, indicates that the metal sulfide formation may be responsible for curing of epoxy resin thus providing the latent catalytic property. This was further supported by the fact that metal sulfides formed upon thermal annealing beyond the threshold decomposition temperature as reported possess highly catalytically active surfaces [23]. The metal sulfides formed upon reaching threshold temperature while thermally annealing presumably is responsible for curing of epoxy resin composite consisting of metal xanthate [24]. Therefore, higher the decomposition temperature of the metal xanthates longer the time required for the formation of metal sulfide resulting in to prolonged time required for curing of epoxy resin composite. Ga (III) xanthate was found to be the most effective catalyst owing to the lowest decomposition temperature as reveled by the TGA curve among the employed metal xanthates. The energetically active metal stable state of Ga_2S_3 in addition may be responsible for further enhancement of catalytic efficiency of gallium xanthates.

4.8 XRD analysis of cured epoxy resin composite with metal xanthates

To confirm the curing of epoxy resin composite by metal xanthates via in-situ formation of metal sulfide upon thermal annealing, finally cured epoxy resin composite containing 20 % of metal xanthates was subjected for annealing at 200 ^{0}C followed by the XRD investigations. The XRD pattern of the final cured epoxy resin including metal xanthates shown in figure 4.9 confirms the formation of metal sulfides in-situ in the epoxy resin matrix as the XRD patterns matches well with the XRD of the metal sulfides obtained by thermal decomposition of only metal xanthates shown in figure 4.4.

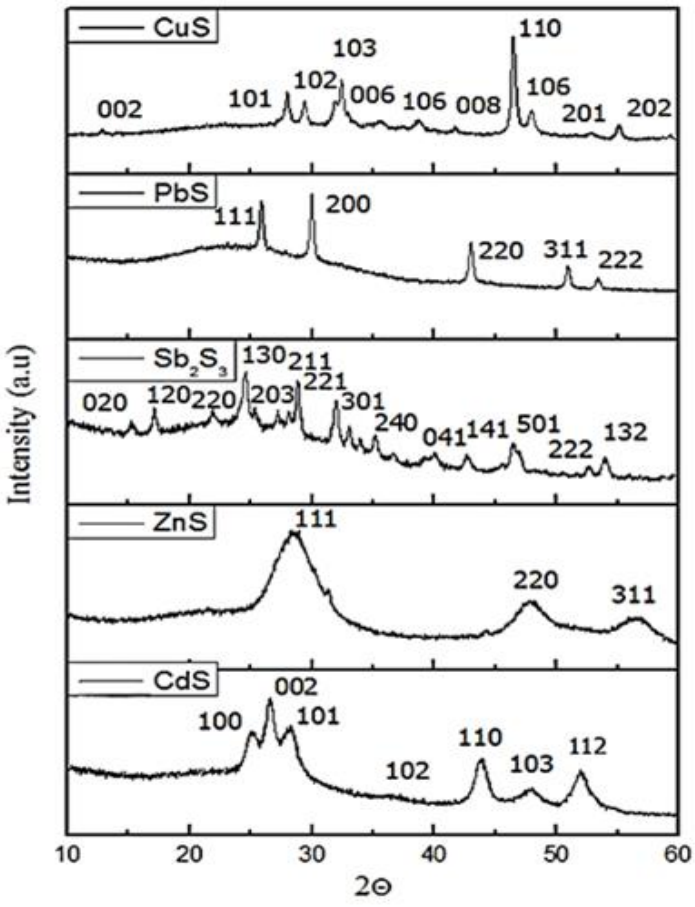

Figure 4.8: The XRD pattern of cured epoxy resin consisting of metal xanthates after thermal annealing (in-situ) at 200 ^{0}C.

4.9 EDS analysis of cured epoxy resin composite including indium (III) and gallium (III) xanthates

It has been explained earlier that In (III) and Ga (III) xanthates annealed at 200^{0}C, yielded amorphous metal sulfides, therefore, EDS was utilized to analyze the finally cured epoxy resin composite which was subjected to curing by 20 % In (III) and Ga (III) xanthates as catalysts.

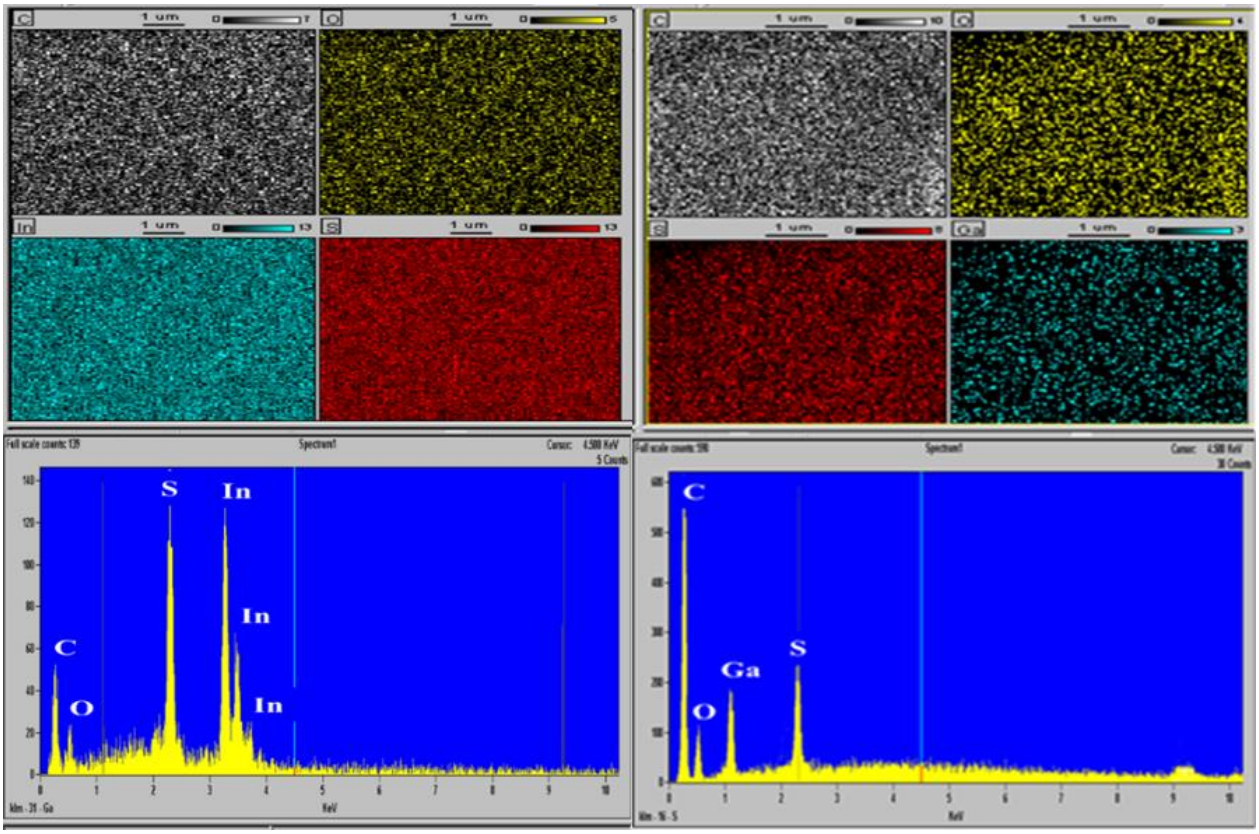

Figure 4.9: The EDS spectra of cured epoxy resin consisting of In (III) xanthate (left) and Ga (III) xanthate (right) after thermal annealing at 200^{0}C.

Both of the formulations based on and In and Ga xanthates with epoxy resin were cured by thermal annealing at 200 ^{0}C for 20 min. The EDS spectra of cured epoxy resin including In (III) and Ga (III) xanthate respectively by thermal annealing presented in Figure 4.9. The similarity between the EDS shown in the figure 4.9 with that of the EDS spectra obtained for the thermally decomposed product of the In (III) and Ga (III) xanthates alone (Fig. 4.5 and 4.6) confirms the in-situ decomposition of In (III) and Ga (III) xanthates into InS and GaS in their

respective composites. At the same time, generalized representation of in-situ generation of metal sulfide during curing process is also shown in the figure 4.10.

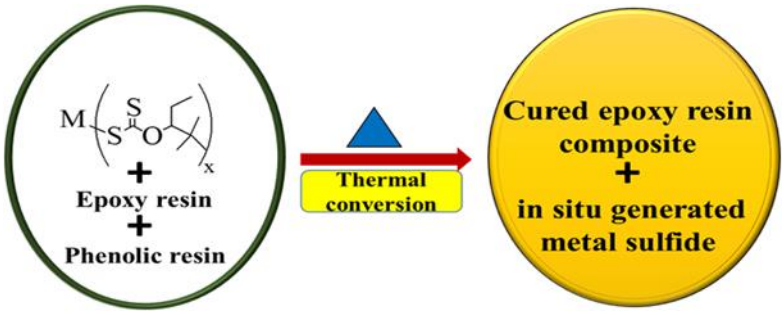

Figure 4.11: Curing of epoxy resin utilizing metal xanthates as curing catalysts.

4.10 Conclusion

Metal xanthates with 2, 2 - dimethyl-3-pentyl ligand were synthesized and characterized owing to their capability of forming stable xanthate precursor with various metals. Their thermal decomposition behavior and final product of thermal decomposition was analyzed by TGA. A perusal of TGA thermograms for various metal xanthates and analysis of the residual mass after the onset of decomposition indicated that final product upon thermal decomposition as corresponding metal sulfides. The metal sulfides obtained were characterized by XRD and EDS techniques. Curing time of epoxy resin composite at various temperatures utilizing various metal xanthates as catalysts was studied and their curing ability was compared. In-situ metal sulfide formation in the cured epoxy resin matrix after thermal annealing was characterized by XRD and EDS techniques. Since curing by the metal xanthates was observed only beyond 170^0C and the order of curing by metal xanthates followed the same order as their thermal decomposition temperatures. Amongst various metal xanthates in this work for the curing of the epoxy resin, Ga (III) xanthate was found to exhibit the best catalytic property. It can be concluded that the active catalytic surface of the metal sulfide formed in-situ in the epoxy resin matrix upon reaching the thermal decomposition temperature instigates curing of epoxy resin.

Reproduced by permission of Elsevier publications © from my publication (Reference no 13)

4.11 References

[1] N. Pradhan, S. Efrima, Journal of American chemical society, 2003, 125, 2050.

[2] D. P. Dutta, G. Sharma, Materials Letters, 2006, 60, 2395.

[3] M. A. Khwaja, T. J. Cardwell, K. J. Magee, Analytica Chimica Acta, 1973, 64, 9.

[4] D.P. Dutta, G. Sharma, A.K. Tyagi, S.K. Kulshreshtha, Materials Science and Engineering B 138 (2007) 60.

[5] M. A. Malik, M. Afzaal, P. O'Brien, Chemical Reviews, 2010, 110, 4417.

[6] N. Pradhan, B. Katz, S. Efrima, Journal of Physical Chemistry, 2003, 107, 13843.

[7] N. Alam, M. S. Hill, G. Kociok-Kohn, M. Zeller, M. Mazhar, K. C. Molloy, Chemistry of Materials, 2008, 20, 6157.

[8] H. C. Leventis, S. P. King, A. Sudlow, M. S. Hill, K. C. Molloy, S. A. Haque, Nano Letters, 2010, 10, 1253.

[9] D. P. Dutta, G. Sharma, Materials Letters, 2006, 60, 2395.

[10] Y. Li, X. Li, C. Yang, Y. Li, Journal of material chemistry, 2003, 13, 2641.

[11] T. Rath, M. Edler, W. Haas, A. Fischereder, S. Moscher, A. Schenk, R. Trattnig, M. Sezen, G. Mauthner, A. Pein, Advanced Energy Materials, 2011, 1, 1046.

[12] L. Wua, H. Xub, Q. Hana, X. Wang, Journal of Alloys and Compounds, 2013, 572 (25), 56.

[13] Tarun C. Vagvala, Shyam S. Pandey, Yuhei Ogomi, Shuzi Hayase, Inorganica Chimica Acta, 2015, 435C, 292.

[14] A. Fischereder, A. Schenk, T. Rath, W. Haas, S. Delbos, C. Gougaud, N. Naghavi, A. Pateter, R. Saf, D. Schenk, M. Edler, K. Bohnemann, A. Reichmann, B. Chernev, F. Hofer, G. Trimmel, Monatshefte für Chemie, 2013, 144 (3), 273.

[15] S. Dowland, T. Lutz, A. Ward, S. P. King, A. Sudlow, M. S. Hill, K. C. Molloy, S. A. Haque, Advanced materials, 2011, 23 (24), 2739.

[16] N. O. Boadi, M. A. Malik, P. O'Brien, J. A. M. Awudzab, Dalton Transactions, 2012, 41, 10497.

[17] A. Keys, S. G. Bott, A. R. Barron, Chemistry of materials, 1999, 11 (12), 3578.

[18] C. Wu, S. H. Yu, M. Antonietti, Chemistry of materials, 2006, 18, 3599.

[19] S. H. Choi, K. An, E. G. Kim, J. H. Yu, J. H. Kim, T. Hyeon, Advanced Functional Materials, 2009, 19, 1645.

[20]. J. Rodriguez‐Castro, M. F. Mahon, K. C. Molloy, Chemical Vapor Deposition, 2006, 12, 601.

[21] C. Liang, Y. Shimizu, T. Sasaki, H. Umeharab, N. Koshizaki, Journal of Material Chemistry, 2004,14, 248-252.

[22] D. Mondal, G. Villemure, G. Li, C. Song,J. Zhang, R. Hui, J. Chen, C. Fairbridge, Applied Catalysis A: General, 2013, 450, 230.

[23] S. K. Yadav, P. Jeevanandam, Ceramics International, 2015, 41, 2160.

[24]J. Kundu, D. Pradhan, ACS applied materials & interfaces, 2014, 6, 1823.

5. Investigation with gallium (III) xanthate and standard commercial catalyst

5.1 Introduction

In the 3rd chapter we have employed metal-xanthates using Zn as representative metal to explore their possibility in the curing of epoxy resin. It was found that amongst various alkyl substituents 2,2-dimethy-pentyl branched alkyl chain as ligand was best owing to formation of stable xanthates with various metals. This made the foundation of 4th chapter to explore the nature of metals on the performance of their curing behavior of epoxy resin and concluded that Ga was the best giving not only the latent catalytic behavior but shortest time taken for the curing also. To further analyze and understand the curing of epoxy resin employing metal xanthates as catalysts, it is vital to compare the catalytic activity and cure kinetics with that of the standard commercial catalyst. To assist this study, a commercial epoxy curing catalyst UCAT3512T was also employed. The cure time trend with varying temperature, cure kinetic analysis and shelf life study was utilized to compare the curing process of epoxy resin by our best performing Ga (III) xanthate with that of commercial catalyst UCAT3512T.

From the cure time study as a function of temperature, latent capability of both the catalytic formulations can be compared. If the catalyst formulation exhibits cure over a broad rather than a narrow range of temperatures then the catalyst cannot be favored as a latent catalyst. As a broader temperature range means no control over the curing conditions and facilitates premature curing [1]. Although curing of epoxy resin was conducted at various temperature as a function of time, but this cure-time investigation alone is not sufficiently enough to completely analyze the curing behaviors. Information such as degree of cure, reaction rate and kinetic model for mechanism which are very much necessary cannot be obtained without performing the curing kinetics. The study of the cure kinetics facilitates precise understanding of the curing process for determining the optimal processing parameters that assure the highest productivity rate along with satisfactory product properties [2]. Curing kinetics allows to compare the curing behavior of different compositions utilizing different matrices, catalysts, fillers and additives [3]. The curing parameters such as degree of cure and reaction rate influences the physical properties and processability of cured epoxy resins and these in turn are dependent on curing conditions such as curing time and

temperature [4]. Curing of epoxy resins is an activated process and differential scanning calorimeter (DSC) is popularly used to elucidate the key cure process parameters [5]. Another pertinent aspect of curing catalyst for epoxy composite is its shelf-life [6]. A longer pot-life for a given formulated mixture consisting of catalyst contributes potential benefits such as facile transportation [7], ease of storage [8], easy handling of cure processing and reducing the overall process cost in the production line [9].

Since 2,2- dimethyl- 3-pentyl gallium (III) xanthate showed the most efficient catalytic properties compared to all other metal xanthates under investigation, Ga (III) xanthate was chosen for further in-depth investigation of the curing of epoxy resin and comparing its performance with that of a commercial catalyst. This section gives the cure time study comparison of gallium (III) xanthate as a latent catalyst with that of standard commercial catalyst UCAT3512T. Further characterization of the cured epoxy resin consisting of gallium (III) xanthate as catalyst was performed by electronic absorption and EPMA analysis. The kinetics of curing for both of the catalyst systems were investigated and analyzed by non-isothermal differential scanning calorimetric (DSC) technique. To calculate the activation energy, DSC data under dynamic conditions was applied to Kissinger's [10] and Flynn-Wall-Ozawa methods [11]. Using the activation energy obtained by Flynn-Wall-Ozawa method [12], the conversion rate and conversion degree with respect to the temperature was determined for the entire range of curing. The kinetic model of the curing process was evaluated by employing Friedman method [13]. Finally the shelf-life study of the epoxy composite formulation including catalyst for a period of 6 months was also conducted.

5.2 Materials and methods

Standard commercial catalyst UCAT3512T, epoxy resin (CNE200ELB65) and phenol (BRG556) used in this work were kindly supplied by Kyocera Company, Japan. A 1:1 mixture of phenol and epoxy resin with varying concentration of both of the commercial catalyst and Ga (III) xanthate was employed for detail investigations pertaining comparative curing behavior, shelf-life by storing at room temperature and curing kinetics.

5.3 Curing of epoxy resin by gallium (III) xanthate and standard commercial catalyst

Curing of epoxy resin as a function of time was investigated by varying temperature in the temperature range 150 to 200^{0}C. A 1:1 molar ratio of epoxy resin and phenol was grinded homogenously with the 5% of respective catalysts and curing time at various temperatures was recorded. The curing time versus temperature plot is presented in figure 5.1. 5% Ga (III) xanthate cured the epoxy resin composite within 39 s at 200^{0}C while it was 34 s for the standard commercial catalyst UCAT3512T. A decrease in curing time with increase in temperature was observed for both the catalysts. Nevertheless curing beginning at lower temperature and over the broad temperature range by UCAT3512T. On other hand, there was no curing below 150^{o}C and significant curing was observed only after an optimum temperature of 170^{0}C in case of Gallium (III) xanthate. This clearly emphasises the efficient latent curing catalytic activity of Ga (III) xanthate over standard catalyst, since the curing was initiated in the former case only upon reaching a threshold specific temperature range. On the other hand in the latter case curing was observed over a broad range of temperatures thus reducing the latent potency of this catalyst.

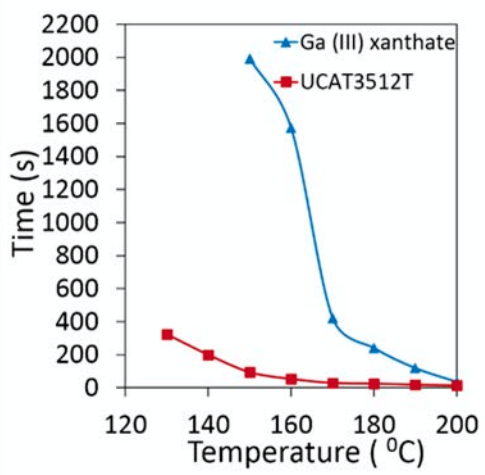

Figure 5.1 Curing time versus temperature with 5% catalyst content for the 1:1 epoxy/phenolic resin.

5.4 Electronic absorption spectroscopic study

To further confirm the mechanism of curing of gallium xanthate via in-situ decomposition reaction forming gallium sulphide, electronic absorption spectral study was conducted. Electronic absorption spectroscopic measurement was performed for two different temperatures viz., below the curing temperature (120^0C) and above the optimum curing temperature (200^0C) for 1:1 molar ratio of Epoxy resin/phenol composite films made on glass substrate. In either of the cases of temperature under investigation, no absorption peak was observed for the films without xanthate catalyst. On the other hand, for the film containing Ga (III) xanthate baked at 200^0C absorption in the range from 380 to 420 nm was observed which was absent for the film baked at 120^0C (Figure 5.2). It is reported that electronic absorption in this wavelength region is exhibited by gallium sulphide confirming the thermal decomposition of gallium (III) xanthate precursor film baked at 200^0C forming gallium sulphide [14].

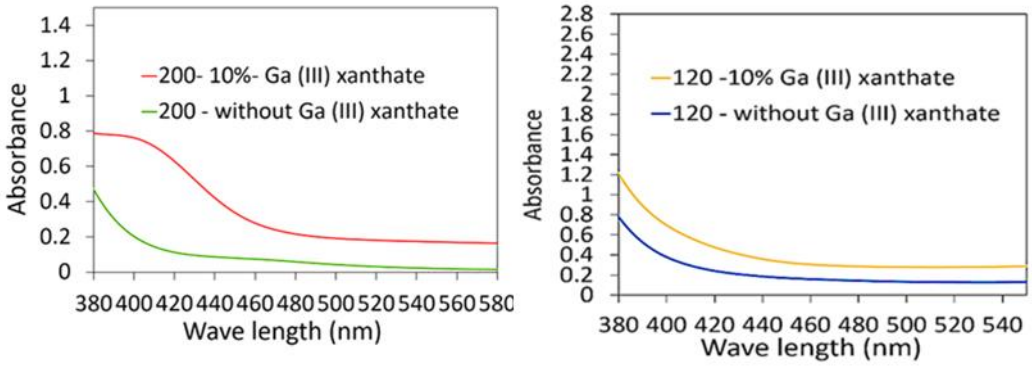

Figure 5.2: Electronic absorption spectra of epoxy composite in the presence and absence of Ga (III) xanthate baked at and 200 ^{0}C (left) and 120 ^{0}C (right) .

Rath et.al, has reported about formation indium sulphide upon the thermal decomposition of Indium (III) xanthate confirmed and the decomposition mechanism also [15] which was also characterized by electronic absorption studies to be Indium sulphide as reported by Malik et al [16]. Therefore, gallium xanthate is also expected to yield the gallium sulphide from the gallium xanthate in the similar fashion since both belongs to the same family in the periodic table. Further confirmation for the formation of gallium sulphide was also made in this work by estimation of optical band gap (Eg) from the analysis of optical absorption spectrum utilizing Tauc plot which

is basically plot of $(\alpha hv)^n$ vs. hv and has been used extensively for the characterization of optical properties of amorphous semiconductors [17] [18]. This value of n varies depending the materials e.g. it is ½ for direct band gap while 2 for indirect band gap semiconductors. Since gallium sulphide is reported to have indirect band gap [19] Tauc plot in the form of $(\alpha hv)^2$ vs. hv was used to calculate its optical band gap as shown in the Fig. 5.3.

Eg was estimated by linear extrapolation as shown by the dotted line. It has been reported that gallium sulphide and indium sulphide belong to the class of wide band gap semiconductor having the band gap in the region about 3.4 eV and 2.2 eV, respectively [20, 21]. Since gallium sulphide formed was non-homogenously distributed in the resin matrix, and lack of exact thickness of gallium sulphide, value of absorbance (A) was used in place of (α) as representative for the Eg calculation. Based on the electronic absorption spectrum for 5 % gallium sulphide in the epoxy resin film shown in the figure 5.3, optical band gap was calculated by Tauc plot and was found to be about 3.2 eV. This indicates the formation of gallium sulphide after thermolysis of gallium (III) xanthate at 200 ^oC in the epoxy resin composite. This clearly indicates that the gallium (III) present in the matrix of epoxy composite decomposes in-situ to form gallium sulphide probably is the cause for curing of epoxy resin.

5.5 Electron probe microanalysis (EPMA) study

As discussed in the previous chapters that gallium sulfide formed after thermal decomposition was amorphous in nature and difficult to characterize it by XRD spectra. Therefore, EPMA was conducted for the product obtained after annealing Ga (III) xanthate at 200 ^0C to confirm the mechanism of curing by formation of in-situ formed gallium sulfide upon thermal annealing. The EPMA image with mapping of Ga and S (figure 5.4) shows that gallium and sulfur both are present at the same place. At the same time analysis of their atomic abundance clearly reveals that they are present in the ratio of 2:1 which gives an atomic stoichiometry of 1:1 indicating the formation of gallium sulfide (GaS).

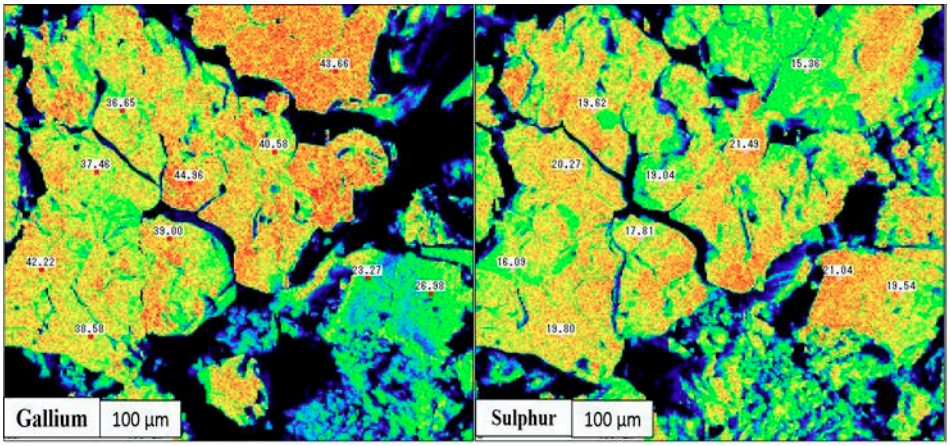

Figure 5.4: EPMA micrograph with elemental distribution mapping for Ga (III) xanthate after annealing at 200 ^{0}C. Left mapping for Ga while right mapping for S.

5.6 Differential scanning calorimetric analysis

It has been widely accepted that curing of the epoxy resins by conventional catalysts is activated process and this activation energy for curing was determined using the differential scanning calorimetric (DSC) analysis [22]. The reaction mixture was cured in DSC under non-isothermal conditions at heating rates of 5, 10, 15 and 20^{0}C min^{-1} in the temperature range from 30 ^{0}C-300^{0}C under constant flow of nitrogen with flow rate of 10 ml min^{-1}. A 1:1(w/w) ratio of epoxy resin and phenolic resin composite with 5 % catalyst was used for the DSC study in an aluminium cell. An identical empty cell was taken as reference. The heat flow data, as a function of temperature and time, were obtained using the area under the peak of the exotherm. DSC curves at different heating rates for 5% Ga (III) xanthate and 5% UCAT3512T compositions are presented in figure 5.5. DSC thermograms reveal a single exothermic peak associated with gelation (crosslinking) of the epoxy resin composite for both of the catalyst compositions.

It is interesting to note that in the case of both UCAT3512T and Ga (III) xanthate catalysts, it takes 3.5 min to complete the cross-linking when dynamic DSC was run at the scan rate of 20 ^{0}C/min. It is clear that exotherms shift towards higher temperatures as a function of heating rate. Compared to standard catalyst, the composite including Ga (III) xanthate shows an overall higher onset temperature. The peak temperature values which determine the nature of curing at various heating rates for both of the catalytic compositions are shown in table 5.1. The values shift to

higher temperatures as the heating rate increases. The increase in peak values with increasing heating rate is due to shortened reaction time with higher heating rate.

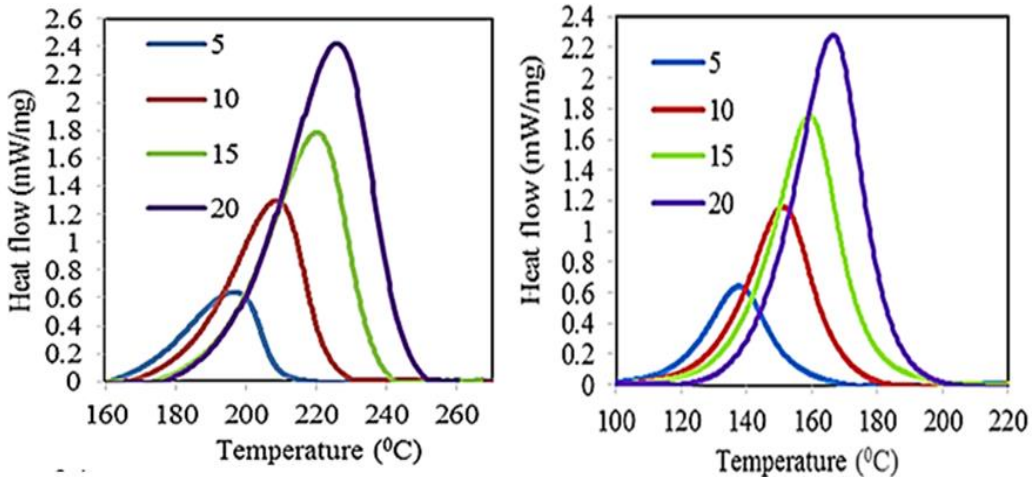

Figure 5.5: Dynamic DSC thremograms for curing of epoxy composite consisting of Ga (III) xanthate (left) and commercial standard catalyst UCAT3512T (right) at different heating rates (^{0}C/min).

It has been explained that exothermic peak appeared in the DSC thermogram is associated with the curing of epoxy resin but one can argue that whether curing has reached to completion or not after the end of one DSC thermal cycle.

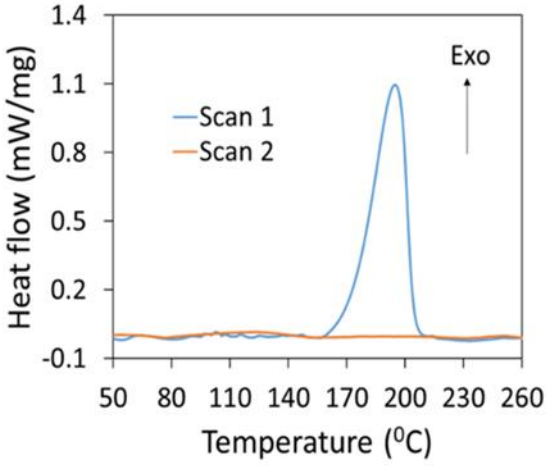

Figure 5.6: Differential scanning calorimetric analysis curves for curing of epoxy composite consisting of 5% Ga (III) xanthate at 10 ^{0}C/min heating rate. Scan 1: First scan from 30 ^{0}C to 300 ^{0}C. Scan 2: A repeated scan from 30 to 300 ^{0}C for the same sample used for first scan.

To verify completion of curing using gallium xanthate, a second DSC run (figure 5.6) was repeated after the completion of first DSC cycle (heating rate 10^0C min^{-1}) for the same sample at the same heating rate in the similar temperature range of 30-300^{o}C. The absence of the exothermic peak in the second DSC run cycle unlike in the first scan confirms that curing of the resin was completed.

5.6.1 Dynamic kinetic methods

Kinetic characterization of epoxy resin curing in terms of curing rate, temperature dependence of curing and energy of activation are of fundamental importance in understanding the structure, property and processing relationships of thermoset resins. The dynamic and isothermal methods have been widely used for detailed understanding of the cure kinetics. The advantage of utilizing the dynamic methods over isothermal methods in determining the cure kinetic parameters lies in the fact that a prior knowledge of the reaction mechanism is not required in order to quantify kinetic parameters [23]. A very widely implemented Flynn-Wall-Ozawa and Kissinger's methods were employed to determine the activation energy (Ea) in the present investigation before discussing the kinetic model in detail.

5.6.2 Flynn-Wall-Ozawa method

The integral form of the rate equation by Flynn-Wall-Ozawa method [24] is generally expressed as

$$\log \beta = \mathrm{A`} - 0.4567 \frac{E_a}{RT} \quad \text{---------- (1)}$$

$$\mathrm{A`} = \log \frac{\mathrm{AE}_a}{g(\alpha)R} - 2.315 \quad \text{---------- (2)}$$

where, β is heating rate, E_a is activation energy, T is temperature, R is ideal gas constant, A is pre-exponential factor, g(α) is an integrated form of the reaction model. Assuming that the degree of conversion is independent of the heating rate at the peak temperature [25], plot of log β versus $1/T_p$ (peak temperature) gives a straight line with a slope of $-0.4567E_a/R$ leading to the estimation of E_a from the Ozawa plot.

5.6.3 Kissinger`s method

Kissinger's method has been widely used for the investigation of curing of epoxy resins in order to estimate the kinetic parameters such as E_a and A from dynamic DSC data. At the peak temperature where, the rate of curing is maximum [25] activation energy can be obtained by utilizing the following equation 3.

$$\ln\left(\beta/T_2\right)^2 = \ln\left(AR/E_a\right) - E_a/RT_p \quad \text{-------- (3)}$$

Eq. 3 indicates that by plotting $\ln(\beta/T_p)^2$ against 1/Tp, we can estimate E_a and A from slope of the linear fit and intercept at the Y-axis, respectively [26]. Linear plots by Flynn-Wall-Ozawa method and Kissinger`s method applying at the maximum rate of conversion for both of the catalyst systems are shown in figure 5.7. Activation energy obtained by both the catalyst formulations are shown in table 5.1. The values obtained by Kissinger's method are similar to Flynn-Wall-Ozawa method even though slightly lower. This behavior is in accordance with the literature reports on curing kinetics [27]. Activation energy is the energy barrier required to overcome the curing reaction to proceed. Since the activation energy of Ga (III) xanthate is higher than that of the standard catalyst UCAT3512T, it can be concluded that the former possess better latent catalytic activity than the later.

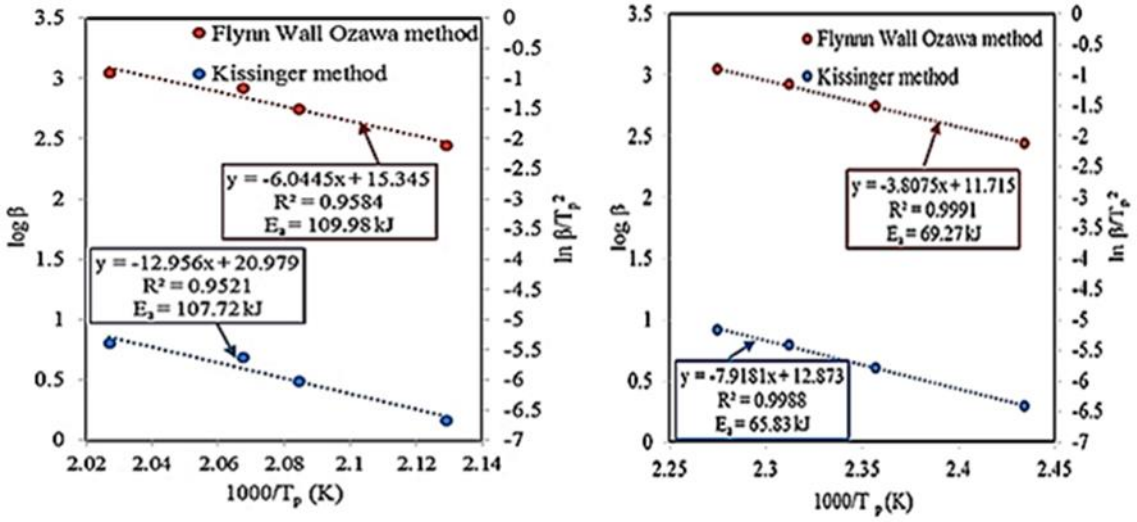

Figure 5.7: Ozawa and Kissinger's plot for curing of epoxy resin composite utilizing 5% of catalysts Ga (III) xanthate (left) and 5% UCAT3512T (right).

Table 5.1:Kinetic parameters for curing reaction of 5% Ga (III) xanthate and 5% UCAT3512T epoxy resin composites.

Curing agent (5% by mass)	Heating rate [^{0}C / min]	Peak temperature (^{0}C)	Activation energy Flynn-Wall-Ozawa method (kJ)	Activation energy Kissinger's method (kJ)
Ga (III) xanthate	5	196.51	109.98	107.72
	10	206.55		
	15	210.51		
	20	220.17		
			69.27	65.83
UCAT3512T	5	137.70		
	10	151.17		
	15	159.36		
	20	166.49		

5.7 Non isothermal kinetic modeling and mechanism

Non-isothermal methods have been widely used for detailed understanding of the cure kinetics. The advantage of utilizing non-isothermal methods over isothermal methods in determining the cure kinetic parameters lies in the fact that a prior knowledge of the reaction mechanism is not required in order to quantify kinetic parameters. Constitutive modeling equations for the cure kinetics of epoxy resins fall under two general categories: n^{th}-order and autocatalytic [28]. In case of n^{th}-order model conversion rate is proportional to concentration of unreacted material. The reaction rate is dependent only on the amount of unreacted material remaining and the reaction products does not involve in the reaction [29]. For instance the formation of cured polymer poly [(phenylsilylene) propargyl–hexafluorobisphenol-A] prepared by dehydrogenative coupling reaction between hexafluoro-bisphenol A and phenylsilylene in the presence of $LiAlH_4$ was reported to follow n^{th} order Kinects [30]. On the other hand autocatalyzed model assumes that at least one of the reaction products is involved in propagating the reaction and characterized by maximum degree of conversion [31] between 20 and 40%. The cure kinectic model of epoxy-

hexaanhydro-4-methylphthalicanhydride system obtained by reaction of diglycidyl ether of bisphenol-A, hardener hexahydro-4-methylphthalic anhydride and tertiary amine 2,4,6-Tris (dimethylaminomethyl)phenol was reported to follow autocatalytic mechanism [32]. To predict the cure kinetics over the whole range of conversion for the current study, the analysis by isoconversioanl Friedman method was employed for non-isothermal dynamic DSC data.

5.7.1 Friedman method

This method is one of the isoconversional methods based on assumption that kinetic parameters E_a and A vary with extent of the reaction [33]. The Friedman method is based on the following equation.

$$\frac{d\alpha}{dt} = q\frac{d\alpha}{dT} = kf(\alpha) \quad \text{---------- (4)}$$

Where, f(α) function is degree of reaction model, k is rate constant and is a function of temperature. dα/dt is the reaction rate. Friedman's isoconversioanl method relates the logarithm of reaction rate to the inverse of temperature for a given cure degree. By introducing Arrhenius equation [34]. The Friedman equation can be rearranged as follows:

$$\ln\frac{d\alpha}{dt} = \ln q\frac{d\alpha}{dT} = \ln[Af(\alpha)] - \frac{E_a}{RT} \quad \text{---------- (5)}$$

The plots of curing conversion rate as a function temperatures for both the catalytic systems is presented in figure 5.8. In either of the cases the peak maxima advanced with increasing heating rate. This behavior was very similar to dynamic DSC thermograms at different rates as shown in the figure 5.5. The values of these curing reaction rates at different temperatures were utilized to estimate ln [Af(α)] values as shown in equation (5).

5.7.2 Reaction rate

Reaction rate can be obtained from non-isothermal DSC data using the following equation.

$$\frac{d\alpha}{dt} = \frac{dH/dt}{H_{tot}} \quad \text{--------- (6)}$$

Where, dH/dt is given by the peak height of the DSC thermogram at time t, H_{tot} is the total heat of reaction for complete curing [35].

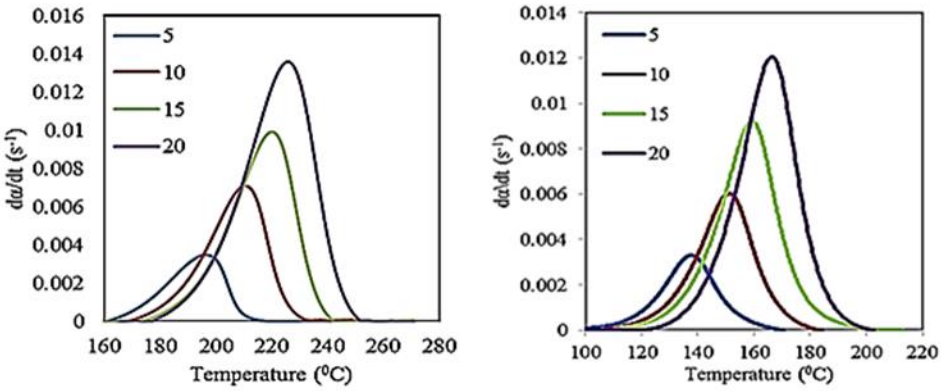

Figure 5.8: Curing reaction rate as a function of temperature at different heating rates (^{0}C/min) for epoxy resin composite curing utilizing 5% Ga (III) xanthate (left) and 5 % UCAT3512T (right).

5.7.3 Degree of cure

Curing degree [36] (α) is defined as the ratio between heat released up to time t (ΔH_t) and total heat of reaction ΔH_{tot}.

$$\alpha = \frac{\Delta H_t}{\Delta H_{tot}} \quad \text{---------- (7)}$$

Non-isothermal dynamic DSC conducted at different heating rates has been widely accepted to provide relatively more accurate kinetic parameters in a short period of time. Figure 5.9 exhibits the plot of extent of conversion (α) as a function of temperature obtained from dynamic DSC data using 5 % Ga (III) xanthate and standard catalyst UCAT3512T composites. It's very clear that heating rate implied under dynamic DSC run affects the extent of conversion as a function of temperature. It is well known that heating rate has great influence on curing process, with exothermic peaks having lower temperatures at lower heating rates. The nature of conversion with respect to temperature gives the latent capability of the catalyst. The curing reaction was initiated at much lower temperature in case of UCAT3512T composite compared to Ga (III)

xanthate. This indicates the superiority of Ga (III) composite over UCAT3512T in extending the working life of a formulated mixture by passivation of the catalyst activity until triggered up to a threshold temperature by the external stimulus.

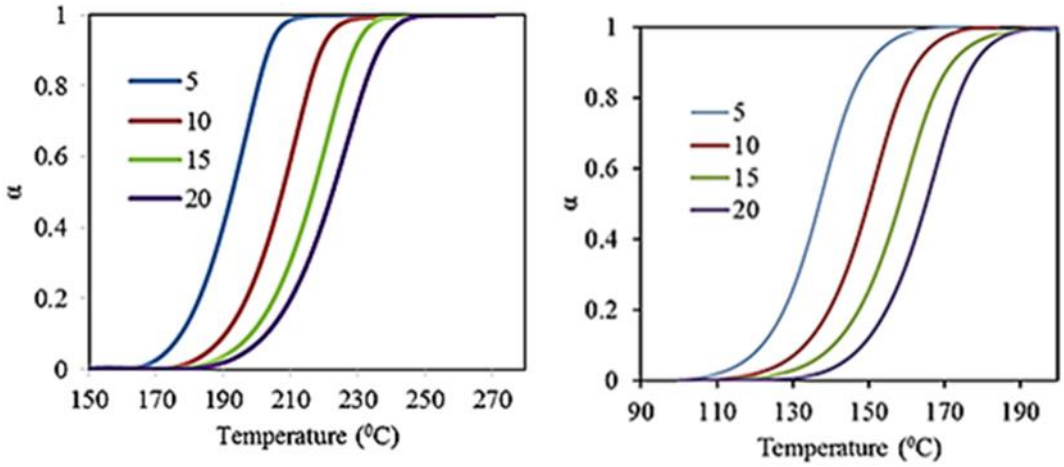

Figure 5.9: Degree of conversion as function of temperature at different heating rates (^{0}C/min) for epoxy resin composite curing utilizing 5% catalytic composition of Ga (III) xanthate (left) and 5% UCAT3512 (right).

Thus after obtaining the rate of conversion and conversion degree at various heating rates, the Friedman method can be successfully applied to predict the reaction model during the epoxy curing process. In case of autocatalytic conversion, f(α) in the Friedman model can be expressed as

$$f(\alpha) = (1-\alpha)^n \alpha^m \text{ ------- (8)}$$

While in the case of nth order reaction kinetics, f(α) can be defined as

$$f(\alpha) = (1-\alpha)^n \text{ ---------- (9)}$$

Where, n and m are the order of reaction.

Substituting both the equation (8) and (9), in equation (5) will yield the following equations [37]

$$\ln \frac{d\alpha}{dt} + {}^{E_a}/_{RT} = \ln A + n\ln(1-\alpha) \text{ ---------- (10)}$$

$$\ln \frac{d\alpha}{dt} + {}^{E_a}/_{RT} = lnA + n\ln(1-\alpha) + m\ln(\alpha) \text{ ---------- (11)}$$

The values of ln[Af(α)] in equation (5) can be obtained from the known values of ln[dα/dt] and E_a/RT. The plot of ln[Af(α)] and ln(1-α) can be used to determine the nature of mechanism. If a straight line is obtained, the slope and intercept gives the reaction order (n) and the natural logarithm of the frequency factor and is predicted to follow nth-order kinetics.

For autocatalytic process, the plot of ln[Af(α)] and ln(1-α) is nonlinear with a peak maximum approximately around -0.51 to -0.22 which is equivalent to degree of curing [34] of 0.2 to 0.4. This could be attributed to the fact that autocatalytic mode of epoxy curing exhibits the maximum rate of reaction [38] at 20-40% completion of conversion. ln(1-α) values were derived from degree of conversion. Thus the obtained ln[Af(α)] and ln(1-α) values at various heating rates were used for the investigation of curing kinetics using the Friedman plots. The Friedman plots of ln[Af(α)] and ln(1-α) for both catalyst systems are presented in figure 5.10.

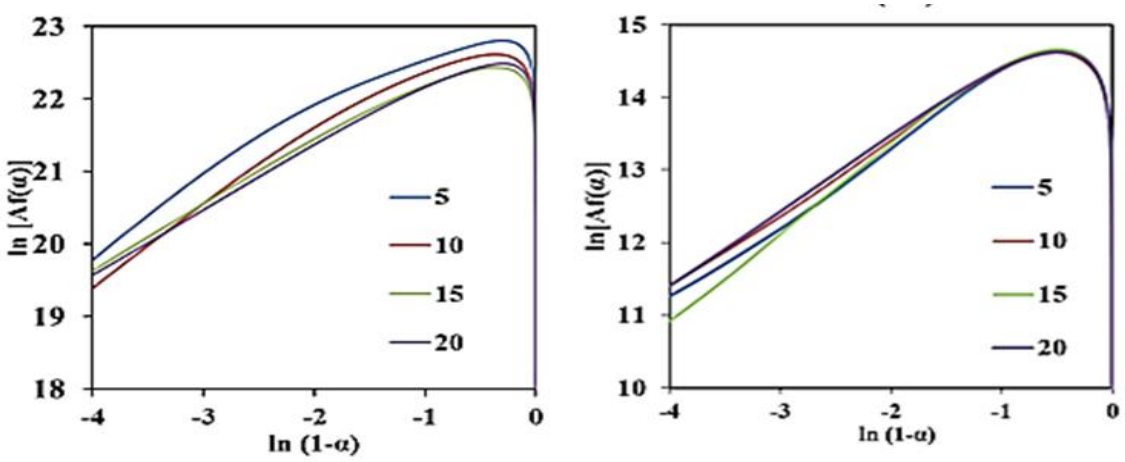

Figure 5.10: The Friedman plot for epoxy resin composite curing at different heating rates (^{0}C/min^{-1}) utilizing 5% Ga (III) xanthate (left) and 5 % UCAT3512T (right).

A perusal of figure 5.10 clearly corroborates that in the case of both of the catalytic compositions there is a nonlinear increase before the peak reaches its maximum between -0.51 to -0.22 followed by linear decrease as function of ln(1-α). This indicates that the curing of epoxy resin composite by catalytic systems under investigation follows autocatalytic mechanism.

To further verify the validity of autocatalytic mechanism in the present system, equation (11) was solved by multiple linear regression. The ln(dα/dt) was taken as dependent variable, and lnα, ln(1−α) and 1/T were taken as independent variables. The average activation energy obtained

by Flynn-Wall-Ozawa method was utilized for estimating the values of A, m, and n. The degree of curing employed to solve regression is from the beginning and until the maximum peak for degree of curing [40] which is ranging from 0.1 to 0.5. The multiple linear regressions analysis results for all heating rates for both of the catalytic compositions were listed in table 5.2 and 5.3.

Table 5.2: Kinetic parameters for the epoxy resin composite curing utilizing 5 % Ga (III) xanthate using Freidman model.

Heating rate (^{0}C / min)	ln A (S^{-1})	Mean	n	Mean	m	Mean
5	23.23	23.20	0.8	0.8	0.3	0.3
10	23.26		0.7		0.4	
15	23.12		0.8		0.3	
20	23.20		0.9		0.3	

Table 5.3: Kinetic parameters for the epoxy resin composite curing utilizing 5 % UCAT3512T using Friedman model.

Heating rate (^{0}C / min)	ln A (S^{-1})	Mean	n	Mean	m	Mean
5	15.77	15.66	1	0.9	0.6	0.5
10	15.59		0.9		0.4	
15	15.69		0.8		0.5	
20	15.61		0.9		0.5	

Based on results obtained for ln A, reaction orders (n and m) by multiple linear regression and average E_a values obtained by Flynn-Wall-Ozawa method. The validity of autocatalytic mechanism by Friedman plot can be crosschecked by equation (11). The equation (12) and (13) are framed autocatalytic equations for the curing of epoxy resin using Ga (III) xanthate and UCAT3512T respectively by introducing the calculated values of lnA, reaction orders (n and m) and activation energy.

$$d\alpha/dt = \exp(23.20).\exp(-13228/T).(1-\alpha)^{0.8}.(\alpha)^{0.3} \text{ ---------- (12)}$$

$$d\alpha/dt = \exp(15.66).\exp(-8331/T).(1-\alpha)^{0.9}.(\alpha)^{0.5} \text{ ---------- (13)}$$

The calculated results of conversion rate ($d\alpha/dt$) obtained by solving these autocatalytic equation (12) and (13) are plotted as a function of temperature and shown in figure 5.11 along with the experimental results as shown in Figure 5.8. It can be clearly observed that a very good match

between the calculated (dotted line) and experimental (solid line) results exists. Since a very good fit can be observed for the calculated and experimental results an autocatalytic mechanism can be proposed for both the catalyst systems. An autocatalytic mechanism can be explained by the acceleration of the reaction process by the free phenol groups generated while the epoxy group begins to open during the reaction process.

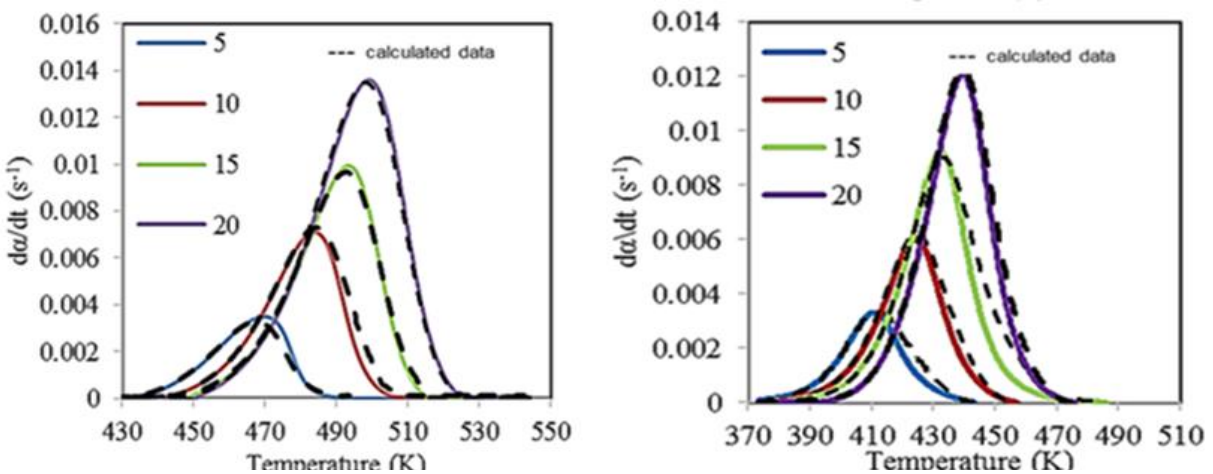

Figure 5.11: Plot of curing rate as a function of temperature at different heating rates (^{0}C/min) for the curing of epoxy resin composite utilizing 5% Ga (III) xanthate (left) and UCAT3512T (right). Dotted lines: calculated values; solid lines: experimental values.

5.8 Shelf-life study

To verify the superiority of Ga (III) xanthate over the standard industrial catalyst in curing of epoxy resin shelf-life study was conducted to determine and compare the pot-life of the formulation consisting of resin-catalyst systems. A 1:1 mixture of the epoxy resin/phenol including 5% catalyst was stored at room temperature for six months to conduct shelf-life study. The curing time at 200^{0}C was monitored for UCAT3512T and was compared with that of Ga (III) xanthate (Figure 5.12 and table 4) at definite time intervals.

Curing time of epoxy resin/phenol composite with UCAT3512T decreased from 14.5 to 12 s while with Gallium (III) xanthate it remained unchanged. Thus the formulation of epoxy composite with UCAT3512T exhibited premature curing while the gallium xanthate formulation showed no

premature curing. This study demonstrates that that Gallium (III) xanthate exhibits better latent catalyst properties than standard catalyst UCAT3512T.

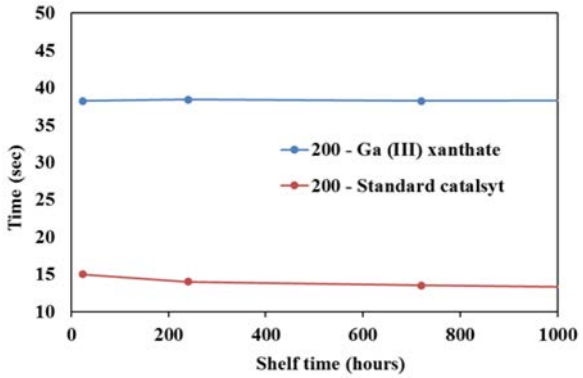

Figure 5.12: Curing time of epoxy resin composite conducted at 200 ^{0}C after storage at room temperature for different time intervals (5% catalyst content).

Table 5.4: Curing time at 200 ^{0}C after storage at room temperature.

Shelf life time (h)	Curing time (s) with 5% standard catalyst at 200 ^{0}C	Curing time (s) with 5% Ga (III) xanthate at 200 ^{0}C
24	14.5	38.2
240	14.0	38.4
720	13.5	38.2
1440	13	38.3
2160	12.3	38.2
4320	12	38.3

5.9 Conclusion

Electronic absorption study and the EPMA analysis both confirmed the in-situ formation of gallium sulfide in the epoxy resin matrix, thus confirming the most probable mechanism of curing of epoxy composite by thermal decomposition reaction of metal xanthate resulting in to metal sulfide. The cure kinetics for Ga (III) xanthate and UCAT3512T epoxy resin composite were studied using dynamic DSC technique. Activation energy determined using Flynn-

Wall-Ozawa method and Kissinger methods was found be almost similar. The activation energy was higher for Ga (III) xanthate composite than UCAT3512T composite. The rate of curing and cure degree as a function of temperature was estimated for both of the formulations followed by for Friedman isoconversioanl kinetic modeling. An autocatalytic model was found to well describe the curing reaction of epoxy resin by both of the catalysts used in the present investigation. Calculated rate of curing determined using the parameters obtained by solving the autocatalytic equation were in good agreement with the experimental cure rate. Shelf-life study was performed to study the pot life of the formulations under investigation. The composite consisting of Ga (III) xanthate had very long shelf life-time since the curing time remained unchanged even after storage for six months at room temperature. On the other hand, composite including standard commercial catalyst UCAT3512T exhibited premature curing due to change in cure time of the composite with time.

5.10 References

[1] T. C. Vagvala, S. S. Pandey, Y. Ogomi, S. Hayase. RSC Advances, 2014, 4, 24658.

[2] M.V. Alonso, M. Oliet, J. Garcia, F. Rodriguez, J. Echeverria, Chemical Engineering Journal, 2006, 122, 159.

[3] F.Y.C. Boey, W. Qiang, Polymer, 2000, 41, 2081.

[4] G. Francucci, F. Cardona, N. W. Manthey, Journal of applied polymer science, 2013, 128, 2030.

[5] N. Sbirrazzuoli, S. Vyazovkin, A. Mititelu, C. Sladic, L. Vincent, Macromolecular Chemistry and physics, 2003, 204 (15), 1815.

[6] M. Kirino, I. Tomita, Macromolecules, 2010, 43, 8821.

[7] S. Naumann, M. R. Buchmeiser, Macromol. Rapid communications, 2014, 35, 682.

[8] S. Naumann, M. Speiser, R. Schowner, E. Giebel, M. R. Buchmeiser, Macromolecules, 2014, 47, 4548.

[9] A. M. Tomuta, X. Ramis, F. Ferrando, A. Serra, Progress in Organic Coatings, 2012, 74, 59.

[10] M. Ghaffari, M. Ehsani, H. Ali Khonakdar, G. Van Assche, H. Terryn, Thermochimica Acta, 2012, 533, 10.

[11] Y. Chen, S. Zhou, H. Zou, M. Liang, Polymer Science Series B, 2014, 56 (5), 623.

[12] Q. Tao, L. Su, R. L. Frost, H. He, B. K.G. Theng, Applied Clay Science, 2014, 95, 317.

[13] I. Hong, S. Lee, Journal of Industrial and Engineering Chemistry, 2013, 19 (1), 42.

[14] N. Kuroda, Y. Nishina and T. Fukuroi, Japan Physical society, 1970, 28 (4), 981.

[15] T. Rath, M. Edler, W. Haas, A. Fischereder, S. Moscher, A. Schenk, R. Trattnig, M. Sezen, G. Mauthner, A. Pein, D. Meischler, K. Bartl, R. Saf, N. Bansal, S.A. Hague, F. Hofer, E. J. W. List and G. Trimmel, Advanced energy materials, 2011, 1, 1046.

[16] M.A. Malik, M. Afzaal and P. O'Brien, Chemical reviews, 2010, 110, 4417.

[17] J. Tauc, Materials Research Bulletin, 1968, 3(1), 37.

[18] D.P Dutta, G. Sharma, A.K. Tyagi, S.K. Kulshrestha, Material Science Engineering B, 2007, 138, 60.

[19] C. H. Ho, S. L. Lin, Journal of applied physics, 2006, 8, 083508.

[20] M. Ohyama, H. Ito, M. Takeuchi, Japanese journal of applied physics, 2005, 44, 4780.

[21] S.L. Loredo, Y.P. Méndez, M.C. Rodriguez, S.M. Fernández, A.A. Gallegos, A.V. Dimas, T.H. García, Thin Solid Films, 2014, 550, 110.

[22] C. Jubsilp, K. Punson, T. Takeichi, S. Rimdusit, Polymer degradation stability, 2010, 95, 918.

[23] M.V. Alonso, M. Oliet, J. Garcia, F. Rodriguez, J. Echeverria, Chemical Engineering Journal, 2006, 122, 159.

[24] L. Barral, J. Cano, J. Lopez, I. LoPez-Bueno, P. Nogueira, M. J. Abad, C. Ramirez, J. Polymer Science Part B: Polymer Physics, 2000, 38, 351.

[25] G. Yang, Z. Yuan, Z. Yang, M. Zhang, Journal of applied polymer science, 2013, 127 (4), 3178.

[26] T. Yang, C. Zhang, J. Zhang, J. Cheng, Thermochimica Acta, 2014, 577, 11.

[27] Y. Liu, J. Wang, S. Xu, Journal of applied polymer science A Polymer Chemistry, 2014, 52 (4), 472.

[28] H. Xie, B. Liu, Q. Sun, Z. Yuan, J. Shen, R. Cheng, Journal of applied polymer science, 2005, 96, 329.

[29] F. Y. C. Boey1, X. L. Song, C. Y. Yue, Q. Zhao, Journal of applied polymer science, 38, 907.

[30] G. Yang, Z. Yuan, Z. Yang, M. Zhang, Journal of applied polymer science, 2013, 127, 3178.

[31] C. Jubsilp, K. Punson, T. Takeichi, S. Rimdusit, Polymer degradation stability, 2010, 95, 918.

[32] F.Y.C. Boey, W. Qiang, Polymer, 2000, 41, 2081.

[33] C. Jubsilp, S. Damrongsakkul, T. Takeichi, S. Rimdusit, Thermochimica Acta, 2006, 447, 131.

[34] N. Sbirrazzuoli, S. Vyazovkin, A. Mititelu, C. Sladic, L. Vincent, Macromolecular chemistry and physics, 2003, 204 (15), 1815.

[35] C. Zhang, W. K. Binienda, L. Zeng, X. Ye, S. Chen, Thermochimica Acta, 2011, 523 (1), 63

[36] M.V. Alonsoa, M. Oliet, J. Garcia, F. Rodriguez, J. Echeverria, Chemical Engineering Journal, 2006, 122, 159.

[37] Y. Lu, M. Li, L. Ke, D. Hu, W. Xu, Journal of applied polymer science, 2011, 121, 2481.

[38] L. Ke, D. Hu, Y. Lu, S. Feng, Y. Xie, W. Xu, Polymer degradation stability, 2012, 97, 132.

[39] C. Jubsilp, K. Punson, T. Takeichi, S. Rimdusit, Polymer degradation stability, 2010, 95, 918.

[40] Tarun C. Vagvala, Gaurav Kapil, Shyam S. Pandey, Yuhei Ogomi and Shuzi Hayase, Journal of Applied Polymer Science, 2015, 132 (26), 42149.

General Conclusion

This thesis presents the synthesis of metal xanthates and to the best of our knowledge is the first element of investigation of metal xanthates as latent catalysts for curing of epoxy resin.

The first chapter deals with the relevance of cured epoxy resins, the process of curing and curing agents. A brief description of conventional curing agents which are broadly classified as Lewis acids and bases. The need and description about the latent curing agents and their ability to circumvent the drawbacks posed by conventional curing agents. A brief introduction about the application of metal sulfides as catalysts along with the benefits of Metal xanthates as precursors of metal sulfides over the direct use of metal sulfides has also been explored. Subsequent section gave the details of basic aim and idea about the current thesis.

The second chapter summarized the various techniques and instrumentation used in the current thesis. Instruments used for confirming the synthesized materials and their characterization along with investigation pertaining to curing of epoxy formulations and its characterization has been discussed.

Third chapter describes the investigation of zinc xanthates as curing catalysts and the influence of alkyl chain on curing of epoxy resin. The synthesis and characterization of linear and branched zinc (II) xanthates with varying alkyl chain length were performed. The Thermogravimetric analysis was performed to analyze and compare the thermal decomposition behavior of the zinc xanthate sunder investigation. The trend of decomposition temperature in case of linear alkyl chain zinc (II) xanthates is observed to be opposite to the trend observed in the case of branched alkyl chain zinc (II) xanthates. Zinc sulfide as the final decomposition product upon thermal annealing for all zinc (II) xanthates under investigation was confirmed by XRD analysis. Cure time for epoxy resin composite consisting of 5 % zinc (II) xanthates at various temperatures was studied. The cure time by zinc (II) xanthates at a particular temperature followed the same trend as followed

by the thermal decomposition temperature. Formation of zinc sulfide in-situ in the cured epoxy resin matrix consisting of zinc (II) xanthates in all cases was characterized by XRD.

Fourth chapter includes the study of influence of metal ion on the xanthate species in catalyzing the curing of epoxy composite. Cu(I), Pb(II), Sb(III), Zn(II), Cd(II), In(III), Ga(III) xanthates (2,2- diemthyl-3-pentane metal dithiocarboanate) were synthesized and characterized by ^{1}H NMR, ^{13}C NMR, infrared spectroscopy and elemental analysis. The metal sulfides obtained by thermal annealing of metal xanthates at $200^{0}C$ were characterized by XRD and EDS techniques. Curing time of epoxy resin composite at various temperatures was studied employing 5% metal xanthates as catalysts. None of the metal xanthates demonstrated any significant curing of epoxy resin composite prior to $170^{0}C$ proving their latent curing potency. Ga (III) xanthate was found to be the most effective curing catalyst amongst the metal xanthates under investigation. The cured epoxy resin including metal xanthate after thermal annealing at $200^{0}C$ subjected to XRD and EDS studies and the formation of metal sulfide in-situ in the cured epoxy resin matrix was confirmed.

Fifth chapter deals with the further study of gallium xanthate as latent thermal curing catalyst for the epoxy resin/phenol composite. Since gallium xanthate exhibited relatively effective catalytic properties among the metal xanthates under investigation, curing behaviour of Gallium xanthate was compared with that of standard catalyst - UCAT3512T. Ga (III) xanthate swiftly cures the epoxy composite within 38.2 s at $200^{0}C$. Unlike standard catalyst which showed curing of epoxy compoiste at lower and over abroad range of temepartures, gallium xantahte observed to intiate singnificant curing of epoxy composite only from $170^{0}C$. Curing of epoxy resin via decomspoition of gallum xanthate leading to in-situ formation of gallium sulfide was further confirmed by utlizing electronic absortion study and EPMA analysis. Determination of kinetic parameters utilizing non-isothermal differential scanning calorimetric technique at different heating rates was made and activation energy for curing was calculated using Kissinger's and Flynn-Wall-Ozawa methods. The activation energy values obtained were noted to be higher for epoxy resin composite consisting of Ga (III) xanthate than UCAT3512T concluding that the former possess better latent properties than later.

Kinetic modelling was performed by applying Friedman`s isoconversioanl method and an autocatalytic model was found to be successful in describing the curing reaction for both of the formulations. The calculated conversion rate as a function of temperature obtained by solving autocatalytic equation showed a very good fit with experimental values. The shelf life is the last study presented in this thesis to investigate and compare the pot life of epoxy composite including gallium xanthate and standard catalyst. The study over six months indicated that the cure time of epoxy composite with Gallium (III) xanthate did not change after storage for six months proving the superior latent propertied of gallium xanthate over standard commercial catalyst under investigation.

Future prospect

For the future, efforts are needed to further enhance catalytic efficiency of the latent catalyst by ensuring the cure time is reduced. The modification of catalyst can either be done by changing the metal species of the xanthate moiety or by altering the alkyl chain ligand. Also the study if mechanical properties such as strength, adhesiveness, stiffens, hardness need to analyzed. The properties such as conductivity, viscosity and modulus are required to assess the commercial use of the catalyst. In addition the decomposition of metal xanthate in-situ in the epoxy resin matrix yield gases which are not favored especially in case of molding applications. As the release of gases leads to increase in porosity of the moldings. In such cases further research lowering the quantity of metal xanthate as catalyst is desired thereby reducing the gases release at the same maintaining low cure time. This also makes the curing process more ecofriendly due to reduction in gas release.

Academically, to the best of our knowledge, there is no report about the implication of metal sulfide for the epoxy curing and the utilization of metal xanthate for curing opens a new area to embark on the latent catalysts of the epoxy resins. We strongly believe that such information is going to help the chemists and material science community in designing the more efficient latent catalyst with much improved pot-life.

Achievements

(A) Publications:

1.Tarun Chand Vagvala, Shyam Sudhir Pandey, Yuhei Ogomi and Shuzi Hayase, Gallium (III) xanthate as a novel thermal latent curing agent for an epoxy resin composite, *RSC Advances*, 2014,4, 24658. DOI: 10.1039/C4RA03151B. IF: 3.7

2. Tarun Chand Vagvala, Gaurav Kapil, Shyam S. Pandey, Yuhei Ogomi and Shuzi Hayase, Nonisothermal curing kinetics of epoxy resin composite utilizing Ga (III) xanthate as a latent catalyst, Journal of applied polymer science, 2015, 132 (26), DOI: 10.1002/app.42149. IF: 1.26

3. Tarun Chand Vagvala, Shyam S. Pandey, Yuhei Ogomi and Shuzi Hayase, Investigation of metal xanthates as latent curing catalysts for epoxy resin via formation of in-situ metal sulfides, Inorganica Chimica Acta, 2015, 435C, 292. DOI: 10.1016/j.ica.2015.07.020. IF: 2

4. Tarun Chand Vagvala, Shyam S. Pandey, Suvratha Krishnamurthy, Shuzi Hayase, Relationship of alkyl chain length and thermal decomposition temperature in Zinc (II) xanthates and its impact on curing of epoxy resin, Inorganica Chimica Acta, under review, manuscript id: ICA-D-15-00530.

Co-authored journals:

Suvratha Krishnamurthy, Venkatprasad Jalli, Tarun Chand Vagvala, T. Moriguchi A. Tsuge, α-Chymotrypsin and l-acylase aided synthesis of 5-hydroxypipecolic acid via Jacobsen's hydrolytic kinetic resolution of epoxy amino acids, *RSC Advances*, 2015, 5, 52154–52160, DOI: 10.1039/C5RA09207H.

Suvratha Krishnamurthy, Venkatprasad Jalli, Tarun Chand Vagvala, T. Moriguchi and A. Tsuge, Crystal structure of (1*S*,4*S*) benzyl 3-oxo-2-oxa-5-azabicyclo[2.2.1]heptane-5-carboxylate, *Acta Crystallographica Section E*, E71, o447–o448, DOI: 10.1107/S2056989015010464.

Suvratha Krishnamurthy, Venkatprasad Jalli, Tarun Chand Vagvala, T. Moriguchi, A. Tsuge, Crystal structure of (1*R*,4*R*)-*tert*-butyl-3-oxo-2-oxa-5-azabicyclo[2.2.2]octane-5-carboxylate, *Acta Crystallographica, Section E*, E71, 2015, o449–o450, DOI: 10.1107/S2056989015010476.

(B) Conference presentations:

International conferences

1. Investigation of metal xanthates as latent thermal epoxy resin curing catalysts, Tarun Chand Vagvala, Shyam Sudhir Pandey, Yuhei Ogomi, Shuzi Hayase, 249 American chemical society meeting, Denver, USA, 2015, March, 24.

2. Gallium (III) xanthate as a novel latent epoxy resin curing agent, Tarun Chand Vagvala, Shyam Sudhir Pandey, Yuhei Ogomi, Shuzi Hayase, 15th IUMRS - International conference in Asia, Fukoaka, Japan, 2014, August, 26.

3. Solution processed organic- inorganic hybrid solar cells fabricated from metal xanthate precursors, Tarun Chand Vagvala, Syota Kimura, Kohei Nishimura, Yuhei Oghomi, Qunig Shen, Kenji Yoshino, Yuhei Ogomi, Quin Shen, kenji Yoshino, Shyam Sudhir Pandey, Taro Toyoda, Tingli Ma, Shuzi Hayase, 15th IUMRS-International conference in Asia, Fukoaka, Japan, 2014, August, 26.

Domestic conferences

4. Solution processed organic- inorganic hybrid solar cells fabricated from metal complex precursors, Minobu Kawano, Tarun Chand Vagvala, Yuhei Ogomi, Quin Shen, Kenji Yoshino, Shyam S. Pandey, Tingli Ma, Taro Toyoda, Shuzi Hayase, Japan applied physics society, Spring meeting, Aoyama Gakuin University, Tokyo, Japan, 2014, March, 17.

5. Fabrication of tghin film solar cells using metal xanthate precurosrs Minobu Kawano, Tarun Chand Vagvala, Syota Kimura, Kohei Nishimura, Yuhei Oghomi, Qunig Shen, Kenji Yoshino, Yuhei Ogomi, Quin Shen, Kenji Yoshino, Shyam Sudhir Pandey, Taro Toyoda, Tingli Ma, Shuzi Hayase, Japan chemical society meeting Nagoya University, Nagoya, Japan, 2014, March, 27.

6. Investigation of Gallium (III) xanthate as latent curing agent for epoxy resin, tarun chand vagvala, Shyam Sudhir Pandey, Yuhei Ogomi, Shuzi Hayase, Japan chemical society meeting, Nagoya, Japan, 2014, March, 29.

7. Metal xanthates as latent epoxy resin curing agents, tarun chand vagvala, Shyam Sudhir Pandey, Yuhei Ogomi, Shuzi Hayase, Kyushu chemical society meeting, Kitakyushu, Japan, 2014, June, 28.

8. Gallium (III) xanthate as a novel thermal latent curing agent for epoxy resin composite, tarun chand vagvala, Shyam Sudhir Pandey, Yuhei Ogomi, Shuzi Hayase, Network polymer meeting, Osaka, Japan, 2014, October, 23.

Acknowledgement

I would like to thank **Associate Prof. Shyam Sudhir Pandey** for providing me this opportunity to join his group and work under his guidance. His vast experience and technical knowledge have given me an excellent support and background to pursue research. I also thank **Prof. Shuzi Hayase** for his valuable ideas and constant encouragement. His zeal and enthusiasm has always inspired me.

My sincere thanks to **Prof. Tingli Maa**, for her valuable suggestions for improving the quality of thesis work and motivation provided to me at all times. .

I would also like to thank **Dr. Gururaj Shivashimpi, Dr. Nishimura** for their valuable support for my research work in Hayase laboratory. I would also like to thank all Hayase lab members for the nostalgic memories during my stay in Japan.

I would like to acknowledge Kyushu Institute of Technology for its support, excellent facilities, aid for conferences and lectures, which helped me a lot both scientifically and socially. Am also grateful to the International student office section, Kyushu Institute of technology for their constant help throughout my period of stay in Japan.

Moreover, I indebted to my family and friends for their love, cooperation and encouragement which was a constant source of inspiration for me.

Appendix

Figure: 1. n-butyl zinc (II) xanthate ^{1}H NMR.

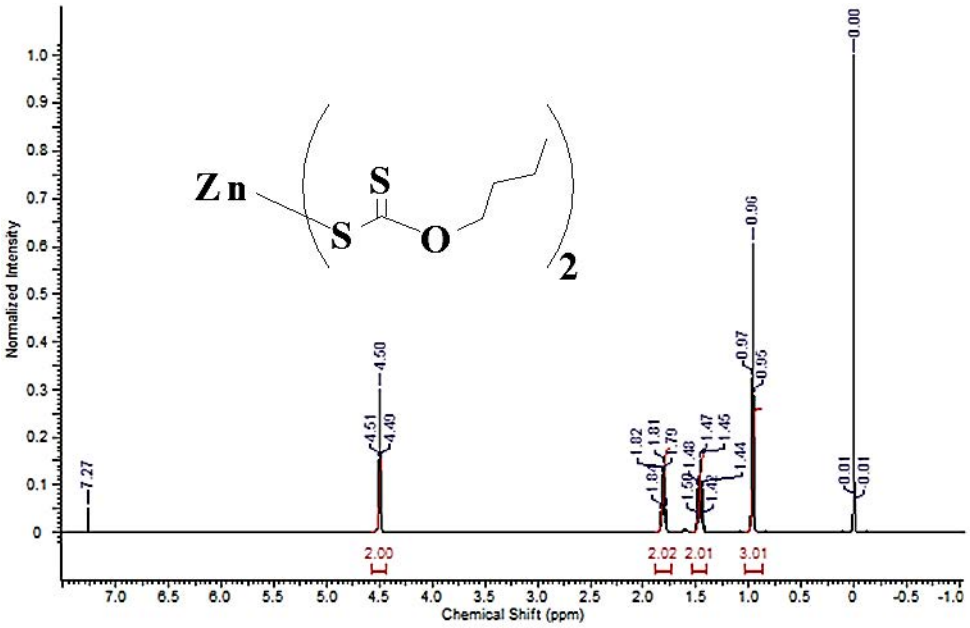

Figure: 2. n-butyl zinc (II) xanthate ^{13}C NMR.

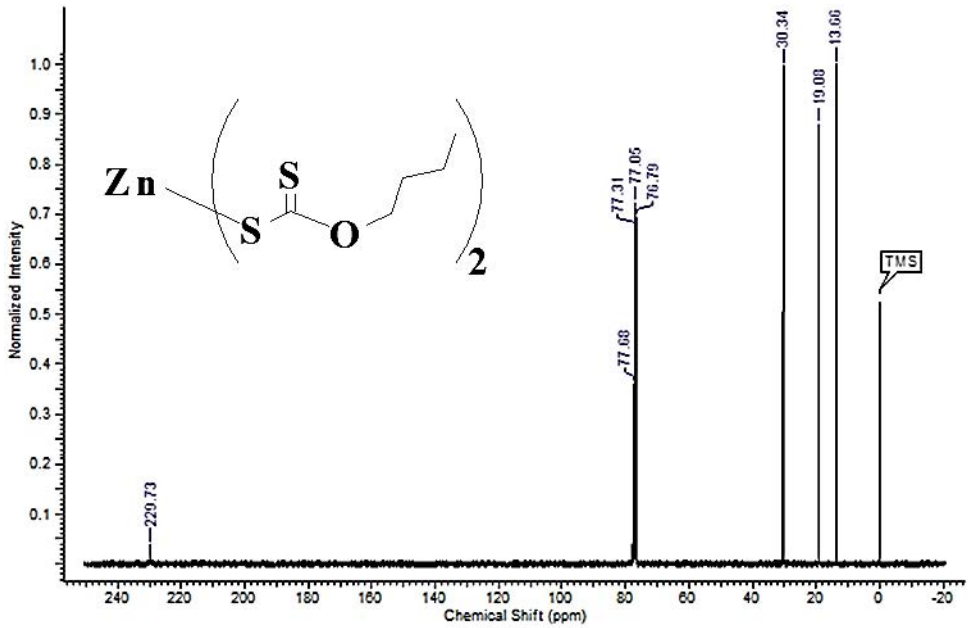

Figure: 3. n-amyl zinc (II) xanthate ^{1}H NMR.

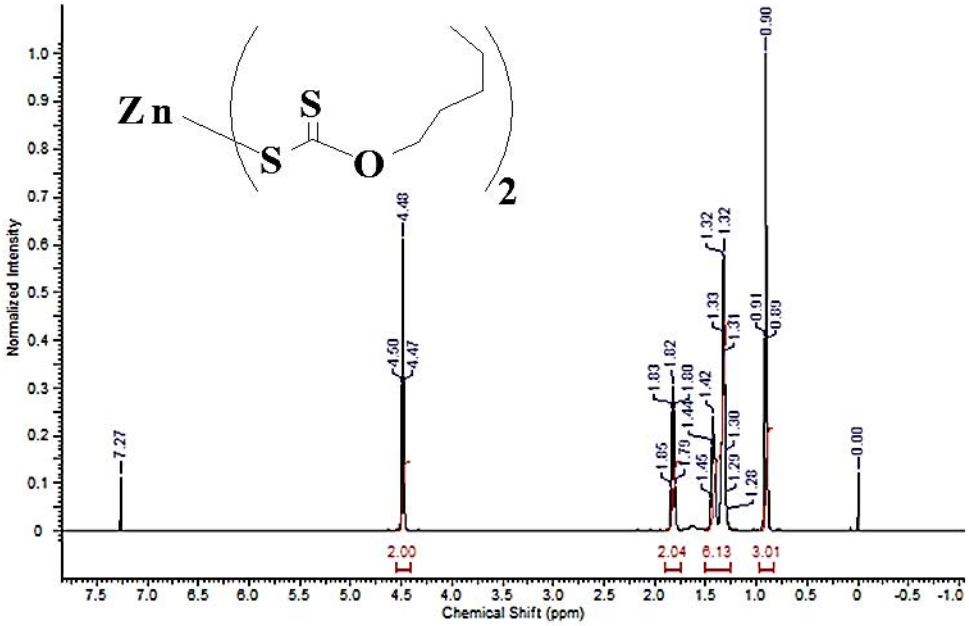

Figure: 4. n-amyl zinc (II) xanthate ^{13}C NMR.

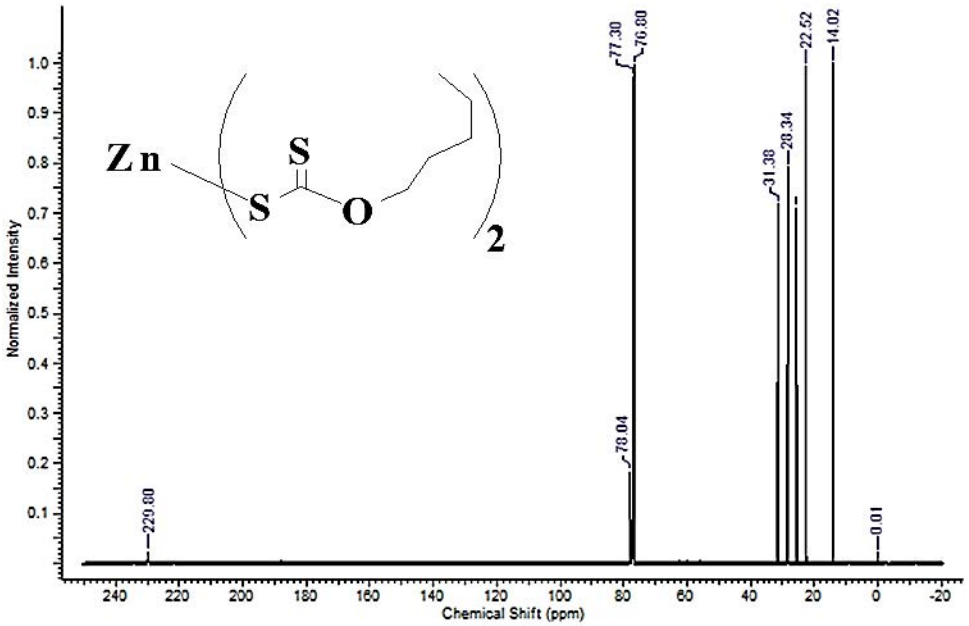

Figure: 5. n-hexyl zinc (II) xanthate ^{1}H NMR.

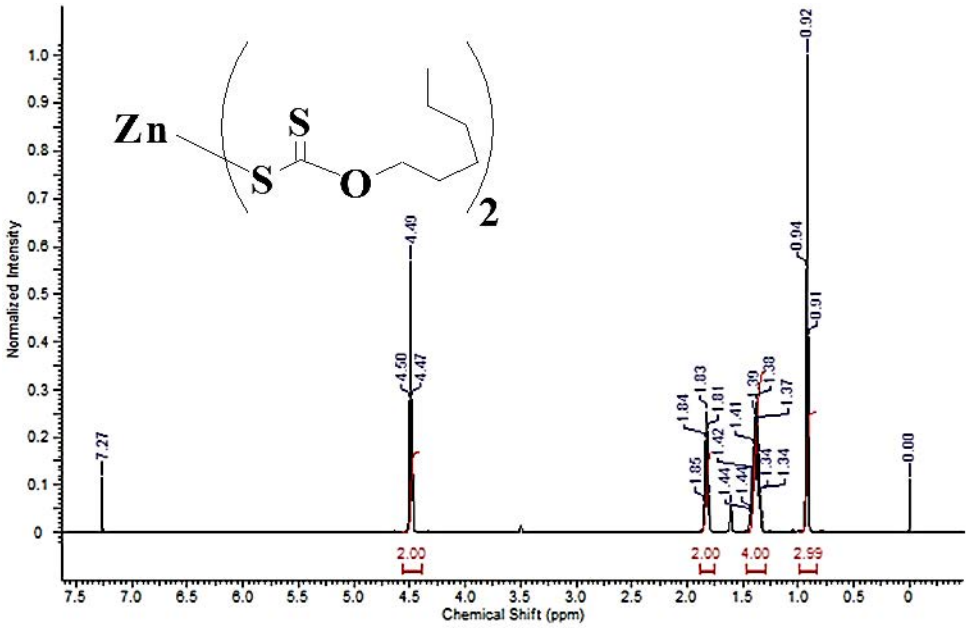

Figure: 6. n-hexyl zinc (II) xanthate ^{13}C NMR.

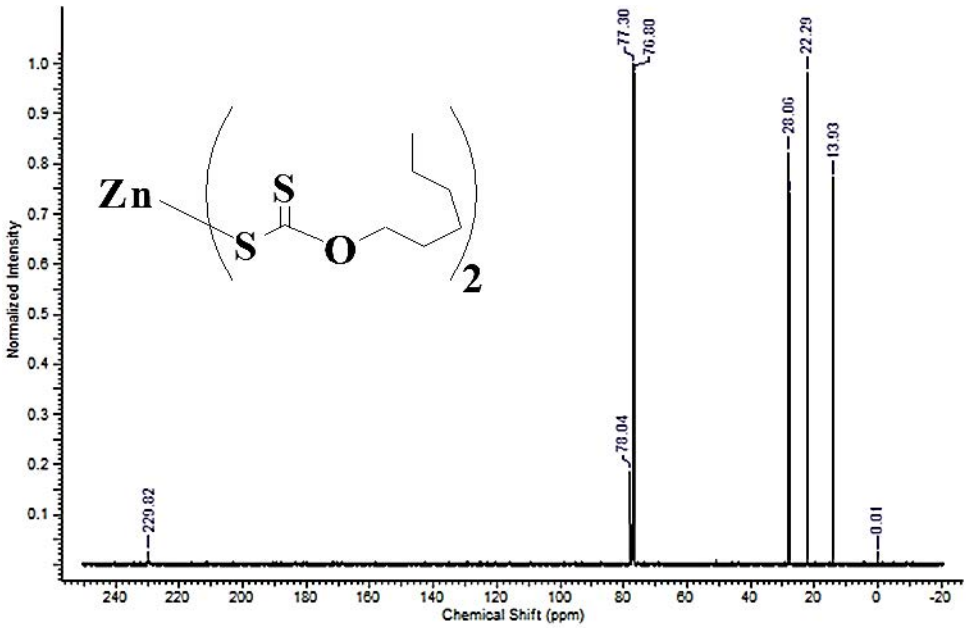

Figure: 7. 2,2-dimethyl-3-butane zinc (II) xanthate ^{1}H NMR

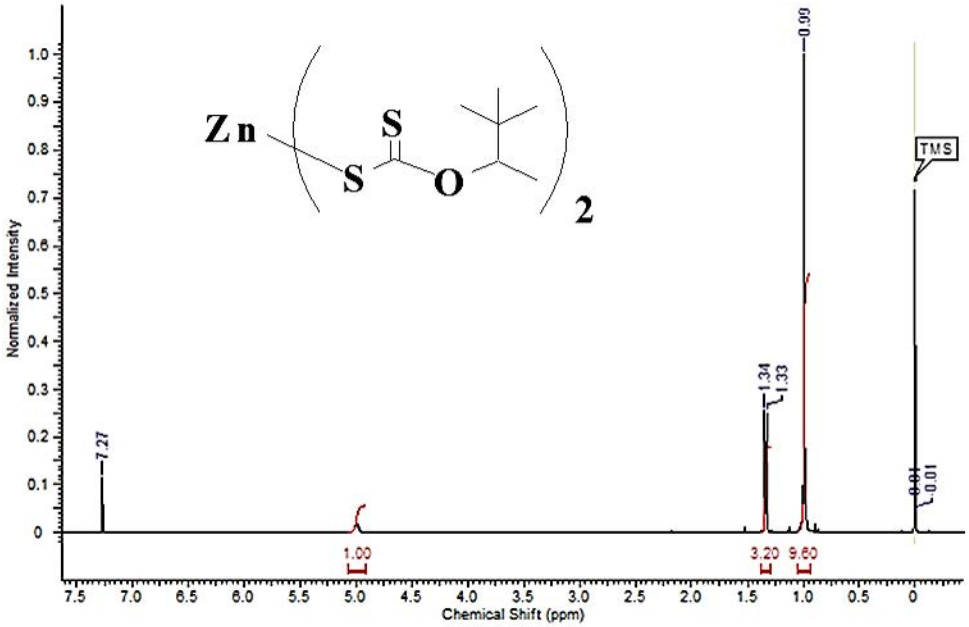

Figure: 8. 2,2-dimethyl-3-butane zinc (II) xanthate ^{13}C NMR

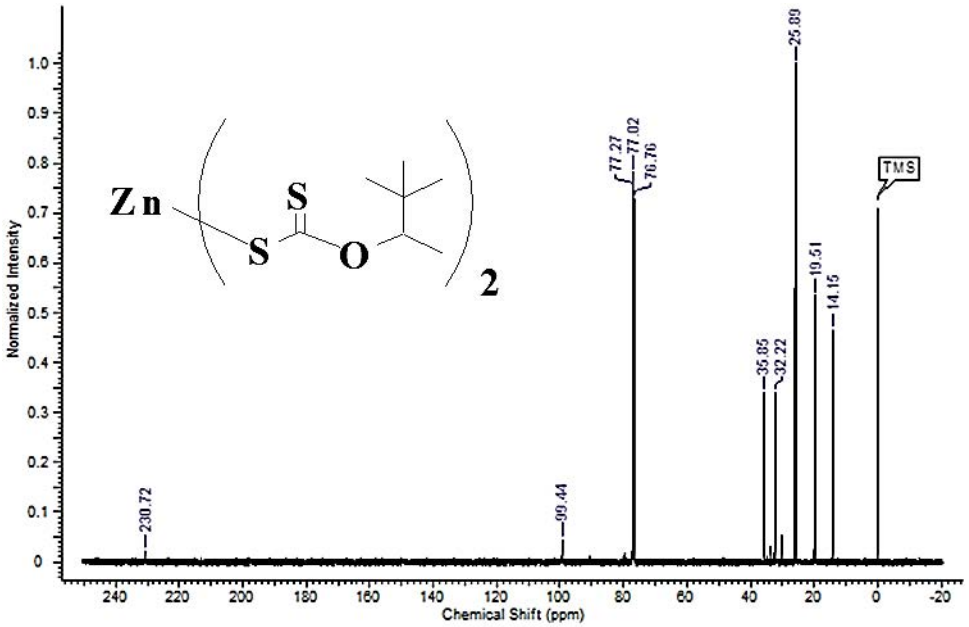

Figure: 9. 2,2-dimethyl-3-hexyl zinc (II) xanthate ^{1}H NMR

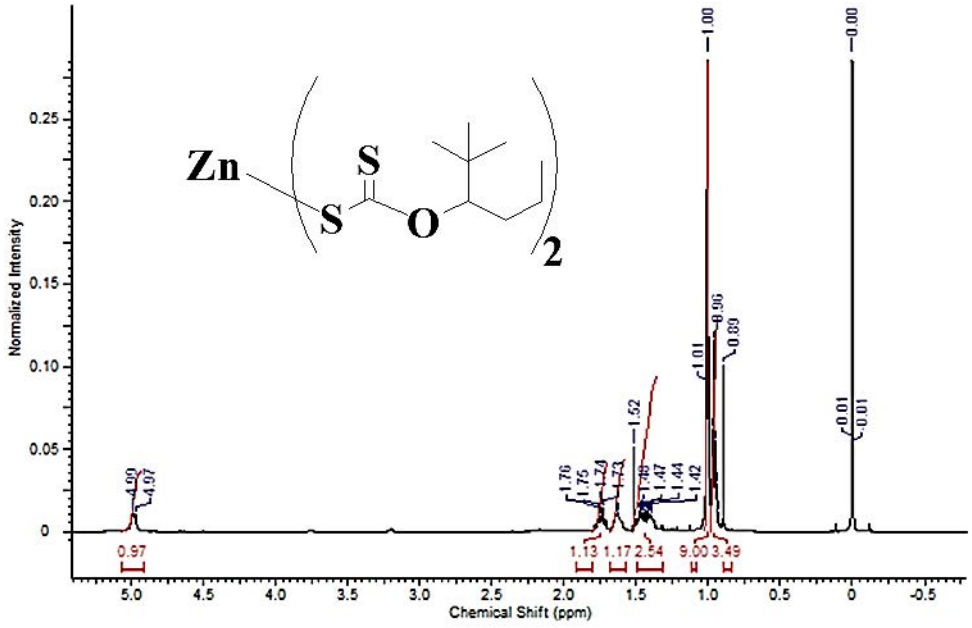

Figure: 10. 2,2-dimethyl-3-hexyl zinc xanthate ^{13}C NMR

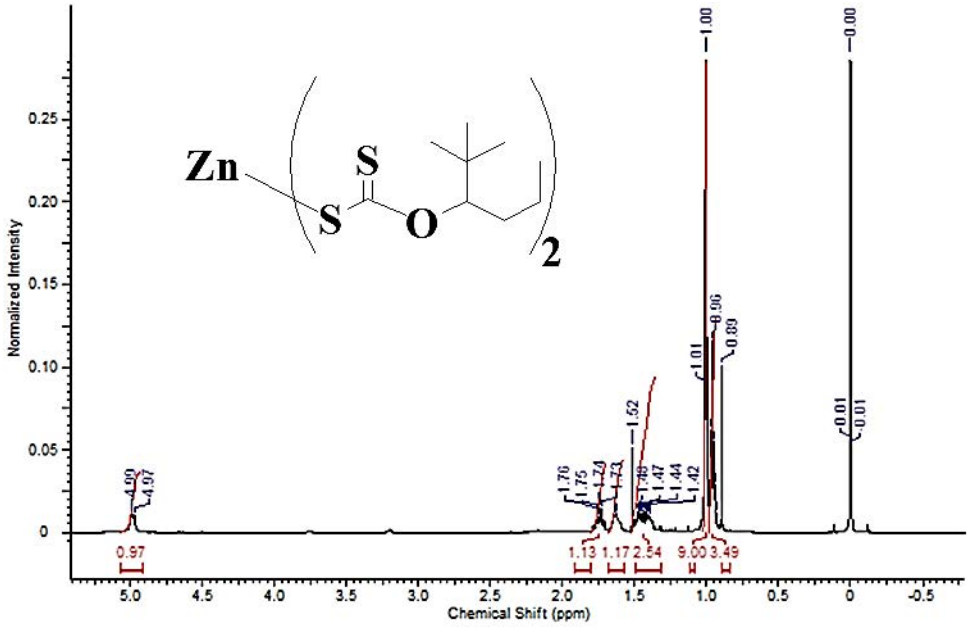

Figure: 11. n-hexyl potassium (I) xanthate ^{1}H NMR

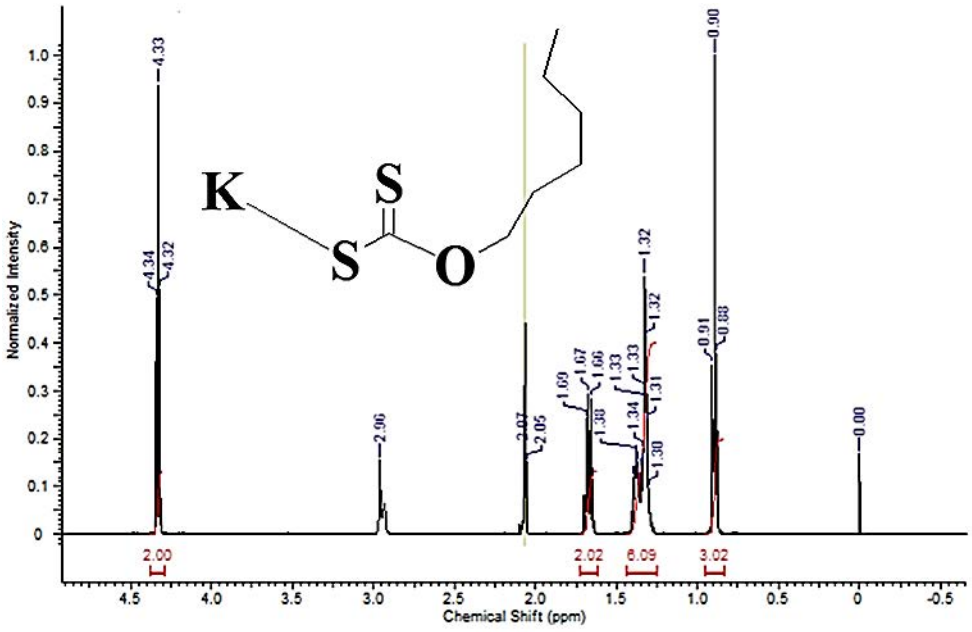

Figure: 12. n-hexyl potassium (I) xanthate ^{13}C NMR

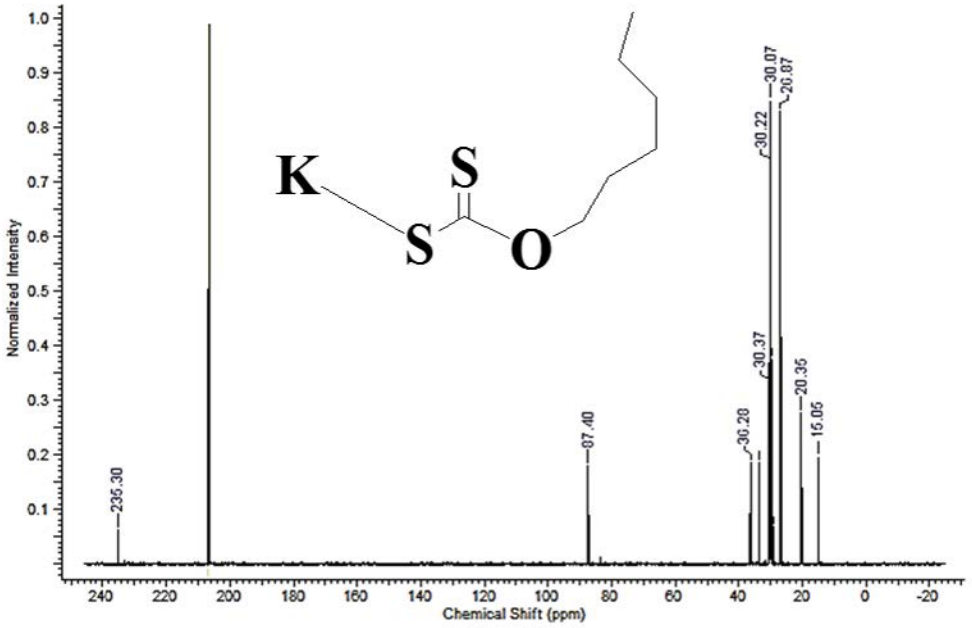

Figure: 13. 2,2-dimethyl-3-hexane potassium (I) xanthate ^{1}H NMR

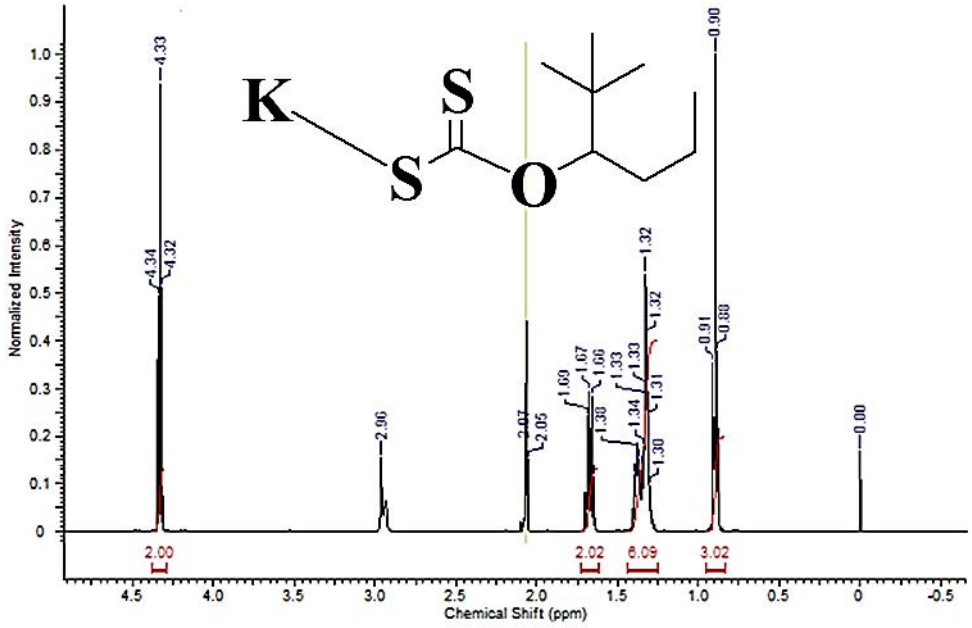

Figure: 14. 2,-dimethyl-3-hexane potassium (I) xanthate ^{13}C NMR

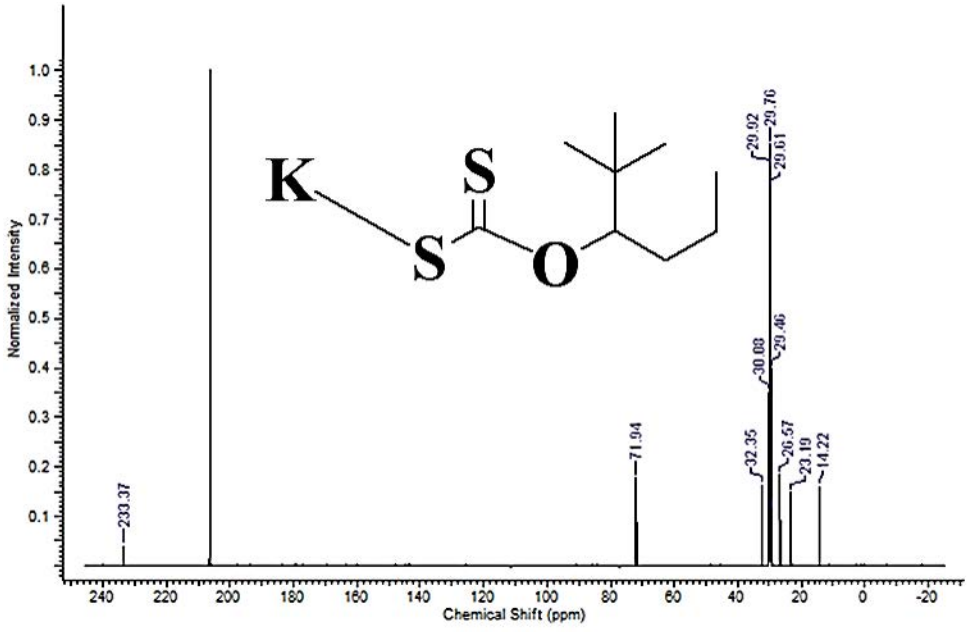

Figure: 15. Cu (I) - 2,2-dimethyl-3-pentane xanthate ^{1}H NMR.

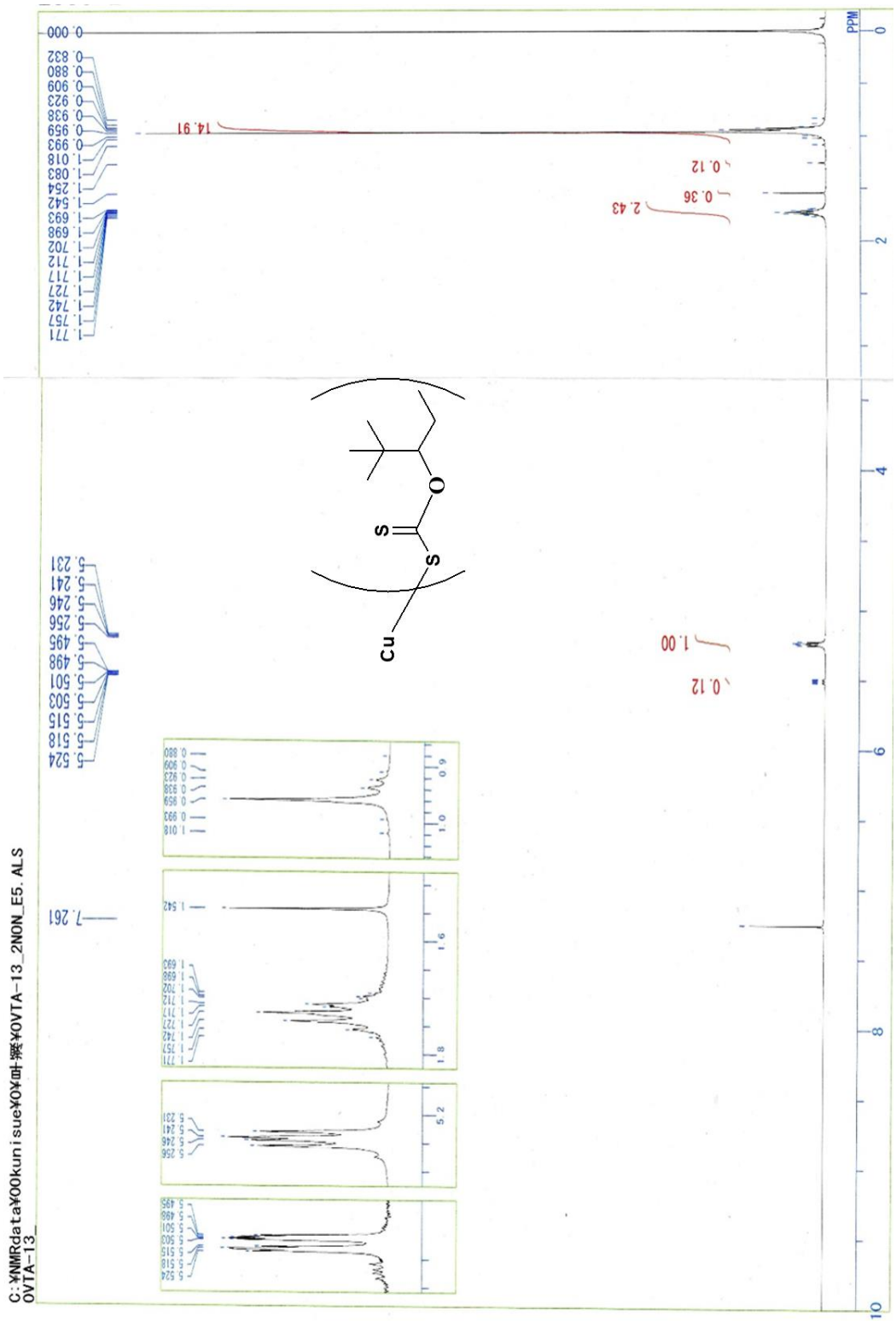

Figure: 16. Pb (II)- 2,2-dimethyl-3-pentane xanthate ^{1}H NMR.

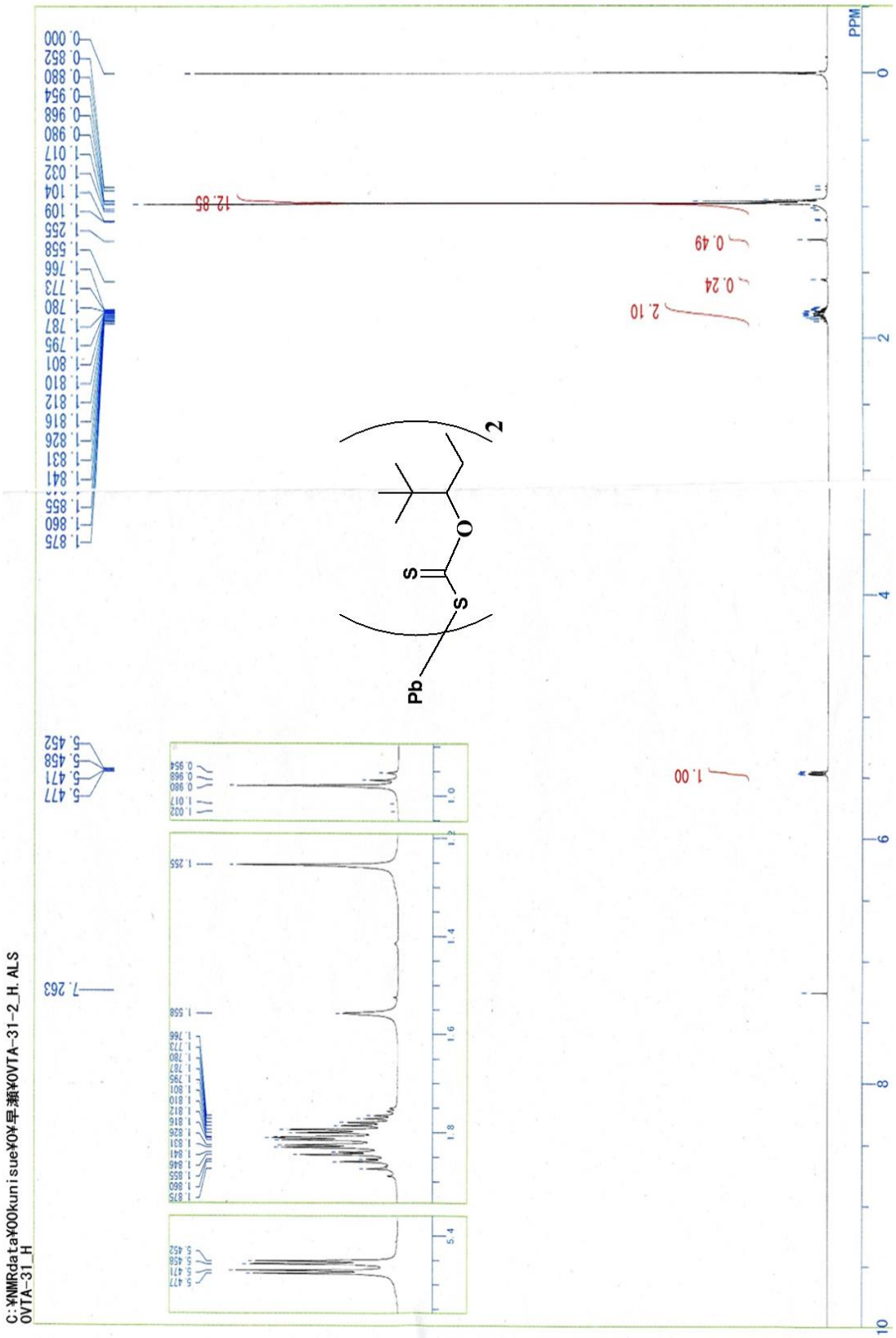

Figure: 17. Sb (III) - 2,2-dimethyl-3-pentane xanthate ^{1}H NMR.

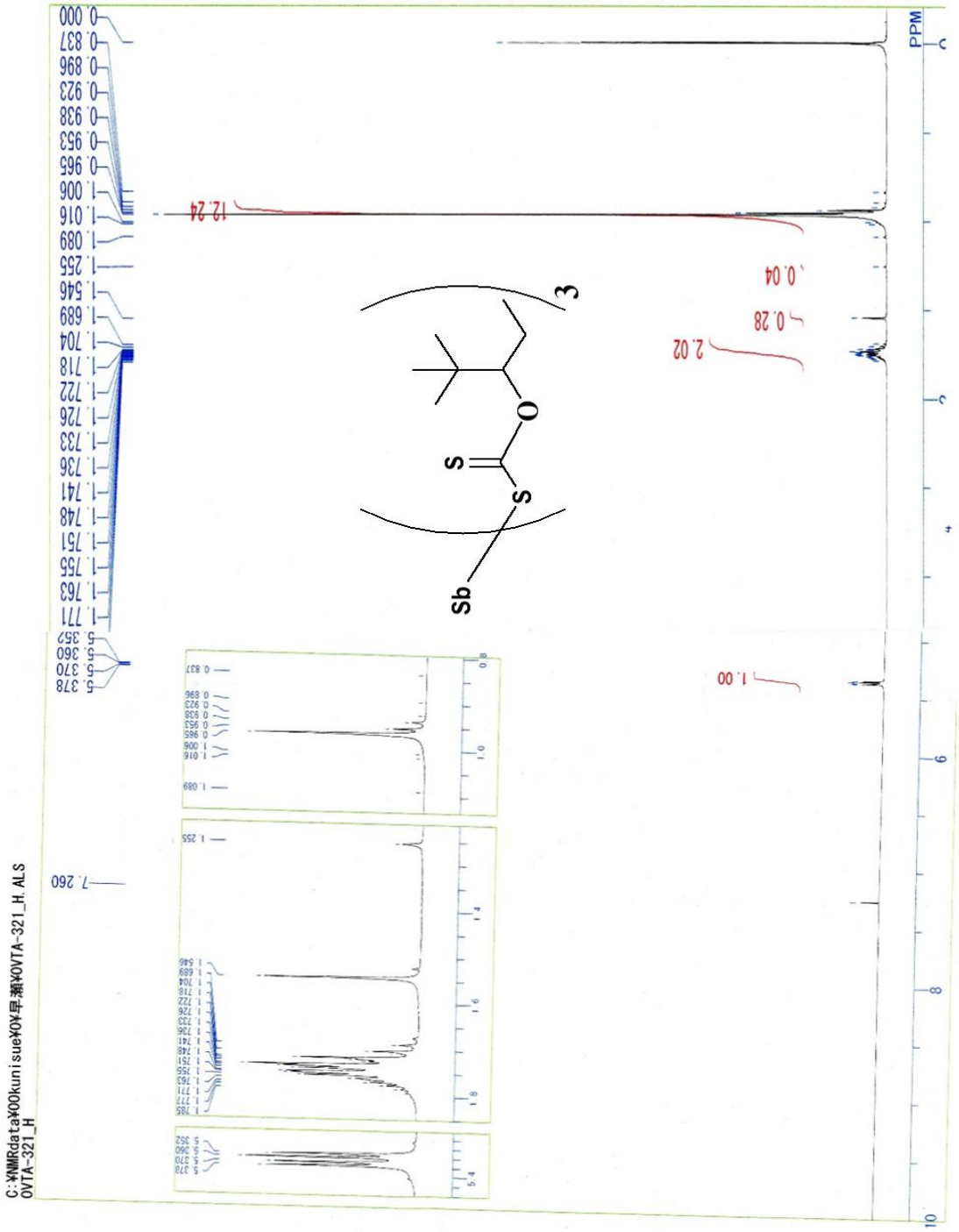

Figure: 18. Zn (II) - 2,2-dimethyl-3-pentane xanthate ^{1}H NMR.

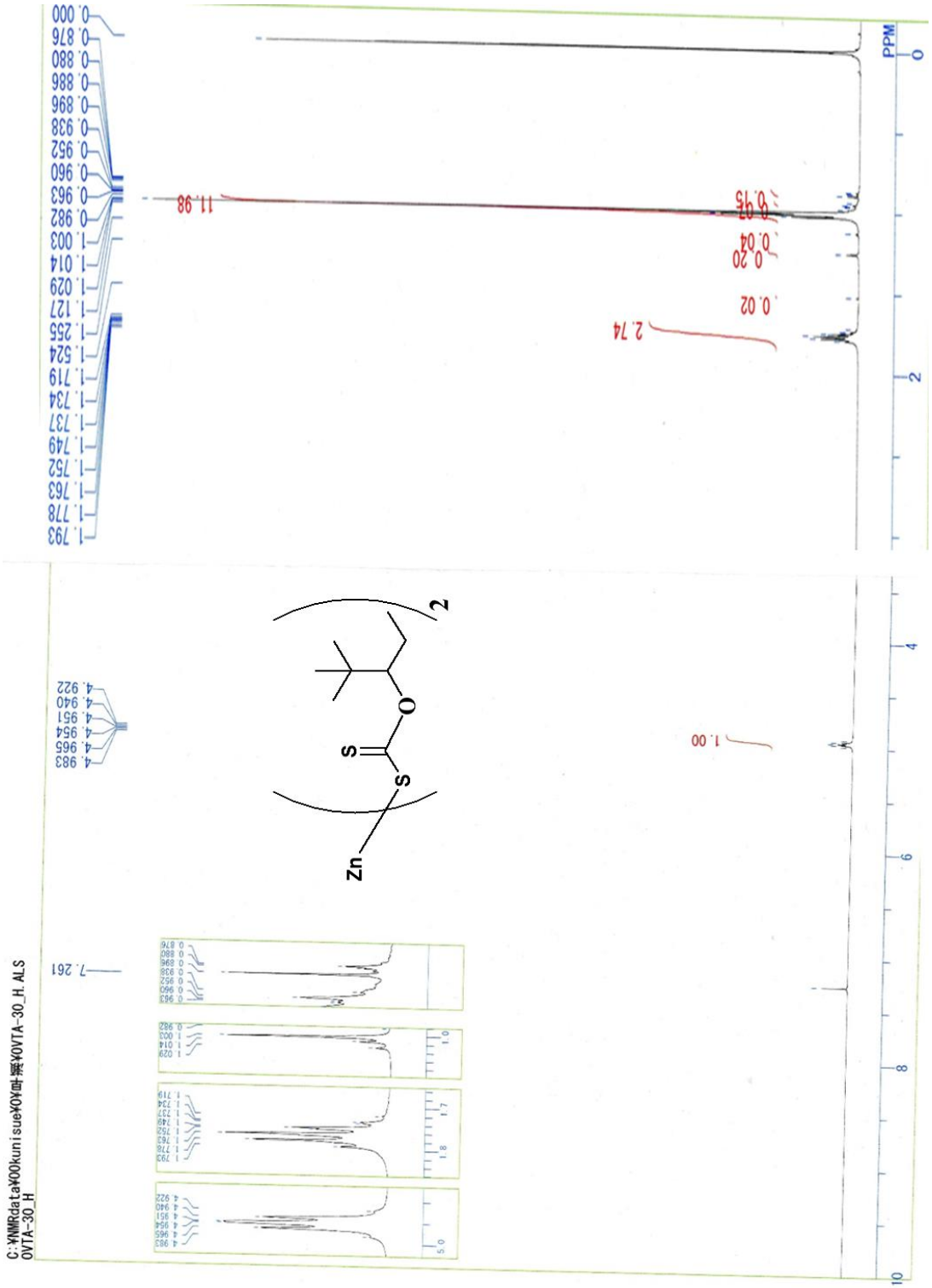

Figure: 19. Cd (II) - 2,2-dimethyl-3-pentane xanthate ^{1}H NMR.

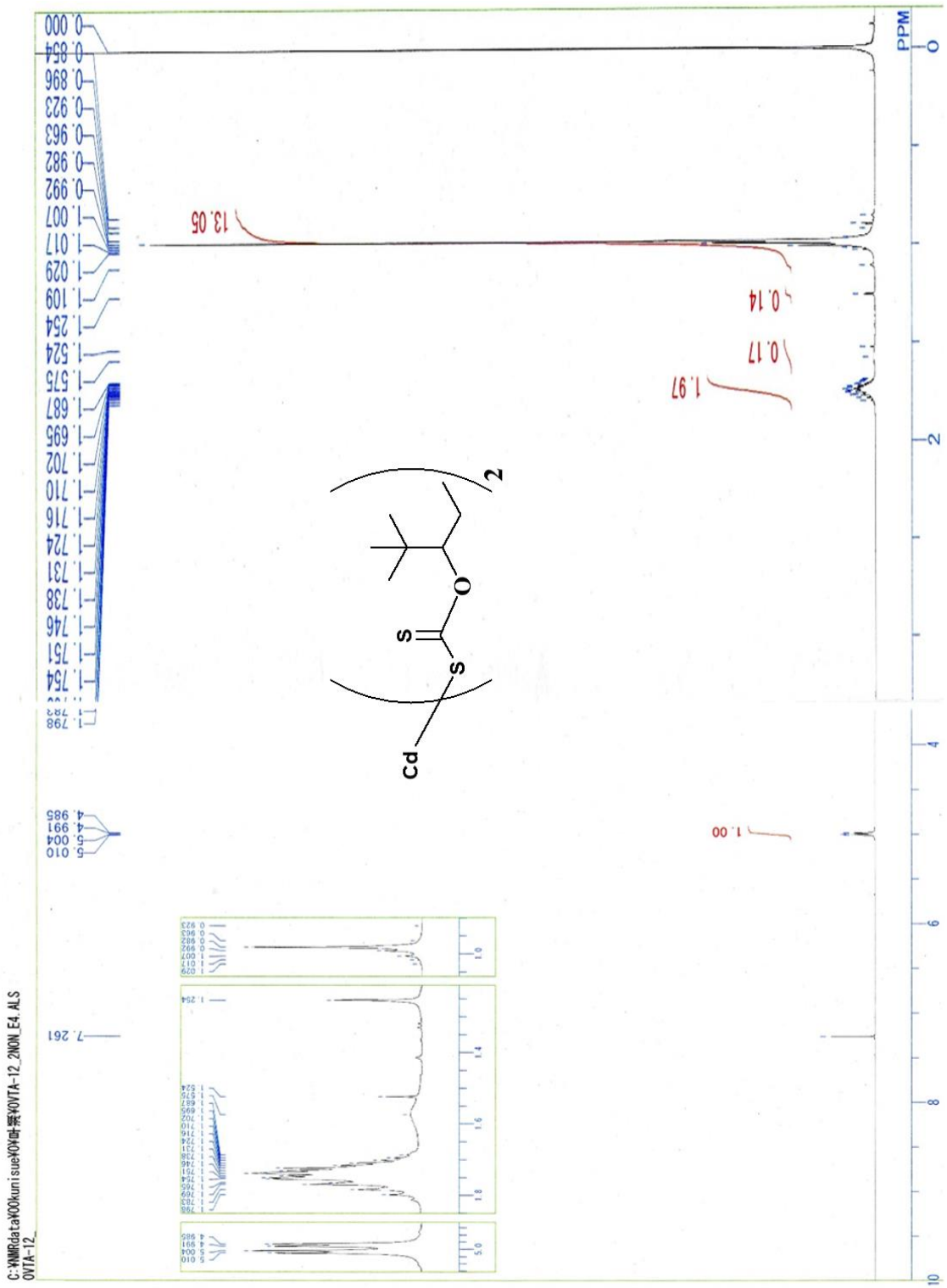

Figure: 20. In (III) - 2,2-dimethyl-3-pentane xanthate ^{1}H NMR.

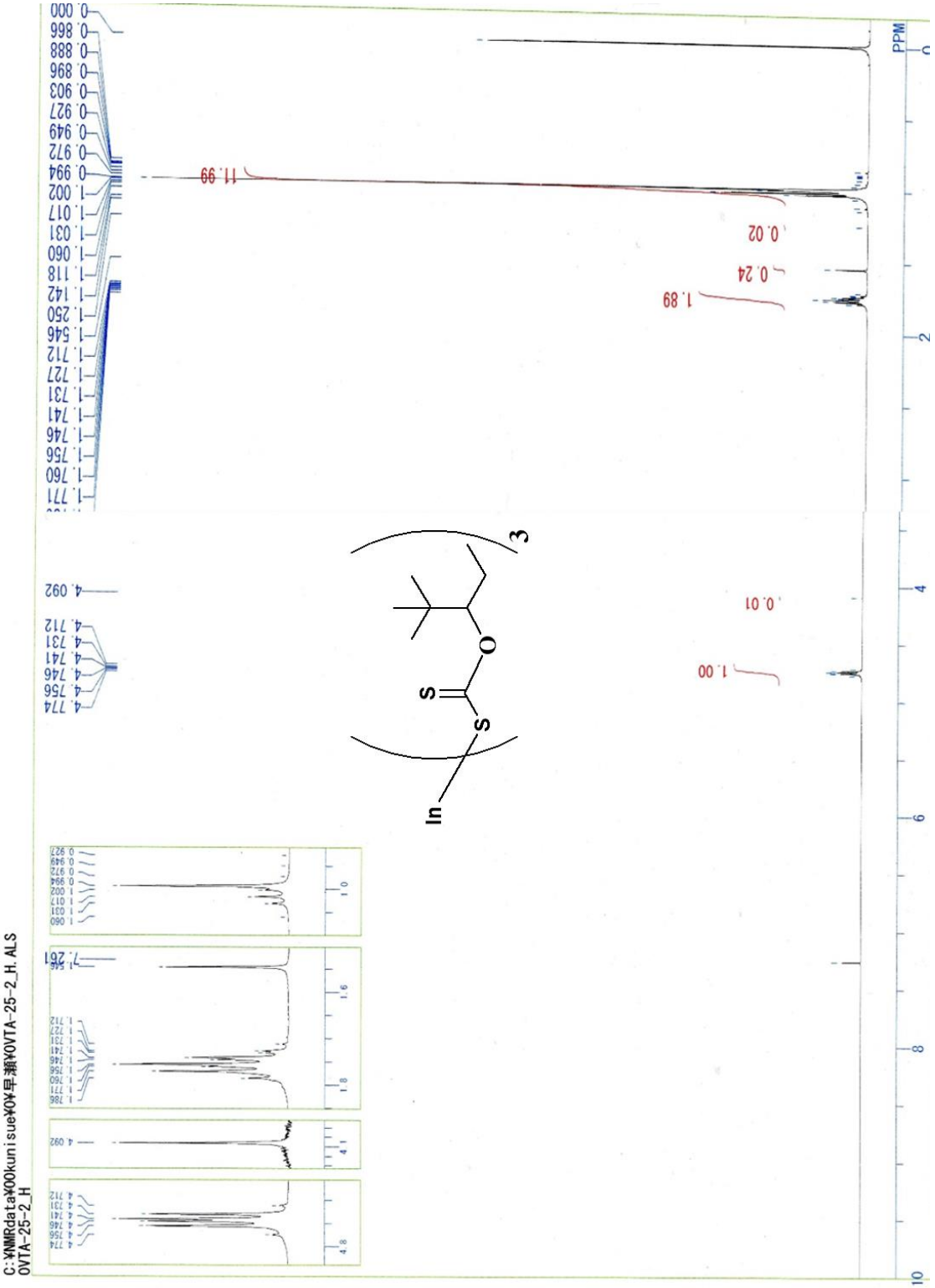

Figure: 21. Ga (III) - 2,2-dimethyl-3-pentane xanthate ^{1}H NMR.

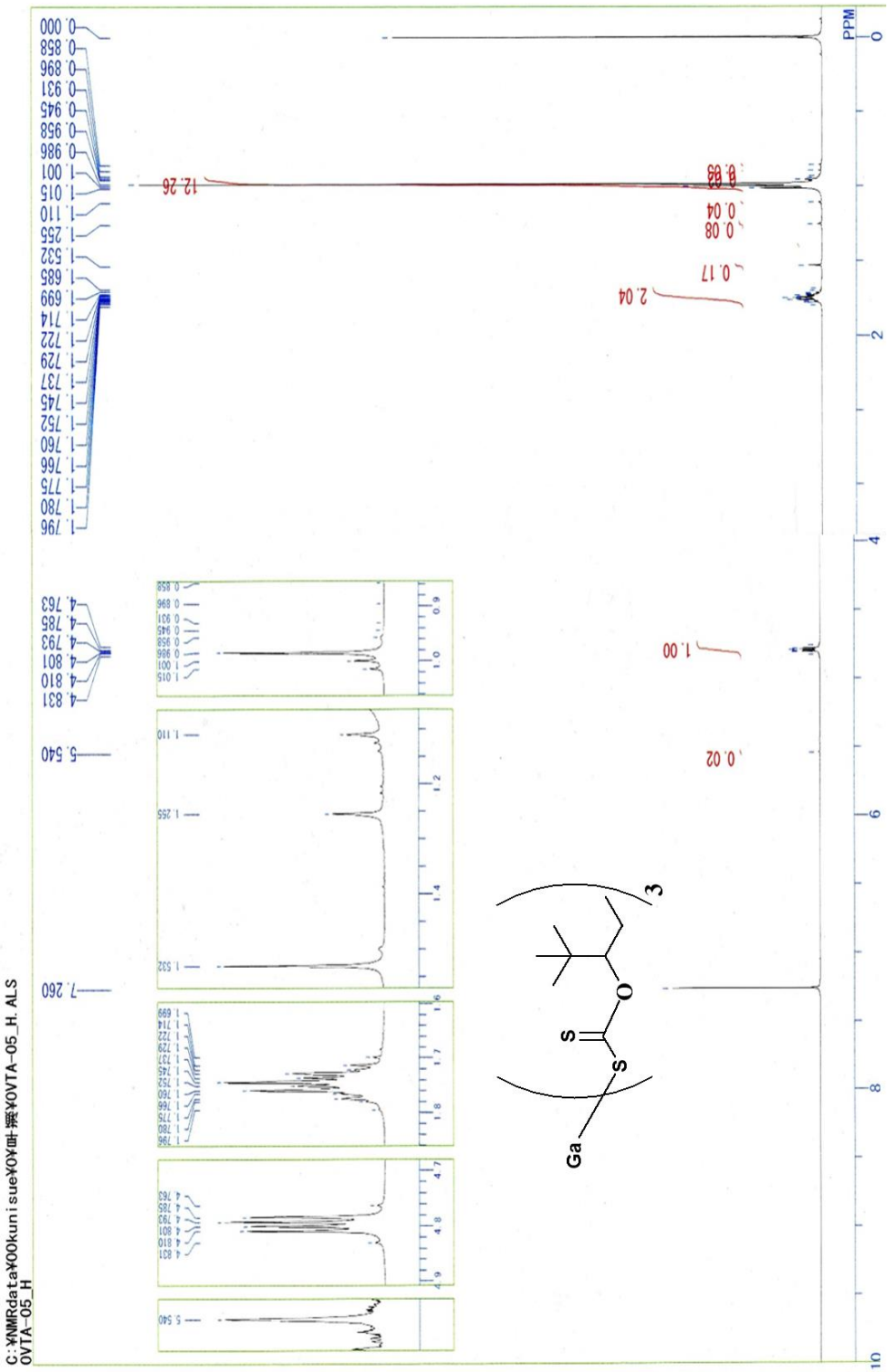

Figure: 22. Cu (I) - 2,2-dimethyl-3-pentane xanthate ^{13}C NMR.

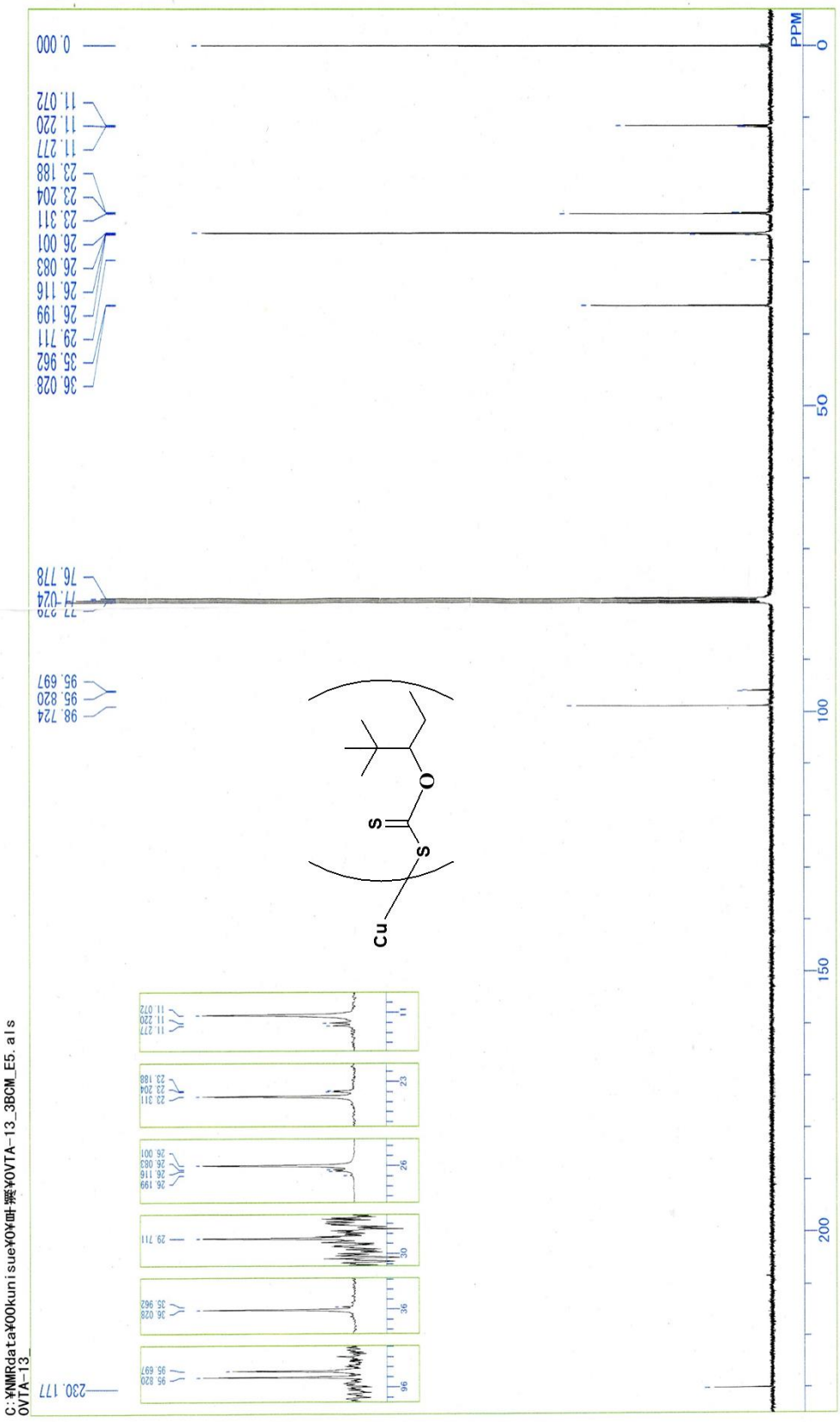

Figure: 23. Pb (II) - 2,2-dimethyl-3-pentane xanthate ^{13}C NMR.

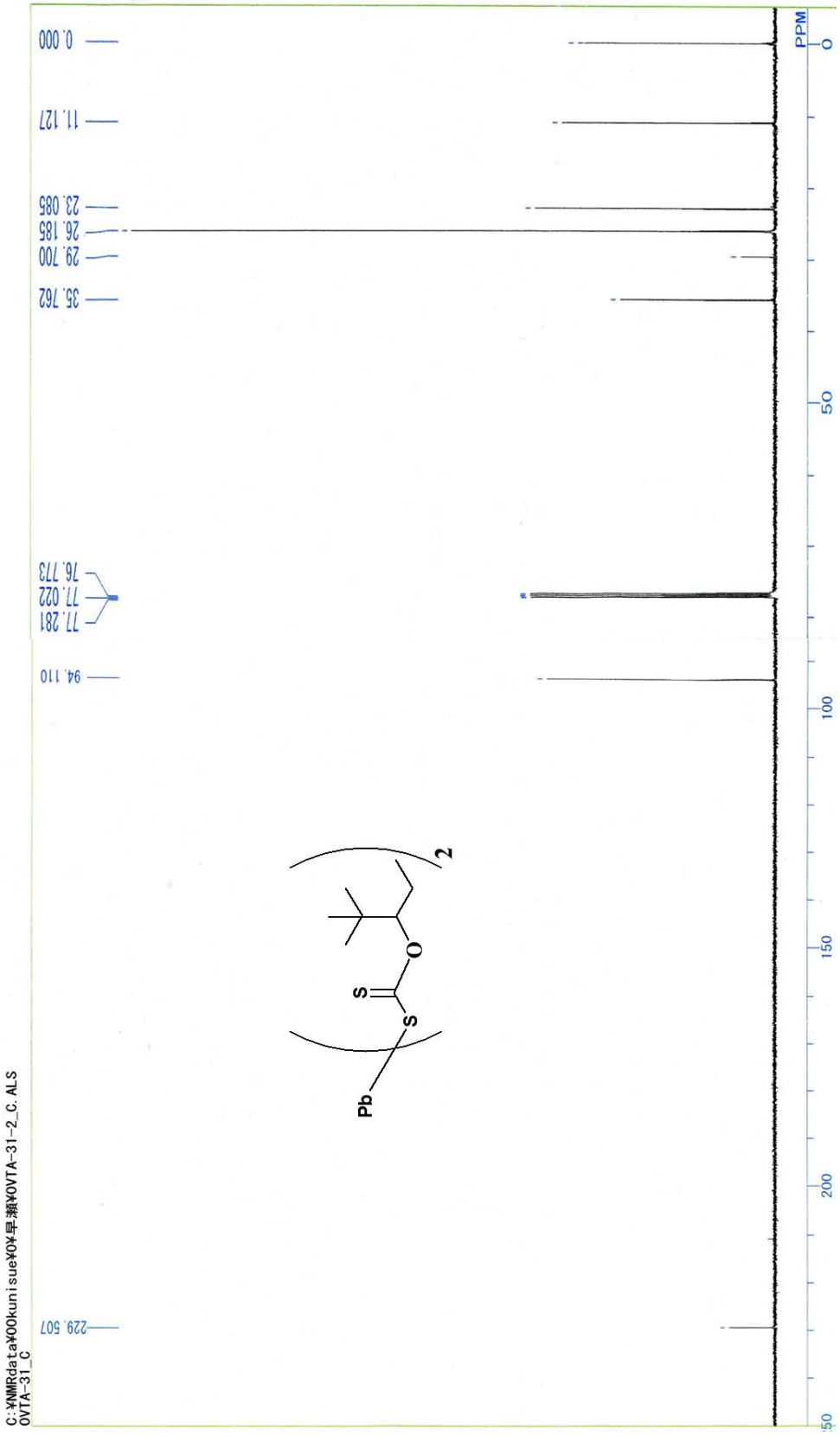

Figure: 24. Sb (III) - 2,2-dimethyl-3-pentane xanthate ^{13}C NMR.

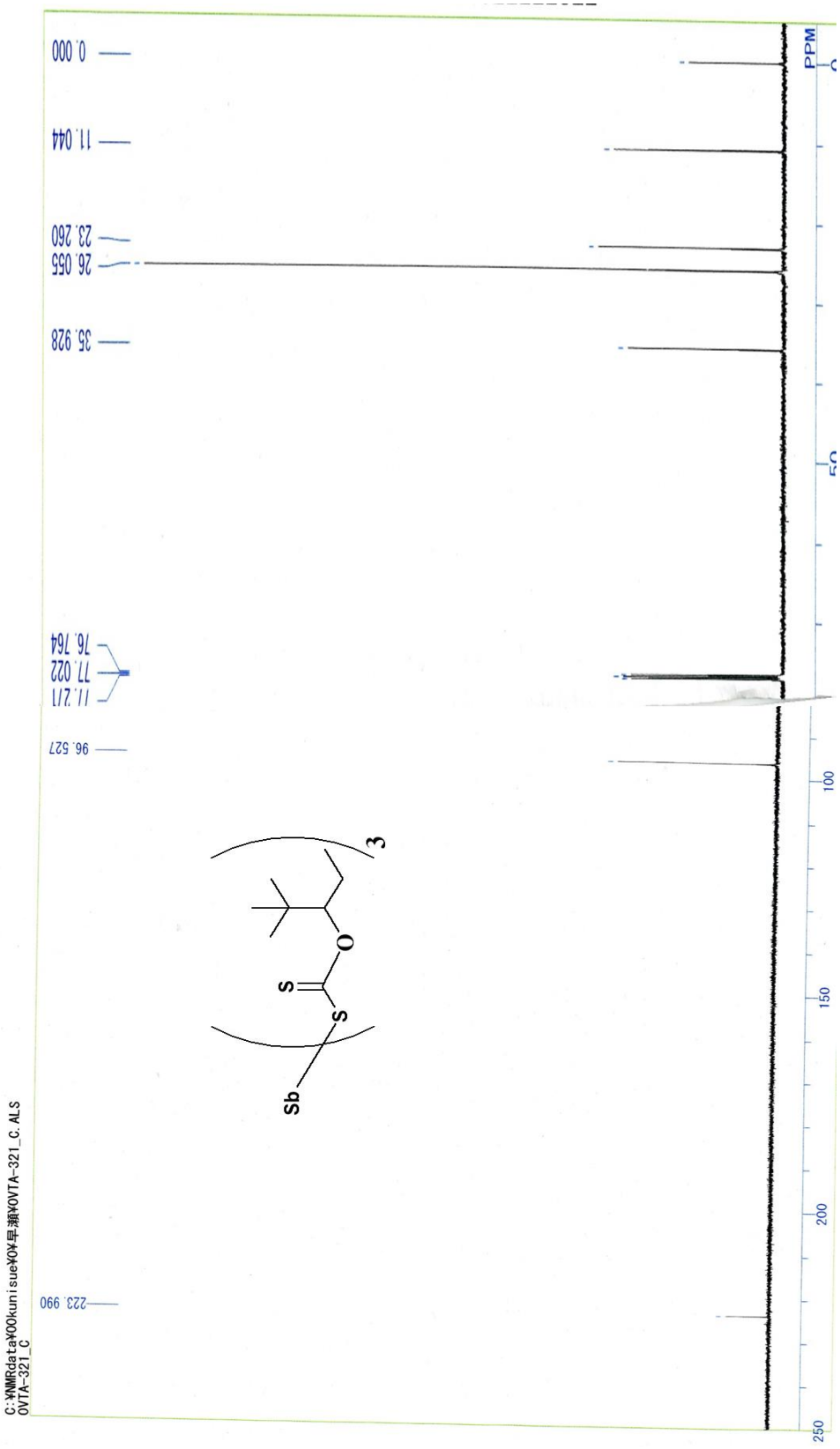

Figure: 25. Zn (II) - 2,2-dimethyl-3-pentane xanthate ^{13}C NMR.

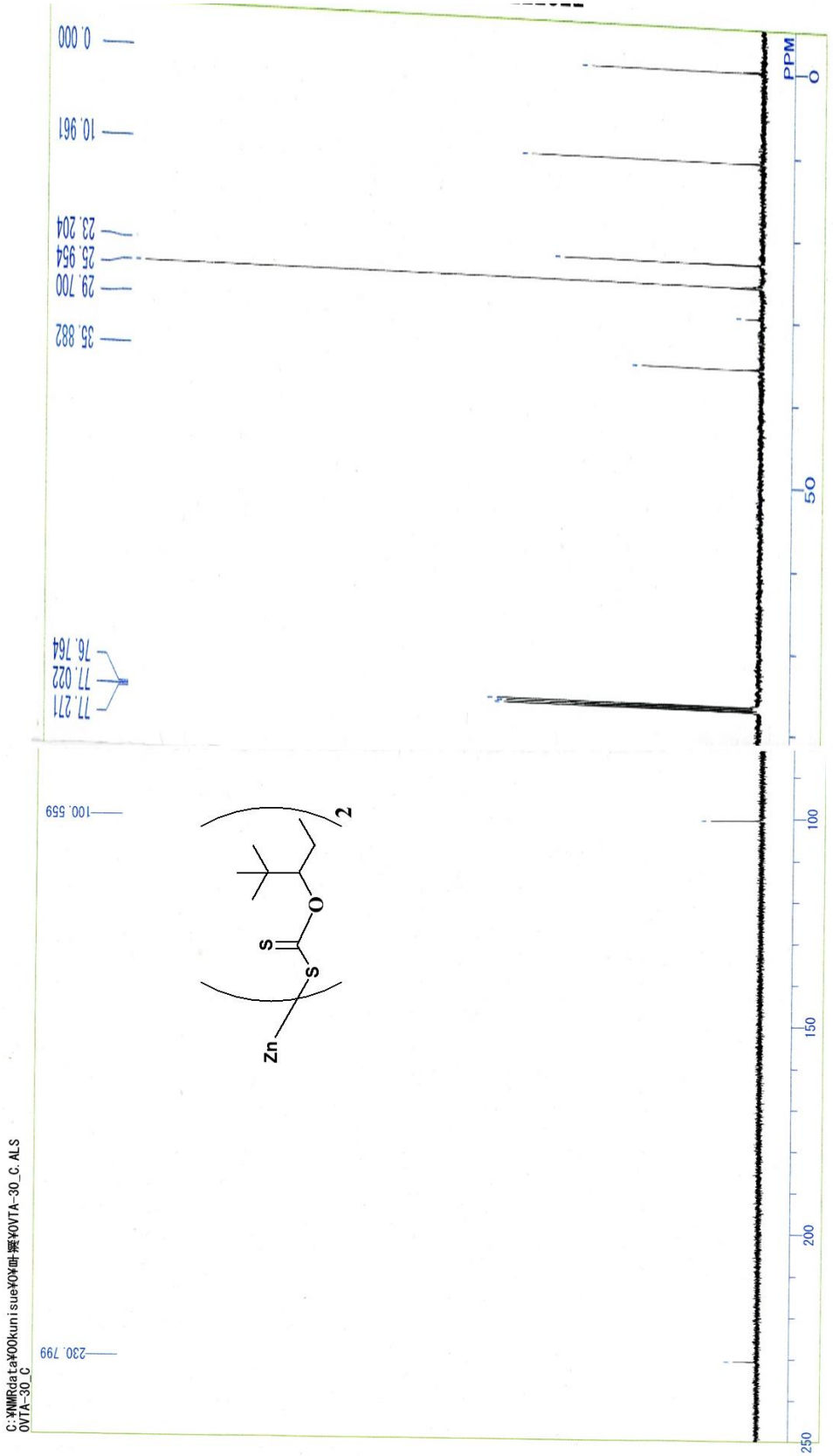

Figure: 26. Cd (II) - 2,2-dimethyl-3-pentane xanthate ^{13}C NMR.

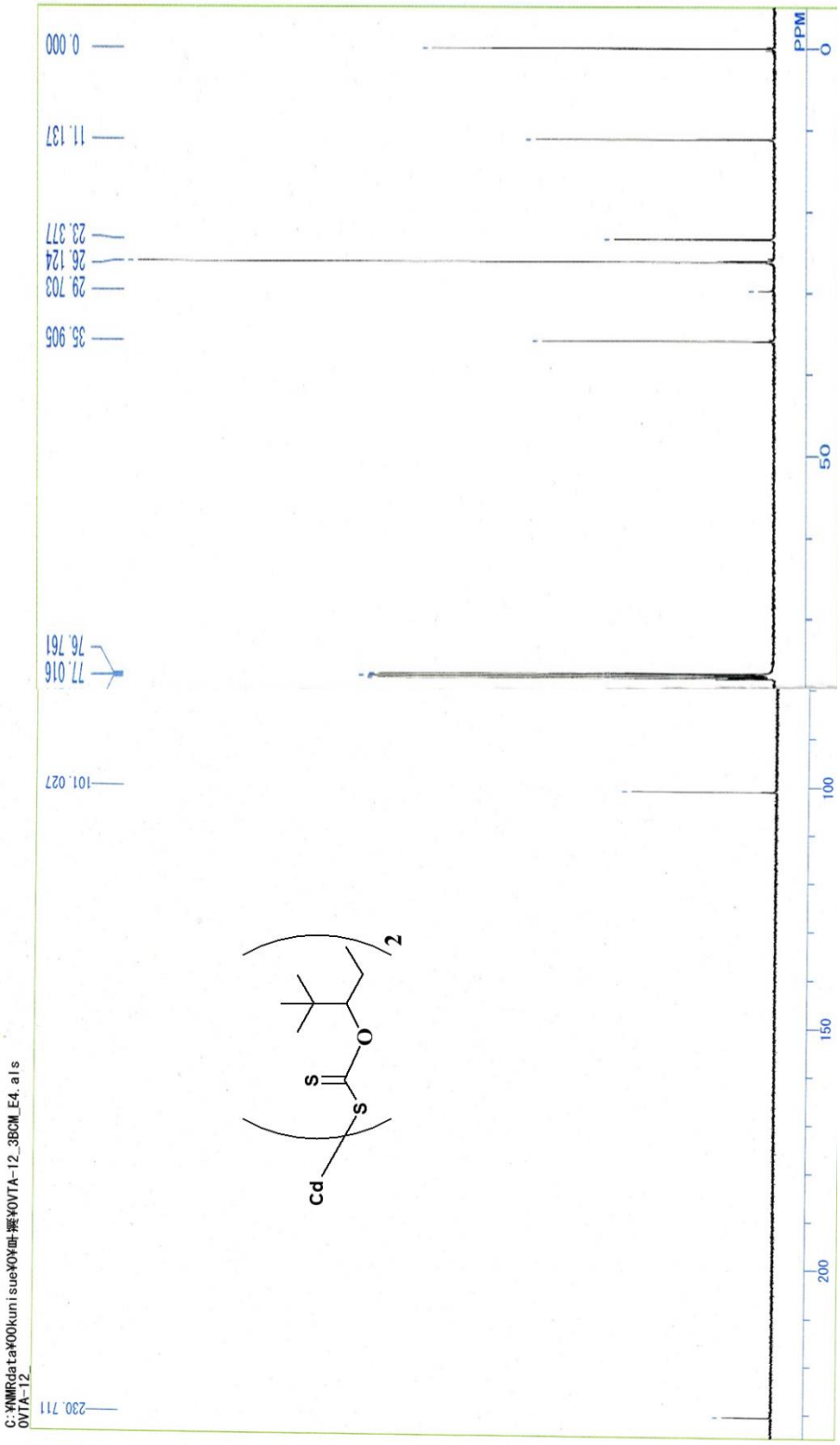

Figure: 27. In (III) - 2,2-dimethyl-3-pentane xanthate ^{13}C NMR.

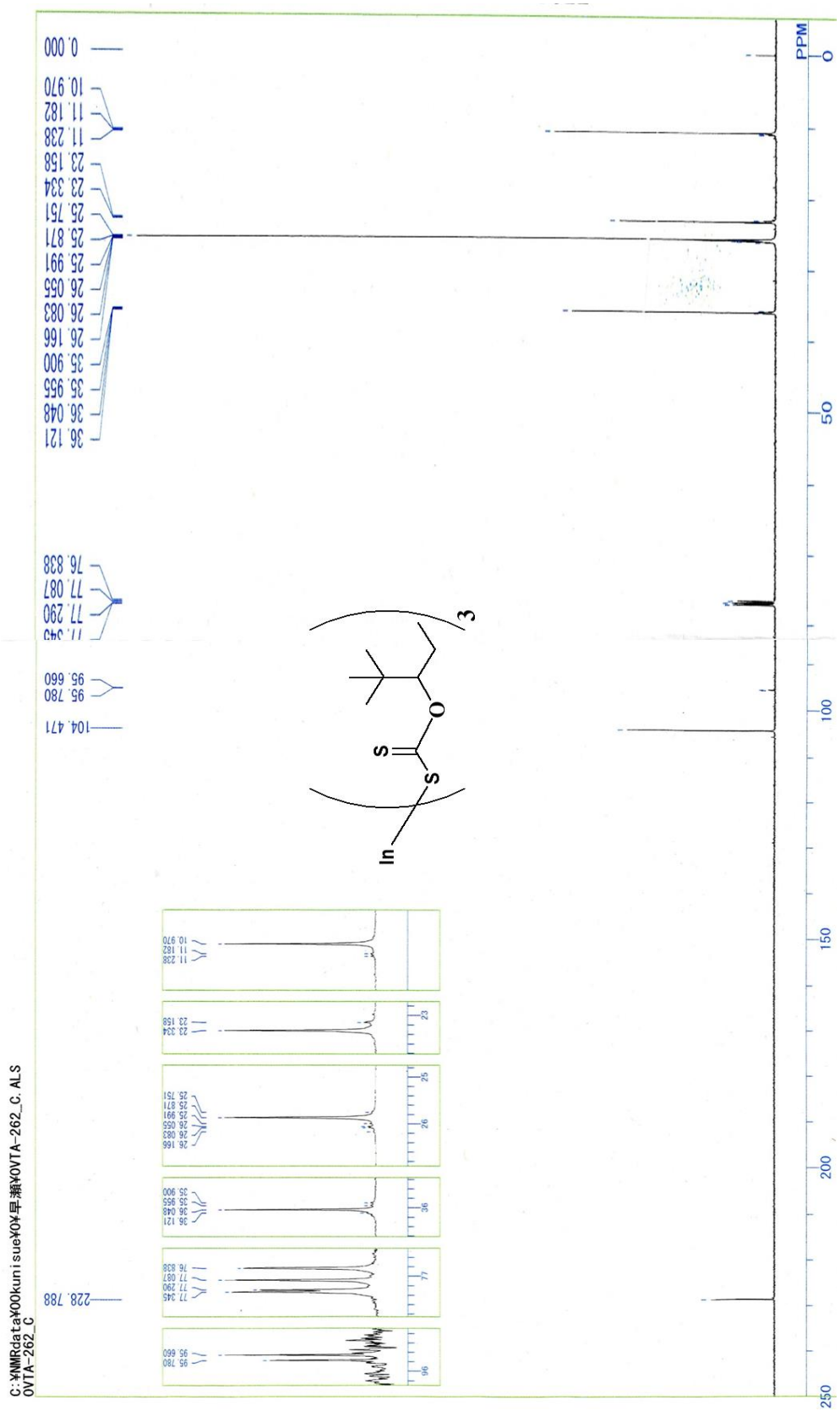

Figure: 28. Ga (III) - 2,2-dimethyl-3-pentane xanthate ^{13}C NMR.